THE UNIVERSITY OF MANITOBA

BIOELECTRIC CURRENT DURING OOGENESIS

IN

RHODNiIlS *PROLIXUS*

WILLIAM LIONEL DIEHL-JONES

A THESIS SUBMITTED TO THE FACULTY OF GRADUATE STUDIES
IN PARTIAL FULFILMENT OF THE REQUIRMENTS
FOR THE DEGREE OF DOCTOR OF PHILOSOPHY

DEPARTMENT OF ZOOLOGY

WINNIPEG, MANITOBA

SEPTEMBER, 1991

ISBN 0-315-76603-4

Canada

BIOELECTRIC CURRENT DURING OOGENESIS IN RHODNIUS PROLIXUS

BY

WILLIAM LIONEL DIEHL-JONES

A thesis submitted to the Faculty of Graduate Studies of the University of Manitoba in partial fulfillment of the requirements of the degree of

DOCTOR OF PHILOSOPHY

ABSTRACT

Previous studies show that the telotrophic ovarioles of the hemipteran Rhodnius prolixus have a dynamic pattern of transcellular ionic currents and a 10 mV electropotential difference between nurse cells and the terminal oocyte. These bioelectric properties may be associated with intraovariole regulatory feedback and intracellular electrophoretic transport. In the present work, the pattern and ionic composition of extracellular currents are further characterized with the two dimensional vibrating probe technique.

Asymmetries exist in the radial pattern of currents around intact ovarioles, especially around the terminal oocyte. Experimental removal of the follicular epithelium indicates that germ cells generate at least part of the extracellular current pattern. Current direction over denuded penultimate oocytes reverses from influx to efflux in late vitellogenic stages of the ultimate oocyte, correlating roughly with the release from developmental arrest. Denuded tropharia show current efflux over the basal region and influx over the apex, which is consistent with earlier observations by Telfer et al. (1981) concerning electrophoretic movement of charged fluorescent dye. Iontophoretic and pressure injection of negatively charged fluorescent latex beads reveals unidirectional transport to the terminal and subterminal oocytes, which is consistent with the electrophoretic theory of transport.

Current efflux over the base and apex of the terminal follicle and over the base of the tropharium is due to active sodium transport. Current influx over the middle of terminal follicle is carried by sodium influx and chloride efflux. Current enters the tropharium via influx of sodium and calcium. Transient inward calcium currents occur over the apex of the terminal follicle in mid- to late vitellogenic ovarioles, and it is speculated that this may serve as a developmental cue. Perturbation of sodium and chloride flux disrupts fluid phase pinocytosis, implying a role of these two ions in regulating fusion of pinosomes during the endocytotic pathway. This study provides a further basis for experimental dissection of endocytotic and transport processes during development.

ACKNOWLEDGEMENTS

I could not have embarked upon this research, much less finished it, had it not been for the support and kindness of many people.

To begin, Dr. Erwin Huebner has been much more than a supervisor - he has been and will continue to be one of my closest friends. Thankyou, Doc, for showing me the "red thread of science". You knew that I would finish the race even when I didn't believe it myself. I have learned much from you, not the least of which is an appreciation of the beauty in science and in life. These lessons I will remember.

I thank Dr. D.B. Stewart who typified, for me and many others, a true gentleman and scholar. His early guidance and faith in me sustained me in some bleak times.

I also thank Dr. T.V.N. Persaud, whose fairness enabled me to try again.

Dr. H. E. Welch left an indelible mark with his own personal courage and integrity, and his memory continues to inspire me and other young scientists.

I thank my committee, Dr. J.G. Eales, Dr. P. MacKay, and Dr. R.I. Woodruff for their thoroughness and patience. Their comments have immeasurably improved this thesis.

I have many friends to thank for helping to maintain my sanity: Larry

Dueck, Alvin 'the mouse' Dyck, Ron Bazin, Dr. Ross McGowan, Irmie Wiebe, Tara Narayansingh, Percy and Rita Hebert, Odd Bres, and all my lab mates past and present. Graduate life was a treat due to these people and many others I cannot name.

To my father - you always knew what my work was about. This meant more to me than I could ever say. Thankyou Dad.

To Charlene, my wife - I could never thank you enough. This thesis is dedicated to you. With you, I know everything is possible.

TABLE OF CONTENTS

Chapter IV: *Intraovariole Bead Transport in Rhodnius prolixus*

LIST OF FIGURES

Chapter I

Chapter II

Chapter **III**

LIST OF TABLES

Chapter II

GENERAL INTRODUcrrON AND LITERATURE OVERVIEW

An underlying concept important to my thesis is that ion pumps and channels are sometimes spatially segregated in the plasma membrane (Harold, 1986; Jaffe, 1986; Nuccitelli, 1990). Ion traffic across the cell membrane results in minute but measurable extracellular voltage gradients; such gradients are discerned as transcellular currents and have been detected around a variety of developing and fully differentiated cells and tissues. To fully establish the nature and possible developmental significance of these currents, this introduction covers the general principles of bioelectricity, and reviews the methodologies and studies pertinent to this work. The final section focuses on bioelectric phenomena around the telotrophic insect ovariole, which is the system investigated in my research.

General Principles of Bioelectricity

The plasma membrane effectively acts as a dielectric by preventing charged molecules or ions from crossing the hydrocarbon phase of the lipid bilayer (Alberts et al., 1990; Kuffler et al., 1984). Ion traffic across the cell membrane is closely regulated by two broad categories of membrane-spanning molecules: carrier proteins and channel proteins.

Carrier proteins act as enzymes which bind specific solutes and transfer them across the plasma membrane by way of a conformational change. Carriers-- or transporters -- move ions against their electrochemical gradients via the expenditure of metabolic energy. Such biological pumps work by the phosphohydrolysis of ATP, and a variety of ATPases have been characterized, including the ubiquitous Na+/K+ ATPase, H+, Ca+2/Mg+2, K+, and HCO_3- ATPases (Alberts et al., 1990; Hille, 1984; Towle, 1984). In a physical sense, such ATPases can act as pumps that generate electrochemical gradients across the cell membrane and regulate cellular concentrations of these and other ions.

Another class of carrier proteins is the so-called 'ion porters' which are driven by ion gradients rather than directly by ATP hydrolysis. These include antiports in which import of one ionic species is coupled to the export of another. Examples include the Na+-H+, K+-H+, $Ca^{+2-H+,}$ and HCO_3-Cl^- antiports found in a variety of cell types (Aickin and Thomas, 1977; Alberts et al., 1990; Strange and Phillips, 1985). By contrast, symports such as the lactose permease, the Na"-glucose porter, and the Na'-methionine porter involve the unidirectional co-transport of one ion with another ion or molecule (Hille, 1984; Kuffler et al., 1984). In the case of both symports and antiports, the movement of one ion or molecule is coupled to another ion flowing down its electrochemical gradient (Hille, 1984; Kuffler et al., 1984).

Ion channels in the plasma membrane differ from other transport proteins in that they allow only passive ion flow. Presently, ion channels are viewed as

water-filled pores and are known to be more permeable to some ions than others. Channel specificity is a key factor in determining both the electrophysiological properties of cells and the ionic balance within cells, and this specificity is derived from pore radius and charged moieties comprising the channel itself, as well as from ionic charge, radius, shape and hydration (Hille, 1984). Channel conductance for a specific ion can be altered - or gated -- by changes in membrane potential (voltage-gating) or by a specific ligand, such as Ca^{+2} or CAMP, binding to the channel protein (ligand-gating) (Alberts et al., 1990; Hille, 1984).

Electrogenic pumps, ion channels and the capacitive properties of the cell membrane together regulate membrane potentials and in some cases excitability; the energy stored in membrane potentials is used for a multitude of cellular processes, from signal transduction and solute transport to high energy bond formation (Nuccitelli, 1990). Inorganic ions themselves play key roles in many cellular processes (Alberts et al., 1990; Eckert and Naitoh, 1972; Harvey et al., 1988; Hille, 1984; Kindle et al., 1988). According to Hille (1984), major cellular roles have been defined for almost all ionic species.

Given the significance of both the energy stored in transmembrane potentials and the regulatory roles of ions themselves, it is clearly essential to know something of the ionic traffic across the plasma membrane. This is especially true in developing systems, wherein steady-state transcellular ion currents appear to be almost a universal phenomenon (Jaffe, 1981; Nuccitelli, 1983, 1990). Such transmembrane fluxes are the result of spatial segregation of ion

influx and efflux sites (Jaffe, 1981, 1986). Many plant and animal developing systems are known to drive transcellular currents through themselves; in numerous cases the spatial and temporal patterns of these currents correlate with morphogenic and developmentally significant events (see reviews by Jaffe, 1981; Nuccitelli, 1983, 1984, 1988, 1990).

A central question is whether or not transcellular ion currents are developmentally determinative or whether they are a consequence of other processes. Harold (1986) summarized four lines of evidence linking ion currents with developmental events: 1) ion currents may predict and precede the onset and location of growth; 2) localized ion influxes may stimulate localized growth; 3) cytoplasmic ion gradients have been observed which correlate with observed extracellular current patterns; and 4) applied electrical fields can induce polarization in several cell types, from fibroblasts to eggs. Taken together, such evidence strongly implies a role for ion currents in developmental regulation. Review of early studies which initially revealed assymmetries in biological current flow is useful.

Classical Studies on Transcellular Currents

One of the first studies to measure the transcellular ion currents in a developing system involved eggs of the marine alga, Fucus furcatus, which can be polarized by white light to form a bipolar embryo (Jaffe, 1966). Since the voltage drop across a single cell was comparable to the then minimum attainable

electrode noise (approximately 0.1 Uv), a method had to be developed to in effect amplify the electropotential differences; the solution was to line-up 100 - 200 fertilized eggs in a small bore, close-fitting capillary tube, thereby placing the transcellular voltages in series. With standard calomel electrodes and a microvolt-ammeter, Jaffe (1966) measured the voltage difference between the ends of the capillary tubes. Tube potentials increased in proportion to the number of germinating eggs, and during the initial rhizoid outgrowth stage it was calculated that at least 60 picoAmps of current flowed through each egg, or approximately 6 uAmp/em? entered the growing area. The importance of these findings was that, for the first time, measurements had been made of a transcellular current which could conceivably play a role in pattern formation. A major limitation, however, was that of a lack of spatial and temporal resolution (Jaffe and Nuccitelli, 1974).

A landmark report in the early literature on transcellular currents involved a fully differentiated, somatic tissue -- the vertebrate rod cell. Hagins et al. (1970) reported on a steady, inward transcellular current flowing from the rod outer segment (ROS) which was balanced by equal outward current over the rest of the cell. The magnitude of current flow was transiently reduced upon exposure to flashes of light, implicating the current as a DC signal carrier in phototransduction. Subsequent papers showed the outward current was generated by the electrogenic Na+-K+ pump, and the inward current is a consequence of Na" channels in the ROS (Stirling and Lee, 1980). In addition to

its function as a signal carrier, the 'dark current' may be capable of producing a longitudinal voltage gradient inside these receptors (Hagins et a1., 1970). It was calculated that the internal voltage gradient inside the ROS may exceed 3 V/ em, which would enable a 20% increase in the equilibrium concentration in the rod tip of a trivalent negative ion such as ATP (Hagins et a1., 1970).

Hagins et al. (1970) used standard metal electrodes positioned relative to rod cells in retinal slices. Differences in potential relative to ground for two adjacent electrodes could be measured in the millivolt range, and current flow calculated by considering the resistivity of the interstitial fluid and by applying Ohm's law. Maximal extracellular currents in unstimulated rods were on the order of 800 Uamp/crrr', which was well within the signal/noise limits set by the recording system. Currents in the same order of magnitude as those calculated for individual Fucus embryos, however, were not large enough to have been measured within the noise limits of this system; furthermore, few biological systems lend themselves to combined series measurements of current flow as does Fucus. Before measurements could be made of small but steady (and presumably biologically significant) transcellular currents, it was necessary to develop a method with the resolution for measuring voltage differences in the nanovolt range.

The Vibrating Probe

One way to measure a stable current density outside a living cell is to position two recording electrodes fixed distances apart within a few microns of the cell surface. The quotient of the voltage drop between the recording electrodes and the bulk resistivity of the extracellular fluid will be proportional, according to Ohm's law, to current density:

$$I = E/p = -(1/\rho)(\Delta V/\Delta r)$$

where I=current density, E=electrical field strength, p=resistivity, ΔV=voltage difference, and Δr=distance between recording locations (from Nuccitelli, 1990).

A major limiting factor in measuring minute electrical potentials is electrode noise, both in the form of low frequency (1/f) noise and in thermal (or Johnson) noise (Dorn and Wiesenseel, 1982; Freeman et al., 1985; Jaffe and Nuccitelli, 1974). Low frequency noise is generated by electrode drift, and the problem is compounded by nonequivalent electrodes (Freeman et al., 1985). Johnson noise is a consequence of the relatively high impedance associated with the electrode/fluid interface, and in standard KCI-filled electrodes is on the order of $10^6\ \Omega$ (Freeman et al., 1985; Nuccitelli, 1984). These elements define the limits of resolution for 3mM KCI-filled glass electrodes at 10 μV (Nuccitelli, 1990).

Bliih and Scott (1950) were the first to show that 1/f noise is reduced when a single electrode, sampling potential at two separate locations, is oscillated linearly between those two points. Johnson noise can be reduced by using metal-filled electrodes, which reduce impedance from $10^6\ \Omega$ to $10^3\ \Omega$ (Nuccitelli, 1984).

Jaffe and Nuccitelli (1974) were the first to use both these principles in developing the ultrasensitive vibrating probe.

The development of vibrating probe technology in 1974 has enabled the detection and examination of extracellular currents in many plant and animal systems. The design of the original one-dimensional vibrating probe and subsequent improvements have been previously reviewed elsewhere (Dorn and Wiesenseel, 1982; Freeman et al., 1985; Jaffe and Nuccitelli, 1974; Nuccitelli, 1984, 1986, 1990). Briefly, the vibrating probe used for my research consisted of a metal voltage-sensing electrode with a platinum-black ball tip with relatively high capacitance. As the probe tip is moved between two points within a graded electrical field, the probe tip capacitively couples to the field, thereby detecting fluctuations in charge (Nuccitelli, 1990). The oscillatory movement of the electrode is driven by a piezoelectric crystal powered by a sine wave signal from a lock-in amplifier, which also multiplies a phase-matched sine wave into the electrode signal. The product is equal to the peak-to-peak root mean square voltage difference between the two recording points (Freeman et al., 1985; Jaffe and Nuccitelli, 1974; Scheffey, 1986). An RC filter with a selectable time constant is used to average the product, which serves to eliminate faster signals and allows through only the slower changing signal components (Scheffey, 1986). Vector addition of in-phase and quadrature components of the electrode signal provides a measure of both current magnitude and direction.

Aside from enabling the detection of nanovolt potential differences, there

are other advantages inherent in the vibr.ating probe technique. With classical intracellular electrodes, a frequent concern is that of ion leaks around the electrode, which can greatly influence resting potential and cellular physiology (Purves, 1988; Brown and Flaming, 1986). Unlike intracellular electrode techniques, the vibrating probe is noninvasive, and therefore minimally perturbs cells or tissues being examined. Moreover, information elucidated with intracellular electrodes indicates bulk or net ion flow across the entire membrane; the vibrating probe reveals the assymmetry of ion flow.

Freeman et al. (1985) developed a circularly-vibrating probe driven by electromagnetic speaker coils capable of measuring perpendicular voltage gradients. This design is mechanically very stable, and an ultra-narrow-band phase-coherent filtering algorithm and low-noise electronics enable consistent measurements of current densities as low as 5 nano-Amps/crrr' (Freeman et al., 1985), which is by far the most sensitive vibrating probe design to date. Presently, twa-dimensional vibrating probes based on piezoelectric parallelogram (Nuccitelli, 1986) or pi (Scheffey, 1988) bender designs are commercially available (Nuccitelli, 1986; A. Shipley, pers. comm.).

A major disadvantage of the vibrating probe is a relatively slow response time. Kline (1986) directly compared the whole-cell patch clamp method with the vibrating probe in measurements of activation currents in frog eggs. Both methods were capable of detecting the inward activation currents (which consisted of a Cl^- efflux), although the vibrating probe showed a more gradual rise

in current influx (Kline, 1986). As well, the vibrating probe does not provide information on membrane potential, which must be intimately related to transcellular ion traffic. Finally, the giga-seal patch clamp is capable of demonstrating single channel activity in the pico-Amp range (Hamill et al., 1981), and this is beyond the resolving power of the vibrating probe.

Vibrating probes described so far are in essence voltage-sensitive electrodes. To determine the identity of current-carrying ions, it is necessary to use ion channel blockers and ion-substituted media, and this has formed the basis for much of my research. Recently (Kuhtreiber and Jaffe, 1990), a $Ca^{+}2$-sensitive vibrating probe has been developed. Essentially, this is an ion-specific liquid ion exchanger-filled microelectrode vibrated at low frequency. Future developments will probably include pH- and K^{+}-specific vibrating probes (Nuccitelli, 1990), and possibly an aerial vibrating probe (Nuccitelli, 1990).

Possible Role(s) of Ion Currents

In a few examples, the biological relevance of spatially segregated ion pumps and leaks is unambiguous; one such illustration is the asymmetry of transport proteins in columnar epithelial cells of the vertebrate gut. Sodium-glucose symport occurs across the apical cell surface, and is driven by Na^{+}-K^{+} ATPase along the baso-lateral surfaces (Alberts et al., 1990). Another clear correlation between channel symmetry and biological function are the Cl^{-} channels localized to the apical surfaces of oxyntic cells of gastric crypts

(Demarest et aL, 1986). Perhaps best known is the channel asymmetry found in neurons: Ca+2 channels are concentrated in the soma (Almers and Stirling, 1984) and Na" channels are highly concentrated in the nodes of Ranvier (Chiu and Ritchie, 1980). Beyond these examples, however, a causal link between ion channel/pump asymmetries and cellular physiology is much more difficult to make. Jaffe (1986) identified two possible consequences of trans cellular current flow: (a) specific ion gradients, and (b) intracellular voltage gradients.

(a) Ion gradients and development

It is well known that ion concentration can be non-homogeneous within the cytoplasm; Ca^{+2} ions are sequestered in organelles and by Ca'<binding proteins in the cytoplasm (Alberts et al., 1990; Jaffe, 1981); and there can be regional pH differences within a single cell (Roos and Boron, 1981; Heiple and Taylor, 1982). Localized ion currents may therefore produce ion concentration gradients within the cytoplasm, and this may have profound physiological effects, especially with respect to morphogenetic and developmental processes (Busa, 1986). For example, Ca^{+2} ions have been shown to regulate cytokinesis (Tombes and Borisy, 1989), actin polymerization and membrane fusion (Tilney et aL, 1978), metaphase/anaphase transition (Poenie et al., 1986), control of cytoskeletal-associated proteins involved in microtubule and microfilament dynamics (Forscher, 1989), and of course regulation of protein phosphorylation/dephosphorylation via calmodulin or other $Ca^{+2\text{-binding}}$ proteins

(Alberts et al., 1990; Dinsmore and Sloboda, 1988; Kakiuchi and Sobue, 1983). Protons also playa pivotal role in many cellular processes, from sperm and egg activation (Gilbert, 1988; Hagiwara and Jaffe, 1979; Shen and Steinhardt, 1979) to regulation of cell proliferation and metabolism (Busa, 1982; Busa and Nuccitelli, 1984; Zivkovic, 1990). The potential therefore exists for specific transcellular currents to regulate cellular/ developmental processes in a variety of ways.

The fucoid egg, on which the initial examination of extracellular currents centered, most clearly demonstrates a causal relationship between ion currents, specific cytoplasmic ion gradients, and development. Inward currents precede and predict the future site of rhizoid development (Nuccitelli and Jaffe, 1974), and are carried by Ca+2 influx/ cr efflux (Robinson and Jaffe, 1975). The Ca+2 component of the current has been demonstrated via $^{45}Ca^{+2}$ uptake experiments (Robinson and Jaffe, 1975), and cytoplasmic Ca^{+2} gradients have been demonstrated with chlortetracycline (Kropf and Quatrano, 1987). This has been confirmed with both Ca'<sensitive microelectrodes and optically with the Ca^{+2}-selective fluorophore Quin-Z (Brownlee, 1989; Brownlee and Wood, 1986).

These findings indicate an increased concentration of Ca^{+2} in the apical cytoplasm of the growing rhizoid. Further manipulations of this system confirm the role of Ca^{+2} in the polarization of the fucoid egg: when placed in a Ca^{+2} concentration gradient, eggs polarize towards the area of highest concentration (Robinson and Cone, 1980), and suppression of cytoplasmic Ca^{+2} gradients with the $Ca^{+2\text{-chelating}}$ BAPTA buffer totally blocked tip polarization without affecting

egg viability (Speksnidjer et al., 1989). It is speculated that the Ca^{+2} gradient controls the process of vesicle localization and subsequent secretion of wall softening enzymes (Brawley and Robinson, 1985; Nuccitelli, 1990).

(b) Voltage gradients

According to Jaffe (1986), "Ion currents, per se, cannot act back on the system." If in a biological system current influx and efflux points are separated, current loops in the external medium must be completed by a corresponding inner, or cytoplasmic current loop. Kirchoff's laws (based on the laws of conservation of charge and energy) indicate two constraints of this system:

1) The algebraic sum of currents entering a nodal point in a circuit is zero; and

2) The algebraic sum of potential around a closed circuit is equal to zero (from Miller, 1977).

In other words, current entering a node (or, in this instance a cell) must equal that leaving the node. The cytoplasm of cells or tissues will exert a resistance to current flow, and basic circuit logic tells us that current flow across this resistance will result in a drop in potential (Miller, 1977). From this it is evident that transcellular ionic currents can result in intracellular voltage gradients. Given that extracellular space is restricted and external resistance is sufficiently high, external current loops could also exert physiologically significant electrical fields (Jaffe, 1981; Poo, 1981).

One of the consequences of the external current loop is a phenomenon termed by Jaffe (1977) as *lateral electrophoresis*. While many integral membrane proteins are immobilized by anchoring proteins such as tubulin, ankyrin, and spectrin, others are freely mobile (Poo, 1981). It has been postulated that channel localization could be brought about by electrophoretic redistribution of mobile channel proteins; the degree of redistribution is a function of the coefficient of diffusion, electrophoretic mobility, and the magnitude of voltage drop across a cell (Robinson, 1985). Poo and Robinson (1977) first demonstrated that fluorescein-labelled, receptor-bound Concanavalin A molecules redistribute themselves along the membrane of embryonic muscle fibres in electrical fields as low as 4 V/em. Orida and Poo (1978) also showed electric field-induced redistribution of acetylcholine receptors, and Stollberg and Fraser (1989) established that the direction of migration reverses upon treatment with neuraminidase. McCloskey et al. (1984) confirmed the same phenomenon occurs with P, receptors on leukaemic white blood cells.

Lateral electrophoresis is one of the mechanisms which has been used to account for the polarization and galvanotropic movement of a variety of cell types subjected to electric fields. Dissociated neurites from bird (Jaffe and Poo, 1979) and amphibian (Hinkle et al., 1981) embryos orient and move towards the cathode (negative) pole in weak (7 mV/em) electrical fields. Neural crest cells (Erickson and Nuccitelli, 1984), epithelial cells from Xenopus embryos (Luther et al., 1983), and fish epidermal cells (Cooper and Schliwa, 1986) also move and/or exhibit

lamellopodial ruffling directed towards the cathode. Gild et al. (1989) indirectly measured current influx at the front end of migrating fibroblasts and Freeman et al. (1985) demonstrated inward Ca+2 currents at the growing tips of individual neurites. Cooper and Schliwa (1986) and Nuccitelli and Smart (1989) stopped galvanotaxis with a variety of Ca+2 channel blockers, and McCaig (1989) reversed nerve galvanotropism with Ca+2 channel blockers and the Ca+2 ionophore A23187.

The broader implications of galvanotaxis are that a) electric fields may help direct the movement of embryonic cells or sheets of cells undergoing morphogenesis and b) they may direct fibroblast movement during wound healing. Barker et al. (1982) examined wound exit currents in guinea pig skin, and reported surprisingly large lateral voltage differences running through the epidermis on the order of 100 mV*fcm.* It is likely that wound repair cells respond in some way to this gradient, which is 10 - 100 times larger than the response threshold shown for other cells (Robinson, 1985).

Arguments against the role of lateral electrophoresis in channel localization include the point that it is a somewhat non-specific process (see Nuccitelli, 1990) and that in some instances, receptor migration occurs in the opposite direction to what would be expected on the basis of charge (Jaffe, 1981). A possible explanation for these apparent anomalies is that some membrane proteins may be carried hydrodynamically by electro-osmosis (Jaffe, 1981). Whatever the mechanism, Robinson (1985) points out that definitive evidence of the role of galvanotaxis in vivo must show a correlation between wound current magnitude

and rate of migration of cells.

Internal voltage gradients have been strongly implicated in *internal electrophoresis*, or the charge-based movement of cytoplasmic molecules and organelles. The first demonstration of an intracytoplasmic voltage gradient occurred in the polytrophic ovarioles of the silkworm moth, Hyalophora cecropia (Woodruff and Telfer, 1973). In the polytrophic follicle, nurse cells are linked via a short cytoplasmic bridge to a single 'developing oocyte; a steady voltage difference up to 6 mV is maintained across the bridge (nurse cell negative). Convincing evidence that the voltage difference is involved in unidirectional transport of charged molecules was provided by Woodruff and Telfer (1980) by microinjection of either negatively charged McFly (fluorescein-labelled, methylcarboxylated lysozyme) or positively charged Fly (fluorescein-labelled lysozyme) into either nurse cells or oocyte. Fly moved from oocyte to nurse cell and not in the opposite direction; McFly moved exclusively from nurse cell to oocyte, clearly showing that the voltage difference is involved in unidirectional transport of charged proteins.

A voltage gradient can be maintained in a cytoplasmic syncytium only by steady transcellular current flow (Nuccitelli, 1990). The transcellular current pattern around Hyalophora follicles consisted of strong (up to 20 p.Amp/crrr) current influx over the anterior or nurse cell region, balanced by more diffuse exit currents over the oocyte; a separate current efflux was measured over the furrow between nurse cells and oocyte (Jaffe and Woodruff, 1979), This pattern

was actually opposite to what would be expected for maintaining the nurse cells at a membrane potential more negative than that of the oocyte since current entry implies either influx of positive charge or efflux of negative charge (Jaffe, 1986).

In light of data then available, Jaffe and Woodruff (1979) initially proposed that an electrogenic pump existed in the furrow region between the oocyte and adjacent nurse cell; current driven across the furrow and into the oocyte reputedly returned to the nurse cells via a low resistance cytoplasmic bridge. When in subsequent experiments the follicular epithelium covering the nurse cells was removed by enzymatic and mechanical means, the current pattern reversed, or exited the naked nurse. cell membrane (Woodruff et al., 1986). This finding indicates that the follicular epithelium probably contributes to the pattern of extracellular currents, and that this pattern, at least over denuded germ cell membrane, reflects the standing voltage difference between nurse cell and oocyte.

Internal voltage gradients have been reported in a variety of insect follicle types (Telfer et al., 1981b; Woodruff and Anderson, 1984; Huebner and Sigurdson, 1986; Miinz and Dittmann, 1987; Woodruff, 1989) and in most of these cases charge-dependent movement has been explicitly shown. There is disagreement over the precise current pathways involved in some of these systems (Overall and Jaffe, 1985; Woodruff et al., 1986) and several different models have been proposed to reconcile observed extracellular current patterns and intracellular potentials.

Apart from insect follicles, there are at least two other examples in the

literature of cytoplasmic voltage gradients in developing systems. Hyphae of the water mold Achlya drive distaloutward proton currents via H+ATPase, thereby facilitating inward H+/ amino acid symport at the tip region (Kropf et aL, 1984). This correlates well with an internal 10 mV difference between the tip and trunk (Kropf, 1986). It remains to be tested whether or not the internal field differences (0.2 V/ em) are· large enough to induce internal electrophoretic transport. The other example of a standing cytoplasmic voltage gradient is in the structurally simple nurse cell-oocyte complex of the marine polychaete Ophryotrocha labronica. Emanuelson and Arlock (1985) reported a 22-32 mV potential difference between the oocyte and nurse cell (n=6). The magnitude of this difference is unprecedented, and is especially surprising when one considers the relative size of the complex (approximately 70 urn in length). I would expect a very large transcellular ion flux to be. involved in maintaining this voltage difference; however, my initial vibrating probe analysis of Ophryotroca nurse cell-oocyte complexes revealed small (0.5-1.0 u.Amp/crrr) and variable current fluxes (n=18) (unpublished data). Clearly, the intracellular voltage gradient must be further examined and an effort made to correlate this with vibrating probe measurements of transcellular ion currents.

Bioelectrical Properties of Insect Ovarioles

(a) Panoistic ovarioles

Panoistic ovarioles consist of single oocytes enclosed in a layer of

mesodermally-derived follicle cells (Geysen, 1988; Telfer, 1975). Ovarioles of Locusta migratoria were the first to be examined electrophysiologically. Younger oocytes developed membrane potentials of approximately -20 mV, while later stage oocytes attained potentials around -50 mV (Wollberg et al., 1975). These authors also found that any two adjacent ovarioles were electrically coupled. Verachtert (1988) studied extracellular ion currents around Locusta ovarioles, and showed that inward transcellular ion currents were limited to the posterior end of the terminal follicle, where the germinal vesicle was located. The rest of the ovariole typically had outward currents, with the exception of the posterior end of the sub-terminal (T-1) follicle, which sometimes had inward currents. It is not known whether follicle cells and/or oocyte plasma membranes contribute to these currents. Additionally, the relationship between inward current and the germinal vesicle has not been explored.

An initial study of extracellular currents around Periplaneta ovarioles (see Huebner and Sigurdson, 1986) revealed that currents exited the interconnectives and entered the lateral surfaces of follicles starting vitellogenesis. Although considerable variation was noted, the stage of the terminal (T) follicle correlated with changes in the current pattern. Current efflux at the interconnectives increased in an apical-basal direction along the ovariole (Huebner and Sigurdson, 1986).

Vitellogenic ovarioles of the German cockroach (Blatella germanica) have a dorsal-ventral polarity, and this is mirrored by the observed patterns of

extracellular currents (Kunkel, 1986). Inward current flows along portions of the ventral surface, which will be the site of the future embryonic axis. Bowdan and Kunkel (1990) have subsequently shown that, as follicles progress through vitellogenesis, the areas of current inflow (sink) and outflow (source) increase in area until most of the respective ventral and dorsal areas are covered. An intriguing link was suggested between these currents and vitellogenin uptake, the rate of which increases as vitellogenesis proceede (Bowdan and Kunkel, 1990). The origin and composition of these currents have not yet been described, although it appears that the current sink may be a property of the ventral oolemma and the current source may be the result of ion pumps in the dorsal follicular epithelium G. Kunkel, pers. comm.).

(b) Meroistic ovarioles

In meroistic ovarioles, an original germ cell undergoes a series of incomplete cytokinetic divisions. The interconnected cells form the nurse cell-oocyte syncytium (King and Akai, 1971; Telfer, 1975; Geysen, 1988). Although meroistic ovarioles lack the relative structural simplicity of panoistic ovarioles, their structural/physiological polarization make them unique. Usually, the presence of diffusible cytoplasmic factors induce synchronous nuclear division and differentiation (Phillips, 1970; Telfer et a1., 1981b), or in the case of insect preblastoderm eggs, induce mitotic gradients (Sonnenblick, 1950). In meroistic ovarioles, "nuclear behaviour in the oocyte-nurse cell syncytium indicates that

developmental cues are not freely exchanged" (Telfer et al., 1981b). A fundamental developmental problem concerns the mechanism by which nuclear polarity can be maintained in a common syncytial environment; the electrical polarity of the meroistic ovariole offers us a model with which to examine this question.

Another associated question concerns the possible mechanism of nurse cell-oocyte transport. The oocyte germinal vesicle does not produce measurable quantities of RNA (Davenport, 1974). The oocyte therefore depends upon nurse cells for much of its biosynthetic activity: nurse cells produce various RNA's, subcellular organelles, and proteins, all of which must pass to the developing oocyte via cytoplasmic bridges (Telfer, 1975; Capco and Jeffrey, 1979; Hyams and Stebbings, 1977; Huebner, 1984a; King and Biining, 1985). Meroistic ovarioles therefore present ideal models for examining both germ cell differentiation and cytoplasmic transport (Sigurdson, 1984; Woodruff et al., 1986). There are two types of meroistic ovarioles - polytrophic and telotrophic -- and I present brief overviews of the morphological and bioelectric properties of each in the following section.

(i) Polytrophic ovarioles

The bioelectric properties of H. cecropia have already been described in a preceding section; the electrophysiology of two other polytrophic follicles have also been studied: Drosophila melanogaster and the fleshfly, Sarcophaga bullata.

Much attention has recently been focused on Drosophila follicles, and the findings with respect to intracellular potentials, trans cellular currents, and intracellular electrophoretic movement are presently the subject of controversy.

Overall and Jaffe (1985) reported an extracellular current pattern around Drosophila similar to that found in Hyalophora: during the main period of follicle growth, current enters the nurse cell region and leaves the oocyte region; current influx was found to be carried by Na" and Ca^{+2} ions. The authors postulated a changing source for the extracellular currents: during the main period of follicle growth, currents were driven by the germ cell membranes, during choriogenesis by the follicle cells, and during the preblastoderm stage currents were hypothesized to be due to the plasma membrane *[sic].*

Bohrmann et al. (1986a) also showed current efflux over the oocyte and influx over the nurse cells, but reported far greater variability in current magnitude (normally between 0.1 and 5 μA/crrr) and direction, even among follicles of the same developmental stage. Patches of follicle cells were removed over the tropharium, revealing small inward currents, while one accidently denuded oocyte showed no measurable current flow. In marked contrast to the results of both Overall and Jaffe (1985) and to a lesser extent Bohrmann et al. (1986a), Sun and Wyman (1989) reported extremely small (usually less than 1 p.Amp/crrr) current patterns around Drosophila follicles, and no consistent pattern of efflux and influx.

A notable disparity also exists in measurements of intracellular potentials

in Drosophila. Bohrmann et al. (l986b) reported membrane potentials on the order of -21 mV, and found no significant differences in potential between nurse cells and oocyte. Sun and Wyman (1987) measured membrane potentials of -85 mV, and also found no differences in potential between nurse cells and oocyte (see Nuccitelli, 1990). In contrast, Woodruff et al. (1988), using the same incubation medium as Bohrmann et al. (1986b), showed a 2.5 mV potential difference between coupled nurse cells and oocytes. With Sun and Wyman's (1987) medium, Woodruff (1989) found nurse cells of stage 10 Drosophila ovarioles to average approximately -66 mV, oocytes approximately -61 mY. The average potential difference between nurse cells and attached oocytes was therefore on the order of 5 mY. One important difference between the medium used by Bohrmann et al. (1986b) (Robb's medium - Robb, 1969) and that used by Woodruff (1989) is K+ concentration: the K+ concentration for Robb's medium was 40 mM; for Sun and Wyman's medium it was 2.5 mM. The concentration of K+ in Drosophila blood has been measured at 25mM (Van Der Meer and Jaffe, 1983).

Electrophoretic redistribution of charged proteins has been observed only where voltage gradients have been detected. Bohrmann and Gutzeit (1987) were not able to show any asymmetry in distribution of native proteins with different isoelectric points. Sun and Wyman (1987) were unable to show differential diffusion of charged fluorochromes. However, Woodruff (1989) demonstrated migration of the negatively charged protein Lucifer Yellow CH according to what

one would expect in the electrophoretic fields he reported; furthermore, Fly and its methyl-carboxylated derivative McFly were also shown to electrophoretically redistribute themselves in the relatively weaker intracellular voltage gradient maintained in ovarioles incubated in modified Robb's medium (Woodruff et al., 1988).

The differences reported by these authors have yet to be reconciled, although a recent paper by Bohrmann (1991) clearly demonstrates that these differences are due, at least in part, to the differences in composition and osmolarity of the various recording solutions. Bohrmann (1991) evaluated the effects of several different culture media with respect to follicle development, RNA and protein synthesis, and K^+ uptake. Bohrmann (1991) demonstrated that external K^+ concentration and osmolarity had marked effects on K^+ uptake, and that the addition of pupal hemolymph from H. cecropia had deleterious effects on the morphology and development of Drosophila follicles. Bohrmann (1991) concluded, on the basis of *in vitro* development, RNA synthesis rates and protein patterns, that a completely defined chemical medium (R-14, designed by Robb, 1969) gave results closest to the *in vivo* situation. By comparison with medium R-14, Woodruff et al.'s (1988) culture medium was hypotonic and did not support *in vitro* development.

Despite criticisms as to the unphysiological nature of these recording solutions -- and implicitly of the existence of intracellular potential differences in Drosophila follicles -- several factors support the existence of such voltage

gradients. First, the reported oocyte membrane potential of -61 mV in lower K+ Ringers (2.5 mM) compares with -63.5 mV reported by Miyazaki and Hagiwara (1976) for unfertilized eggs in Ephrussi and Beadle's (1936) fly Ringer ([K+]=5mM). Second, the fact that Woodruff (1989) showed a doubling of the intracellular voltage gradient concurrent with an over two-fold increase in resting potential shows that, despite differences in external K+, the transbridge difference in potential is maintained in a consistent manner. Third, Verachtert (1988) also reported a 3 mV potential difference between nurse cells and oocytes in coupled measurements on vitellogenic Drosophila follicles in Robb's medium (n=7), although he was not able to show charge-dependent redistribution of Lucifer Yellow CH. Finally, there are morphological and physiological similarities between Drosophila and Hyalophora oocytes. Since intracellular voltage gradients and electrophoretic transport have been definitively shown in the latter, it is not unexpected that a similar phenomenon should exist in Drosophila eggs.

The current pattern around Sarcophaga ovarioles is generally similar to that described for Hyalophora and Drosophila'ovarioles: current generally enters the nurse cell compartment and leaves the oocyte, with maximal current densities reaching 20 jtAmp/crrr' (Verachtert, 1988). A noteworthy finding was that the transition from current influx to current efflux correlated with an alteration in the follicular epithelium from simple squamous over most of the tropharium to columnar over all of the oocyte and parts of the tropharium (depending on the stage of vitellogenesis). On the basis of a lack of dye coupling (and presumably

electrical coupling, although the two are not always synonymous) between follicle cells and the oocyte, Verachtert and DeLoof (1989) proposed a model in which current flow is divided into two loops: one loop is generated by the squamous epithelium and flows through the subepithelial space until it leaks out via spaces between the columnar epithelium. The second loop is thought to be generated by influx over the oocyte and efflux over the nurse cells. Verachtert and De Loof (1989) have suggested this model may incorporate the earlier model of Woodruff et al. (1986). A further analysis of these models will be presented in the discussion section in Chapter 1.

Intracellular potentials in nurse cells and oocytes of Sarcophaga varied according to stage and whether or not measurements were coupled (Verachtert, 1988). During one stage of vitellogenesis, however, a statistically significant potential gradient of 3 mV exists between nurse cells and oocytes (nurse cell negative). Lucifer Yellow pressure injected into either nurse cell or oocyte spread throughout the entire ovariole (Verachtert, 1988).

(ii) Telotrophic ovarioles

Telotrophic ovarioles are characteristic of polyphage coleopterans, hemipterans, and megalopterans (Telfer, 1975; Biining, 1978, 1979). Extracellular currents around telotrophic ovarioles have been examined in four insect species: Dysdercus intermedius (Dittmann et al., 1981); Rhodnius prolixus (Sigurdson and Huebner, 1984; Diehl-lones and Huebner, 1989a; this thesis); and Sialis velata and

Ips perturbatus (Sigurdson and Huebner, 1984). Before summarizing what is known about bioelectric properties in specific instances, it is important to review some of the salient morphological and physiological properties of the telotrophic ovarioles.

Similar to polytrophic ovarioles, telotrophic ovarioles exhibit a high degree of morphological and physiological polarization: in contrast, the endopolyploid nurse cells occupy lobes around a common, anterior syncytial chamber, the center of which is filled with microtubules surrounded by an F-actin mesh (Huebner and Anderson, 1972c). Long (up to 1 mm) microtubule-filled trophic cords are in cytoplasmic continuity with developing oocytes (Huebner and Anderson, 1972b,c; Telfer, 1975; Burring, 1979; Hyams and Stebbing, 1979a). The entire ovariole is encased by a somatic epithelium (Huebner and Anderson, 1972a) which is coupled to the germ cells via gap junctions during various stages of development (Huebner, 1981b).

In Rhodnius, oocyte growth is highly regulated: only one oocyte commences vitellogenesis in each ovariole, while subterminal oocytes remain arrested in previtellogenesis (Huebner and Anderson, 1972b; Pratt and Davey, 1972, Huebner, 1984b). After severance of the trophic cord to the terminal oocyte during mid vitellogenesis, the adjacent oocyte increases in size and enters vitellogenesis, implying a tightly regulated ovarian feedback mechanism (Pratt and Davey, 1972a,b; Huebner, 1981a, 1983). By comparison, telotrophic ovarioles of Dysdercus intermedius have multiple. vitellogenic follicles which lose their

trophic connections at the beginning of vitellogenesis (Dittmann et al., 1981). Huebner (1981a, 1983) has suggested that the T oocyte inhibits development of previtellogenic oocytes by means of the trophic cord.

The first description of transcellular ionic currents around a telotrophic ovariole was provided by Dittmann et al. (1981) working with Dysdercus intermedius. Two current loops were evident around intact ovarioles; one circuit consists of current efflux from the regions between vitellogenic follicles coupled to a current influx along the lateral surfaces of the oocytes. The second loop involves current efflux from the region of previtellogenic follicles to influx over the tropharium. Furthermore, a 4 mV potential difference between the tropharium and previtellogenic oocytes (tropharium negative), although the pattern of external currents does not correspond with the intracellular potential, and it is not known whether the external currents are a product of the germ cells, the follicular epithelium, or both.

Microinjection experiments analogous to those performed by Woodruff and Telfer (1980) revealed that negatively and positively charged proteins injected into the tropharium of D. intermedius ovarioles redistributed themselves according to the potential gradient, but the counter experiment wherein charged proteins were injected into previtellogenic oocytes did not show a functional polarization (Miinz and Dittmann, 1987). These workers also found that microinjected mitochondria aligned themselves along microtubules in the trophic core (Munz and Dittman, 1987) and are transported along trophic cords at rates corresponding to fast and

slow axonal transport, suggesting dual mechanisms for intraovarian transport, both electrophoretic and microtubule-based.

Three other types of telotrophic ovarioles have been examined electrophysiologically: those of the elm bark beetle Ips pertubatus, the megalopteran Sialis velata, and the hemipteran Rhodnius prolixus (see Huebner and Sigurdson, 1986). Differences in the current pattern around these ovarioles will be reviewed in more detail in chapter one. With respect to R. prolixus, a dynamic pattern of transcellular ionic currents has been demonstrated around intact ovarioles (Sigurdson, 1984; Huebner and Sigurdson, 1986) and an intracellular voltage gradient has been detected between the tropharium and early vitellogenic oocytes (Huebner, Woodruff, and Telfer, unpublished data). As will be addressed later in this thesis, a juvenile hormone analogue alters the external current pattern (Sigurdson, 1984) and increases the magnitude of the voltage gradient (unpublished results, see Telfer et al., 1981b). Telfer et al. (1981b) have also shown charge-dependent migration of microinjected proteins, and Diehl-lones and Huebner (1989b) have demonstrated unidirectional transport of charged latex beads. Moreover, the exciting finding by O'Donnell (1985) that $Ca^{+2\text{-driven}}$ action potentials are generated by the oolemma has interesting implications with respect to the possible role of Ca^{+2} as an intracellular signal, as does the observation that cyclic AMP modulates this excitability (O'Donnell and Singh, 1988).

Based on these background data it is apparent that a correlation exists between the electrical properties of Rhodnius ovarioles and oogenesis, and it has

been speculated that such electrophysiological properties could be related to nurse cell-oocyte transport, germ cell differentiation, and/or intraovariole regulatory feedback (Huebner and Sigurdson, 1986; Sigurdson, 1984; Telfer et al., 1981b). The existence of any causal relationships between the electrophysiological properties of Rhodnius ovarioles and oogenesis has yet to be established, and much basic information regarding the origin and ionic basis of the extracellular current pattern has hitherto been lacking.

OBJECTIVES OF THIS THESIS

It is clear from previous studies that transcellular ionic currents are, at the very least, correlated with developmental events. Before the exact role of these currents may be discerned, the complete circuit pathways, the identities of the ionic species, and their mechanisms of crossing the cell membrane must be known. Armed with this information, it should be possible to experimentally manipulate a developing system and determine the developmental significance of transcellular currents. Within this framework, my thesis is divided into four chapters with the following objectives:

In chapter one, the aim is to more fully delineate the pattern of transcellular currents and their origines). The previous findings of Sigurdson

(1984) are extended to show a three dimensional map of the transcellular current pattern around Rhodnius prolixus ovarioles. I also present data on experimentally denuded ovarioles in an attempt to determine the origin of the ionic currents.

The focus in chapter two is on determining the identity of the current-carrying ions via ion substitution and inhibitor experiments. Previous work (Diehl-Jones and Huebner, 1989a) indicates that several ionic species are involved in generating transcellular currents, and refined experimental protocols imply major roles for an electrogenic Na" pump and Na"/Ca^{+2} influx.

In chapter three I establish a link between Na" flux and a dynamic cellular process, fluid phase endocytosis, using the marker Lucifer Yellow CH. Finally, in chapter four I present a preliminary experiment (previously published in abstract form) demonstrating unidirectional movement of charged fluorescent latex beads.

GENERAL MATERIALS AND METHODS

Insects

Rhodnius prolixus (Stahl) were maintained at constant temperature (27C) and relative humidity (70%) in jars containing strips of Whatman"

chromatography paper. Insects were fed blood meals on female New Zealand white rabbits as previously described (Huebner and Anderson, 1972a). Ovarioles of adult R. prolixus were dissected in a modified Rhodnius Ringers (O'Donnell, 1985) and desheathed immediately prior to each experiment. The modified Ringers was used in preference to Madrell's (1969) Ringers because ovarioles appeared healthier for a longer period of time and it reduced fouling of the vibrating probe tip. Ovarioles were not used after 1 hour post dissection, and obviously damaged or atretic follicles were discarded, except where otherwise indicated.

Ovarioles were divided into 9 different size classes based on terminal oocyte (T oocyte) length, starting at 300-400 urn (previtellogenic, size class 1) and increasing in 100 urn increments until late vitellogenic-chorionating stages (1500-2000 urn, size class 9) (see Pratt and Davey, 1972a). T oocyte length was measured on a video screen which had been calibrated to account for screen curvature and geometric distortion (Inoue, 1986).

Recording Chamber

A custom-built recording chamber based partly on a design by A. Shipley and E. Bowdan was used for all experiments except for tetrodotoxin trials. It consisted of a lower specimen chamber and an upper fluid reservoir (see Appendix, Fig. 2a). A fluid intake port in the lower chamber and a suction port in the upper chamber permitted either constant fluid exchange via a gravity feed

or rapid fluid exchange via a push-pull syringe system.

Platinum-blacked reference and ground electrodes were permanently incorporated into the recording chamber, thereby eliminating the need for a second, bimorph-mounted reference electrode and enabling calibration of the vibrating probe in the recording chamber. An auxiliary opening in the specimen chamber permitted introduction of a suction pipette which was used in some experiments for holding ovarioles by the pedicel (see Appendix, Fig. 2a). Fluid temperature was monitored via a Sensortek" thermocouple probe, and the entire chamber assembly attached to a plexiglass gliding stage on a Zeiss IM35 inverted phase contrast microscope. The microscope and probe manipulator assembly rested on a vibration-free table (Micro-G) and was enclosed by a wire-mesh Faraday cage (Appendix, Fig. 1).

Yibrating Probe

Two-dimensional vibrating probe measurements were made with equipment purchased from the Vibrating Probe Company, (Davis, California). This consisted of a low noise differential FET preamplifier (gain=10) connected to a two phase lock-in amplifier (Model NR 2000). Lock-in outputs were digitized with a labmaster analog-digital converter (Tekmar Co., Solon, Ohio), and were analyzed by an IBM PCXT computer. Video images were recorded with an AG-6050 Panasonic time-lapse video recorder. In-phase and quadrature outputs were monitored on a dual channel Tektronix 2205 oscilloscope. A glass current-

injecting microelectrode driven by a WPI iontophoresis module (model no. S-7061A) was used as a known current source for probe calibration. Resistivities of media were obtained by calculating the inverse of the conductivity values given by a conductivity meter (Electromark Analyzer, Markson Science Inc., Del Mar, CA.).

Several modifications to the original apparatus significantly improved the noise characteristics of the probe. Original gold-plated wire socket connectors were replaced with gold plated R30/c socket pins (Vector Electronics, Sylmar, CA.). These provided a much more mechanically stable connection between the vibrating probe and the bimorph. The original reference electrode arrangement was replaced with a permanently installed reference wire, and a 66Ω signal terminator on the probe input eliminated internally-reflected voltage spikes from the coaxial signal cable. Finally, extensive grounding of equipment and metal fittings via a common grounding bus further reduced noise.

Vibrating probe measurements were typically carried-out with 30 μm platinum-tipped electrodes vibrated between 650-750 Hz at a time constant of 0.3 sec, except where otherwise indicated. Reference values relative to ground were collected by taking measurements well away from potential current sources; this procedure was repeated at least once every 30 sec, and actual measurements were performed only if in-phase and quadrature reference values were less than 0.5 p.Amp/ em'. Probe phase and accuracy were checked according to a known current, and all probes were checked for barrier artifact.

Each current measurement consisted of X (in-phase) and Y (quadrature) components. Bowdan and Kunkel (1990) report that, for two-dimensional current measurements around Blatella germanica oocytes, the Y current component (L) is a more accurate measurement of current normal to the oocyte surface than the X component (I_x) or the integrated, total current (I_t) values. The external geometry of Rhodnius ovarioles is markedly more complex than that of B. germanica oocytes; therefore, it could not be assumed that I_y was always most normal to the ovariole surface except over the middle of mid to late vitellogenic T follicles (recording positions 4-7, see Chapter 1). As a result, I, values were accepted as the most accurate measure of current over the ovariole except at the locations above, where I, was clearly most normal to the surface. Due to an inherent mechanical instability of the bender design, spectacular errors in current magnitude and even direction could be generated if the probe was positioned slightly above or below the most vertical plane normal to the cell surface; consequently, great care was taken to insure correct vertical positioning of the probe. Both positive and negative ions can carry current, and to avoid confusion the following conventions are adopted: inward current refers to either cation influx or anion efflux; outward current refers to either cation efflux or anion influx (see Nuccitelli and Jaffe, 1976). For example, a current influx can be carried either by an influx of Na" ions or an efflux of C1 ions.

CHAPTER I

IONIC CURRENTS AROUND INTACT AND DENUDED *Rhodnius prolixus* OVARIOLES

INTRODUCTION

A central problem in developmental biology concerns the mechanisms by which pattern formation occurs (Jaffe and Woodruff, 1979), and within this framework is the question as to how tissues and cells differentiate and polarize. One of the most striking examples of developmental polarity is found in the insect meroistic ovariole: in this system, two divergent cell types -- nurse cells and oocytes -- maintain a high degree of structural and functional polarity despite sharing a common cytoplasm (Telfer et al., 1981b). This characteristic is in marked contrast to the normally lock-step, synchronous behaviour of other syncytia such as insect and mammalian male germ cells (Fawcett et al., 1959; King and Akai, 1971) or of other ovarian systems (Franchi and Mandl, 1962; Zamboni and Condos, 1967).

The telotrophic ovariole is a meroistic sub-type, and its structural polarization has already been described (Huebner and Anderson, 1972a,b,c). Briefly, endopolyploid nurse cells are located in a common, multi-lobed

tropharium, and are in cytoplasmic continuity with all oocytes via long (up to 1 mm), microtubule-filled trophic cords (Huebner, 1981a; Huebner and Anderson, 1972c; Buning, 1979). This polarization leads to significant physiological dependence of the oocyte on the nurse cells. The oocyte germinal vesicle does not manufacture RNA (Davenport, 1974; Vanderburg, 1963), and may even repress expression of ribosomal DNA (Telfer, 1975). Most biosynthetic activities are performed by the nurse cells, which produce various organelles, proteins, and nucleotides for the oocyte (Huebner and Anderson, 1970; Davenport, 1974; Telfer, 1975; Hyams and Stebbings, 1977; Capco and Jeffery, 1979). All of these materials are transported to the oocyte via the trophic cords. Furthermore, in Rhodnius only one oocyte per ovariole is in vitellogenesis at anyone time, while the remaining oocytes are arrested during previtellogenesis (Huebner and Anderson, 1972b; Pratt and Davey, 1972c). This unique structural/functional polarization lends itself well to the question as to how private or semiprivate compartments can be maintained within a common cytoplasmic milieu (Telfer et al., 1981b), and to examining mechanisms of intraovariole regulatory feedback and cytoplasmic transport (Huebner, 1981a, 1983; Telfer et al., 1981b; Sigurdson, 1984).

Possible effectors of these processes include the inherent electrical polarity of Rhodnius ovarioles. A 10 mV electropotential difference exists between the tropharium and the terminal oocyte (Huebner and Woodruff, unpublished results), and related to this phenomenon, microinjected basic proteins show restricted movement within the tropharium (Telfer et al., 1981b). These

phenomena are analogous to the situation in the polytrophic Hyalophora cecropia ovariole (Woodruff and Telfer, 1980). In addition, a dynamic pattern of extracellular currents has been described around Rhodnius ovarioles, and this generally corresponds to certain stages of oogenesis (Huebner and Sigurdson, 1986; Sigurdson, 1984). Briefly, this current pattern consists of current effluxes from the base, apexand connective of the T follicle, and current influx over the tropharium. Sigurdson (1984) has shown that the overall current density increases over the course of vitellogenesis', and that the current pattern over the previtellogenic region was variable as to direction and magnitude, depending on the stage of vitellogenesis.

Before any definitive links between the extracellular current pattern and ovariole physiology can be made, several properties of these currents must still be delineated. First, previous work has concentrated on changes in current direction and magnitude only along the longitudinal axis; work by Kunkel (1986) and Bowdan and Kunkel (1990) on the panoistic ovariole Blatella germanica has shown an obvious dorsal-ventral axis which correlates with the future site of embryo formation. While there are no clear markers of a dorsal-ventral axis in Rhodnius ovarioles, it is nonetheless worthwhile to determine if there are any lateral extracellular current axes. As stated by Bohrmann et al. (1986a), "... current patterns from the whole follicle cannot be determined from measurements in one plane of the follicle." Additionally, it is of interest to compare the results from the present study which used a two-dimensional vibrating probe and

modified Rhodnius Ringers (O'Donnell, 1985) with the results from Sigurdson's (1984) work which used a one-dimensional vibrating probe.

Secondly, panoistic and meroistic insect ovarioles are covered by a layer of follicular epithelial cells, and it has not previously been shown whether the extracellular current pattern is a property of germ cells, follicle cells, or both. The actual sitets) of current generation and the current pathways are of obvious interest, particularly in terms of resolving the apparent anomaly between the current influx over the tropharium and its relative electronegativity. Since Woodruff et al. (1986) have demonstrated that follicle cells around the trophic region of Hyalophora follicles mask current efflux from naked nurse cells, it is obviously important to. determine if a 'similar situation exists in Rhodnius ovarioles.

The purpose of this work is to further analyze the current pattern around intact Rhodnius ovarioles, and to evaluate extracellular current pattern around ovarioles in which the follicular epithelium has been removed (denuded). New findings include data which demonstrates that lateral asymmetries exist around intact ovarioles, particularly around the T follicle. As well, I found that the extracellular current pattern is largely reflected by a similar, although weaker pattern of currents over the germ cell membranes. Finally, I demonstrate that current enters previtellogenic oocytes, whereas the mean current direction over subterminal oocytes entering vitellogenesis is outward.

MATERIALS AND METHODS

Tissue

Rhodnius prolixus (Stahl) were reared as previously described (see General Materials and Methods); ovarioles were carefully dissected into modified Rhodnius Ringers (O'Donnell, 1985) and the ovariole sheath removed immediately prior to each experiment. Ovarioles may be classified according to stage of vitellogenesis on the basis of terminal (T) follicle size (Pratt and Davey, 1972a). For the purposes of comparing extracellular current patterns, ovarioles from 9 different size classes were examined with the vibrating probe, starting with previtellogenic ovarioles in size class 1 (T follicle length=300-400 urn) and increasing in 100 μm increments until size classes 8 and 9 (late vitellogenic, T follicle length=1000-1500 and 1500-2000 μm respectively). T follicle length was measured on a video screen which had been calibrated to account for screen curvature and geometric distortion (Inoue, 1986).

Twenty positions along the length of the ovariole were chosen for current measurements on the basis of easily recognizable morphological landmarks (Fig. 1). Measurements were also made at 4 circumferential or radial locations at each position. This was accomplished by attaching a suction pipette to the pedicel at the base of each follicle and by placing a glass weight on the terminal filament. After probe measurements were made along one side of an ovariole, it was

rotated 90° on the longitudinal axis and the same measurements were repeated. A consistent reference point was the trophic cord to the T oocyte; the 0° position refers to the trophic cord facing up in a recording chamber, with the vibrating probe positioned on the left side of the -ovariole with respect to the anterior-posterior axis. Subsequent positions refer to the sides of the ovariole as it is rotated 90, 180, and .270° counterclockwise, the 90° position being the side with the trophic cord closest to the vibrating probe By convention, I refer to each such side as a 'quadrant', from 0 to 270. When the trophic cord to the T oocyte had detached and retracted in mid- to late vitellogenic ovarioles, I used the trophic cord to the T-l oocyte as a reference point. Fresh Ringers solution was perfused through the recording chamber each time an ovariole was rotated, or approximately every 5 minutes.

Denuded Ooarioles

In an effort to determine the origin of the extracellular currents, the basal lamina and surrounding epithelium were removed in the following manner. Ovarioles were washed in Ca'<free Rhodnius Ringers with 2 mM EGTA (ethyleneglycol-bis-If-aminoethyl ether) tetraacetic acid) for 15 min, then briefly exposed to 0.5% trypsin (Type ill, Sigma Chemical Co.). When the basal lamina appeared to blister, the ovariole was removed from the trypsin-containing Ringers, gently washed in $Ca^{+2\text{-free}}$ Ringers and then adhered to an acid-washed piece of glass slide which had been coated with 1% high molecular weight poly-L-

lysine (Sigma Chemical Co.), The basal lamina was torn with sharpened tungsten needles, and patches of the ovariole gently "defolliculated" by rolling it over the coated surface.

Recording locations over denuded patches of the T follicles were classified as being either basal, mid, or apical, since it was difficult to assign discrete positions. Likewise, locations measured over the tropharium were regarded as either basal, extending h.alfway from the most basal nurse cell to the most apical nurse cell, or were regarded as apical, extending halfway from the most apical nurse cell to the most basal nurse cell. Damage to the denuded germ cells was evidenced by either a large current influx (25-35 μA/em") at the site of injury or by a current efflux of similar magnitude over adjacent areas. Such injury currents could be elicited by poking the ovariole with a sharpened tungsten needle or by even gentle contact between the vibrating probe and denuded patches of germ cell membrane. Ovarioles exhibiting extracellular currents in this range were therefore discarded. It was found that injury could best be avoided by removing only portions of the follicular epithelium, so most measurements reflect currents over isolated patches of cell membrane. Current measurements were made 30 min post-dissection. One representative measurement was taken from each location. If both current efflux and influx were observed within the same area, neither reading was used. Current measurements were also rejected if the current decayed within 1 hour post-dissection.

Recording Chamber

A custom-built recording chamber based partly on a design by A. Shipley and E. Bowdan (Marine Biological Laboratories, Woods Hole, Mass.) was used for all experiments except for tetrodotoxin trials. The chamber consisted of a lower specimen chamber and an upper fluid reservoir (see Appendix, Fig. 2a). A fluid intake port in the lower compartment and a suction port in the upper compartment permitted either consistent fluid exchange via gravity feed or rapid fluid exchange via a push-pull syringe system.

Platinum-blacked reference and ground electrode were permanently incorporated into the recording chamber, thereby eliminating the need for a second, bimorph-mounted reference electrode and enabling calibration of the vibrating probe in the recording chamber. An auxiliary opening in the specimen chamber permitted introduction of a suction pipette which was used for holding ovarioles by the pedicel. Fluid temperature was monitored with a Sensortek" thermocouple probe, and the entire assembly attached to a plexiglass gliding stage on a Zeiss IM35 inverted phase contrast microscope. The microscope and probe manipulator assembly rested on a vibration-free table (Micro-C. Inc.) and was enclosed in a wire-mesh Faraday cage (see Appendix, Fig. 1).

Current Measurements

Extracellular currents were measured with a two-dimensional vibrating probe purchased from the Vibrating Probe Company (Davis, CA). Technical aspects of the probe design, construction, and operation are described in the General Materials and Methods and Appendix. Briefly, the probe tip consisted of a gold and platinum 30 urn diameter sphere; the probe was usually vibrated at a frequency of 650-700 Hz and an amplitude of 25-30 urn. The probe was routinely calibrated and checked for artifact before each experiment and was periodically checked for capacitance and recalibrated. Probe data were plotted with the Axum Graphics program (Trimetrix, Inc., Seattle, WA) and analyzed on an IBM AT PC with Instat statistical software (Graphpad Inc., San Diego). Statistically-significant differences between different circumferential locations at each position were determined with a one-way analysis of variance. Means were considered statistically significantly different when $P<0.05$ and marginally significant when $0.1>P>0.05$). Since a limited number of comparison were made, P values were corrected with the Bonferroni post-test (Kleinbaum et al., 1988) to avoid Type 1 errors. Conventions regarding current measurement are indicated in the General Materials and Methods; current entering an ovariole is designated as negative, whereas current efflux is designated as positive. Since Sigurdson (1984) thoroughly analyzed changes in current pattern between different positions along the ovariole and between the same position over different size classes, the

analysis in the present study is for the most part restricted to an analysis of differences between circumferential locations at each position.

RESULTS

Intact Ovarioles

At least two current circuits were evident in all size classes: current efflux from the base and apex of the T follicle returned via current influx over the middle of the T follicle, and current efflux from the T connective returned via influx of the tropharium (Figs. 2-10). Current efflux over the apex of the T follicle and the T connective are significantly elevated over vitellogenic oocytes (class 3, Fig. 4), remain significantly elevated during vitellogenesis, then decrease significantly in late vitellogenic-chorionating oocytes (Class 9, Fig. 10). However, there are some notable differences which will be indicated in each size class.

Class 1

Maximal current efflux in class 1 (previtellogenic) ovarioles (T follicle length=300-400 um) occurred at the T connective (position 10) over all four axes, with the greatest current density at the 270° quadrant (4.90 ± 1.17 μA/em', Fig. 3). Mean current influx was greatest over the middle of the T follicle. Current magnitude and direction were highly variable over positions 11-15, and are

evident in the spline plot of mean current densities (Fig. 2). However, axial differences are statistically significant only at position 14, between quadrants 1 and 180, where current direction reverses from 1.76 ± 0.79 μA/crrr' to -0.68 ± 0.63 μA/crrr', respectively (p=0.028). Current reversals at all other locations were not significant (N=9).

Class 2

Current magnitude increased noticeably, but not significantly, around class 2 (late previtellogenic to early vitellogenic) ovarioles (T follicle length=400-500 urn). Maximal mean current efflux occurred over the T connective (mean current densities from 6.36 ± 1.72 to 7.91 ± 2.60 μA/crrr), whereas maximal current influx occurred over positions 11 and 12, the approximate locations of the T-1 and T-2 oocytes (Fig. 3). Axial variations in current direction were especially evident over the base and middle of the T follicle and also over the previtellogenic region. These differences were significant at positions 2,4, and 13. At position 2, current influx over quadrant 1 (-1.40 ± 1.04 μA/crrr) was significantly different from efflux at quadrant 180 (1.60 ± 0.70 μA/crrr'; P=0.034) and marginally significantly different from efflux at quadrants 90 (P=0.050) and 270 (P=O.064). At position 4, current efflux at quadrant 90 (0.80 ± 0.10 μA/crrr') was significantly different from influx at quadrant 0 (-1.25 ± 0.10; P<O.OOl), but not significantly different from the other quadrants (N=7).. At position 13, differences were marginally significant between quadrants 1 and 180 (P=0.090).

Class 3

Early vitellogenic ovarioles in class 3 (T follicle length=500-600 um) showed some axial variations in current density, particularly at the apex of the T oocyte (position 8 and 9), and current reverses at position 2, quadrant 180; this reversal was significantly different from current efflux at the same position, quadrant 270 (P=0.006; Fig. 4). Radial differences at other recording positions were not significantly different. Corresponding increases in current influx were apparent over much of the T follicle, and little variation was apparent over the previtellogenic region (positions 11-14; see spline plot, Fig. 4).

Class 4

Vitellogenic ovarioles in class 4 (T follicle length=600-700 urn) exhibited great variation in radial current patterns. Statistically significant differences were measured at positions 2, 7, and 10, and marginally significant differences were noted at position 9 (Fig. 5). Current efflux at position 2, quadrant 0 was significantly different from current influx at quadrant 180 (P=0.042). Current efflux at position 7, quadrant 0, was significantly different from current influx at quadrant 180 (P=0.003), and marginally significantly different from quadrant 90 (P=0.065) but not significantly different from current efflux at quadrant 270. Current efflux at quadrant 270 was significantly different from influx at quadrant 180 (P=0.004). Current efflux at position 10, quadrant 0 (5.71 ± 1.14 μA/crrr') was

significantly lower than at quadrants 180 (P=O.021) and 270 (P=O.028). Current efflux at position 9, quadrant 0, is marginally significantly lower than at position 9, quadrant 90 (P=0.092). The obvious current efflux at position 4, quadrant 0 (1.59 ± 3.18 μA/crrr)$_r$ was not statistically different from the other quadrants (N=2). Differences between quadrants at other positions were not statistically significant.

Class 5

In contrast to the" previous size class, class 5 ovarioles (T follicle length= 700-800 urn) had relatively less variation in radial current direction (Fig. 6). Current efflux at position II, quadrant 180, was opposite to but not significantly different from current influx observed at other quadrants over position 11. Current direction was consistent over all other quadrants at other positions; however, current efflux at positions 8 and 9, quadrant 0, were marginally lower than at the same position at quadrant 90 (P=0.010), and quadrant 270 (P=0.025). Current efflux at position 10, quadrant 0, were marginally lower than current efflux at position 10, quadrant 90 (P=0.054).

Class 6

Overall current patterns in class 6 (T follicle length=800-900 urn) were similar to that of ovarioles in class 5, although current efflux at positions 8, 9, and 10 were not significantly different (Fig. 7). Fluctuations in current direction at position 7 (influx over quadrants 90 and 180, efflux over quadrants 0 and 270)

were variable and marginally significantly different between quadrants 180 and 270 (P=0.071).

Class 7

Mid-vitellogenic ovarioles (T follicle length=900-1000 μm) which comprised class 7 had radial current patterns which varied at positions 2, 3, 4, and 6. At position 2, current efflux was evident over quadrants 90 and 270; influx was measured over the other quadrants (Fig. 8). At position 3, current exited over quadrant 270, whereas current entered over the other quadrants. Similarly, weak current efflux was measured at position 4, quadrant 0, while current influx was found over the remaining quadrants. Finally, current efflux was measured over all quadrants at position 6, except for quadrant 270 where current efflux was observed. None of these differences were statistically significant. N=S at all other locations except for position 7 (N=3).

Class 8

By class 8 (T follicle length=1000-lS00 μm), the trophic cord to the T follicle has severed its connection. This coincides with large increases in current efflux (26.59 ± 1.84 μA/crrr) at position 7, quadrant 0 (Fig. 9). This is significantly different from current influx measured over quadrant 270 (P=0.023) but the difference is not significant between quadrants 0 and quadrants 90 and 180 (N=2). Current direction over positions 2 to 7 on the T follicle was quite variable, but

these differences are not statistically different. Current at position 15 on the tropharium consists of an efflux over all quadrants except quadrant 90; none of these differences, however, was significant. The radial current pattern over positions 11 to 13 (previtellogenic region) was highly variable, but none of these differences were significant.

Class 9

Late vitellogenic ovarioles (T follicle length=1500-2000 um) had markedly lower current densities over the apex of the T follicle and T connective (positions 8-10) than the same locations in the previous size class, and these decreases were statistically significant between the same and different quadrants at corresponding positions ($P<0.05$; Figs. 10 and 11). Radial variations in current density over the T oocyte are evident in the spline plot of mean current density around class 9 ovarioles (Fig. 10), but these were not significantly different. Likewise, slight variations in current density and direction over the rest of size class 9 ovarioles were not significant. Current efflux was consistent over all quadrants at position 11, when the T-1 oocyte is beginning early vitellogenesis. Current direction at position 11 in the preceding size class was variable; at quadrant 1, current influx is -4.22 (± 2.94) μA/crrr', and this was marginally significantly different from current efflux (1.83 ± 0.45 μA/crrr) over the same position and quadrant in size class 9 ($P=0.08$). Other differences between size classes 8 and 9 were not significant.

Denuded Ovarioles

Extracellular current direction and magnitude around denuded patches of ovarioles are reported in Fig. 11; selected video still frames of partially denuded ovarioles are presented in Figs. 12a-c, 13a-d, and 14a,b.

Regions of weak current efflux were evident over the base of early, mid, and late vitellogenic ovarioles. Current at the base of only 1 late vitellogenic ovariole was measured due to the fragility of large terminal oocytes at this stage. Current efflux at the base of early vitellogenic ovarioles did not differ significantly from current efflux at the base of mid-vitellogenic ovarioles. Weak current efflux was evident over the middle of early vitellogenic oocytes ($0.27 \pm 0.85\ \mu A/crrr$): by contrast, current influx occurred over the middle of mid- and late vitellogenic oocytes, and is strongest ($12.40 \pm 5.25\ \mu A/crrr$) over the latter. Differences were significant only between early and late vitellogenic ovarioles ($P=0.003$).

The apices of early, mid-, and late vitellogenic oocytes all had patches of current efflux (Fig. 12c). Current efflux is strongest over the apex of late vitellogenic oocytes ($4.85 \pm 1.67 \mu A/cm^2$), but no significant differences existed between early, middle, and late stages of v,itellogenesis. Regions of current efflux were also detected over the trophic cord to the terminal oocytes in early and mid-vitellogenesis, although these were quite variable. Current vectors were usually directed towards the T oocyte (Fig. 13c); however, angular errors may have been induced by positioning the vibrating probe slightly above or below the plane tangent to the surface being measured (see General Materials and Methods).

Since the margin for error is much smaller when measuring a narrow structure such as the trophic cord, this result should be viewed with caution.

A remarkable finding concerned the current direction over denuded T-l oocytes. Extracellular current over T-l oocytes in early vitellogenic follicles were directed inwards, averaging -3.62 ± 1.81 μA/em' (Fig. 13a); current influx was also observed over denuded T-l oocytes in mid-vitellogenic ovarioles, averaging 2.02 ± 0.71 $\mu A/cm^2$ (Fig. 13b). However, denuded T-l oocytes from late vitellogenic follicles exhibited patches of current efflux (2.99 ± 1.09 $\mu A/cm^2$; Fig. 12a,b). This roughly corresponded with the current patterns observed around the same areas over intact follicles; current influx were usually measured at position 11 on ovarioles from classes 2, 6, and 7 (Figs. 3, 7, and 8, respectively), and current efflux was consistently measured over class 9 ovarioles (Fig. 10). These differences were statistically significant between early and late vitellogenic oocytes ($P=0.006$) and between mid- and late vitellogenic oocytes ($P<O.OOl$).

Extracellular current flowed outwards over denuded trophic cords connected to T-l oocytes (Fig. 13c). Current vectors were usually directed away from the T-l oocyte in early and mid-vitellogenic ovarioles, and towards the T-l oocyte in late vitellogenic ovarioles, although the same restriction noted above also applied to these measurements.

Current influx is obvious over patches of denuded T-2 oocytes at all stages of vitellogenesis (Fig. 13d). Three trophic cords connected to T-2 oocytes were also measured for extracellular currents. Both cords measured in mid-vitellogenic

ovarioles exhibit tangential current efflux, whereas the single T-2 trophic cord measured in a late vitellogenic oocyte had a tangential current influx. A limitation in all of these measurements was the proximity of the T-2 cords to the base of the tropharium.

The basal portions of denuded tropharia in all three stages of vitellogenic oocytes had mean positive or outward currents, and the apical portions of tropharia had mean negative or inward currents (Figs. 14a,b). Mean current efflux over tropharia of early vitellogenic oocytes was not significantly different from the mean current efflux over the apical portions of tropharia in the same size class (P=O.34). This was mainly due to the weak and variable nature of apical currents (-0.62 ± 1.00 $\mu A/cm^2$). However, basal current efflux and apical current influx were significantly different in mid- (P=0.027) and late (P=0.015) vitellogenic ovarioles. A summary of the current patterns over denuded early, mid-, and late vitellogenic ovarioles is depicted in Fig, 15.

DISCUSSION

Radial Asymmetries

A primary, novel finding of this study is that radial asymmetries exist in the extracellular current pattern around a meroistic ovariole. These asymmetries are statistically significant in previtellogenic (class 1), early and mid-vitellogenic

(classes 2, 4, and 5) and late vitellogenic (class 8) stages of development. Previtellogenic ovarioles are the only group to have statistically significant radial differences over the prefollicular region; all other significant asymmetries occur over the T follicle.

The present study extends and is in general agreement with the Sigurdson (1984) study, although it is worthwhile to note some of the exceptions. Sigurdson (1984) reported current efflux over the lateral aspects of the T follicle of stage 4 ovarioles, whereas I found that current generally entered the T follicle at positions 2 - 7. Over size class 6 ovarioles, Sigurdson reported current efflux at positions 11 and 12, while I consistently found current influx at all quadrants over these positions. In both the latter study and the present one, current efflux from the base and apex of the T follicle return via current influx over the middle of the T follicle, and current efflux at the T connective completes a circuit via current influx over the tropharium. Since efflux at the T connective is sometimes directed anteriorly toward the tropharium, part of the return circuit is probably by way of the tropharium. The increase in current efflux as ovarioles enter vitellogenesis and the subsequent decline in current density in very late vitellogenic ovarioles is also very consistent between both studies. A novel finding in the present study is that the area of current influx over the T follicle is more extensive than previously believed; this was uncovered by measuring current densities over a more extensive area of the T follicle. The importance of this result is that it demonstrates that a general balance exists between total current influx and efflux.

Discrepancies noted between the two studies may be attributable to several different factors. First, different salines are used in the two studies. The modified Rhodnius Ringers used in the present work omits HCO_3^- and HPO_4^{-2} ions (see Table I, Chapter Two), and this may either alter or abolish specific ion activities or conductances. It is unlikely that any substantial currents are carried by these ions, since the general direction and magnitude of transcellular currents are very similar in both Sigurdson (1984) and the present study. Second, it is technically difficult to position the one-dimensional vibrating probe exactly perpendicular to the surface at all positions over the ovariole. Minute deviations in placement of the probe can result in stronger tangential currents from adjacent areas of the ovariole masking currents over the actual site being measured. This problem is especially evident over the T-l follicle, which is immediately adjacent to strong current efflux emanating from the apex of the T follicle and the T connective. Inherent advantages of the two-dimensional vibrating probe include the fact that it is easier to position and, regardless of the orientation of the probe, one may select L, I_y, or I_t vectors, to separate smaller current influx or efflux from larger tangential currents.

It must be reiterated that the morphological reference point for current measurements around the axis of Rhodnius ovarioles is the trophic cord. As such, the trophic cord may in fact not be indicative of more definitive ovariole axes, and other electrical and/or physiological axes may exist but are not discernible. In several instances, currents enter one side of the T follicle or

tropharium and exit via the opposite side of the ovariole; these phenomena cannot be consistently ascribed to any known axis and are obscured in the pooled, averaged data. It is noteworthy that Kunkel (1986) and Bowdan and Kunkel (1990) have reported a dorsal-ventral polarity in Blatella oocytes which have morphologically distinguishable axes. Rhodnius oocytes do not present any distinguishable morphological axes. An alternative marker is the germinal vesicle, such has been used in electrophysiological measurements of Locusta ovarioles (Verachtert, 1988). However, yolk spheres in vitellogenic Rhodnius ovarioles greatly obscure the germinal vesicle; furthermore, the germinal vesicle is usually centrally located in sub-terminal oocytes during early and mid-vitellogenesis.

One possible solution to this problem may be to look for oolemmal or ooplasmic markers. There is precedence for the existence of discrete ooplasmic domains in insect eggs: RNA and protein-rich polar granules are localized in the cortical layer of the posterior pole of Drosophila eggs (Mahowald, 1971; Hay et al., 1988). Thus far, no analogous structures are apparent in Rhodnius oocytes. The discovery of such elements in Rhodnius oocytes and a means by which to visualize them would yield another valuable positional marker and would obviously have broader developmental implications.

Based on the marker chosen, there are no conspicuous electrical polarities which suggest an obvious dorso-ventral axis in Rhodnius ovarioles. This does not preclude the existence of such axes around Rhodnius ovarioles. The asymmetries which are evident imply there are at least subtle electrical polarities

associated with different developmental stages. The longitudinal pattern of transition from current influx to current efflux at the apex of the T follicle, for example, may be physiologically significant with respect to the oocyte cortical cytoskeleton which changes dramatically at this location (Graham and Huebner, unpublished data). Along this line, one can speculate that current asymmetries may relate to localization of mRNA.

It is well known that during early development several classes of mRNA transcripts are localized to either the animal or vegetal poles of Xenopus oocytes (King and Barklis, 1985; Weeks and Melton, 1987). Such mRNA species may either themselves be determinants or may encode proteins that are determinants of embryonic polarity. One mRNA has a particularly clear asymmetrical distribution; this is the Vg1 transcript localized to a crescent in the cortex of full grown Xenopus oocytes (Melton, 1987). The Vgl transcript translocates to the vegetal hemisphere in a manner similar to that of yolk platelet translocation (Browder et al., 1991), although the precise mechanism is obscure. It is clear, however, that Vg1 RNA movement and anchorage in the cortex depends on the cytoskeleton: microtubule inhibitors block Vg1 translocation, and cytochalasin B, a microfilament inhibitor, prevents anchorage (Yisraeli et al., 1990). Furthermore, the Vg1 transcript delocalizes in the unfertilized egg (Yisraeli and Melton, 1988), as do a variety of other mRNA species (see Browder et al., 1991). A clue as to one of the factors involved in transcript delocalization is provided by Larabell and Capco (1988); these authors implicate Ca^{+2} influx in the delocalization of PolyrA)"

mRNA and tubulin mRNA in Xenopus oocytes.

A role for ionic currents in general and current asymmetries in particular as effectors or modifiers of mRNA translocation and/or localization is appealing. Cytoplasmic Ca^{+2} and pH influence the cytoskeleton (see General Introduction and Literature Survey), and localized ion fluxes may influence the cytoskeleton and ultimately the location of message transcripts. Additionally, transmembrane currents may mediate mRNA localization by influencing factors binding mRNA to the cytoskeleton, or by exerting an effect other than via the cytoskeleton. For example, the net negative charge of mRNA could enable electrophoretic redistribution within the ovariole towards areas of positive current influx such as the current entry sites over the tropharium or lateral aspects of the T oocyte. Variations in the extracellular current patterns may influence mRNA localization via any of the mechanisms suggested above. Finally, local variations in the intracellular ionic environment may regulate transcription of message transcripts and the concentration of specific proteins in these regions.

Certainly, we are far from being able to show any such correlations in Rhodnius. We do not presently know if or where either polyrA)" or specific mRNA transcripts are localized in Rhodnius germ tissue, although work in our lab is beginning in this direction. The task is a large one, since most mRNAs are not localized in Xenopus oocytes (Jamrich et al., 1984). One strategy will be to create and screen a eDNA library for mRNA transcripts present in Rhodnius ovarioles, and to use in situ hybridization to ascertain the location of these

mRNAs. A similar approach has already been used by Kastern et al. (1990) to determine the localization of specific mRNA transcripts in Hyalophora ovarioles. If localized transcripts are found, and the next step will be to determine the effects of ion channel blockers and ionophores on transcript distribution.

Ionic Currents Around Denuded Ooarioles

Currents around the T oocyte are generally in the same direction as those over the corresponding areas over intact ovarioles, although they are of lower magnitude. Currents over the trophic cord of the T oocyte are also consistent with the current efflux observed at the T connective (position 10). Current patterns over denuded tropharia, however, are not fully compatible with the current patterns over intact tropharia. The basal current efflux extends over positions where influx is consistently observed in intact tissue; only over the apical half of the tropharium do currents mirror those measured over intact tissues. Since these currents are manifest 30 min post dissection and are within the same order of magnitude as currents over intact ovarioles, it is unlikely they are the result of physical insult to the cell membrane.

Perhaps the most noteworthy finding is that current direction *reverses* over the T-1 oocyte during the transition from mid- to late vitellogenic T-l oocytes. This compares well with the change in direction at position 11 between size classes 8 and 9, and is a tangible electrophysiologicallink between prophase-arrest of subterminal oocytes and their subsequent activation. Two possibilities suggest

themselves. The first is that the reversal in current represents a change in the internal electrophoretic fields between the T-1 oocyte and the tropharium. These changes may set in motion meiotic events and nuclear migrations central to oocyte differentiation. Alternately, such reversals in current flux probably alter the intracellular concentrations of key ions, and it may be this change which signals a change in developmental state. Justification for this idea is strong: Woodruff and Telfer (1990) show that ooplasmic pH increases and nurse cell and oocyte membrane potentials hyperpolarize in activating Hyalophora follicles. This hypothesis in Rhodnius ovarioles.

Woodruff et al. (1986) report current reversals over denuded patches of Hyalophora nurse cells, and they provide convincing evidence that the epithelium over the trophic cap forms a tight barrier to dye movement. By extension, this epithelium could theoretically block or impede current efflux from the trophocytes. Since the transbridge potential between nurse cells and oocytes is maintained after enzymatic and mechanical removal of the follicular epithelium, it is unlikely that the reversal of current over the trophic region is artifactual.

Differences between the current patterns over denuded Hyalophora and Rhodnius trophocytes are difficult to reconcile. They may simply represent differences between polytrophic and telotrophic ovarioles, or could be related to the different procedures used for removing the follicular epithelium. My initial attempts to denude Rhodnius ovarioles according to Woodruff et al.'s (1986) method were unsuccessful, so it is not possible to compare these methods

directly. On the one hand, the convincing nature of Woodruff et al.'s (1986) data and the fact that many epithelia are morphologically adapted to the task of ion transport argue strongly for a broader role for the follicular epithelium in producing transcellular ionic currents. On the other hand, it makes electrophysiological sense that whatever current enters the follicle cells should also enter (or leave) the germ cells (see Nuccitelli, 1990), since the two are known to be well-coupled in both Hyalophora (Woodruff, 1979) and Rhodnius (Huebner, 1981b) ovarioles during certain periods of vitellogenesis. One other concept to consider is whether or not the follicular epithelium offers enough resistance to effectively block current flow. Although Overall and Jaffe (1985) dispute this possibility, there is still no firm evidence either supporting or refuting it. That the epithelium and basal lamina could in fact offer such resistance is not debatable: one has only to remember, for example, that the epithelium and basal lamina in the vertebrate cochlea provide enough charge separation to support endocochlear potentials, and the ion pumping epithelia of the kidney maintain transepithelial ionic differences.

In final analysis, in Rhodnius ovarioles the oolemma is involved in at least a component of the extracellular current pattern. The situation is less clear with respect to the tropharium. The more extensive area of current efflux over the base of the tropharium may signify that the follicular epithelium generates or modifies the current in this region. The fact that both current efflux and current influx are found over different areas of the tropharium argues that relatively

distinct current efflux-influx loops exist over both the T oocyte and the tropharia, although nurse cell-oocyte coupling via the trophic cord insures that the two circuits interact in some manner. This scenario helps to reconcile the differences between extracellular current patterns and intracellular potentials, and this fits well with the suggestion of Telfer et al. (1981b) that a potential gradient radiates outward from the trophic core to the nurse cells; such a gradient could be maintained by a basal-apical current loop over the tropharium. The results of ion substitution and inhibitor experiments add further support for this idea, and are presented in Chapter 2.

The role of the follicular epithelium has not been examined in my research, although it is clearly important in ovarian physiology. Early work by Wollberg et al. (1975) and Woodruff (1979) demonstrate electrical coupling between adjacent follicles in panoistic and polytrophic ovarioles, respectively, and recently Woodruff and Telfer (1990) extend observations on Hyalophora follicles to clearly demonstrate that interfollicular coupling via follicle cells plays a pivotal role in the onset of vitellogenesis. Certainly, future work in the telotrophic Rhodnius ovariole should address this possibility.

Figure 1

Recording positions along intact ovarioles. The lines next to numbers 1-20 are current vectors; current magnitude is indicated by the length of the line, and current direction is denoted by the direction of the line from the point closest to the outer surface of the ovariole (scale not shown).

(a) Numbers 1-10 denote recording positions starting at the base of the T foolicle, extending to the T connective. (b) Numbers 11-20 denote recording positions over the prefollicular region (11-13) and tropharium (14 - 20). This is a bright field image with oblique illumination, recorded on video tape. Images were captured with an image analyzer and hardcopies made with a freeze frame (see chapter 3 for details). The blurred object at the bottom of the field is the vibrating probe. Mag. = 200X.

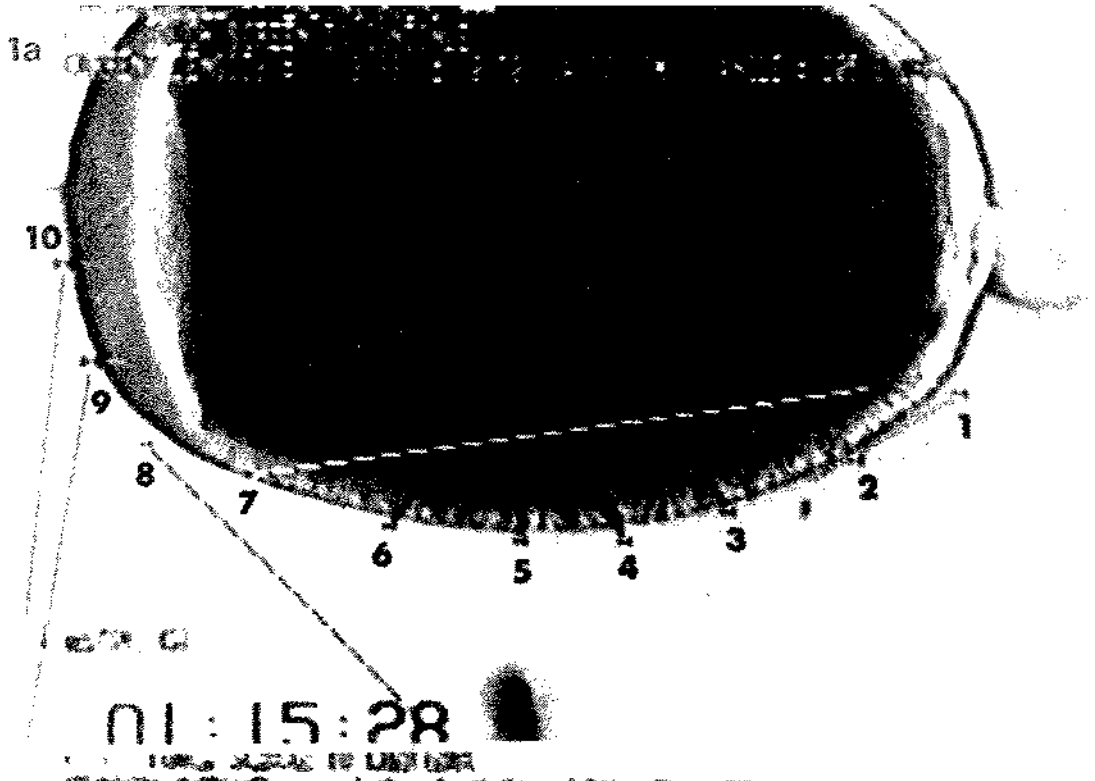

1b

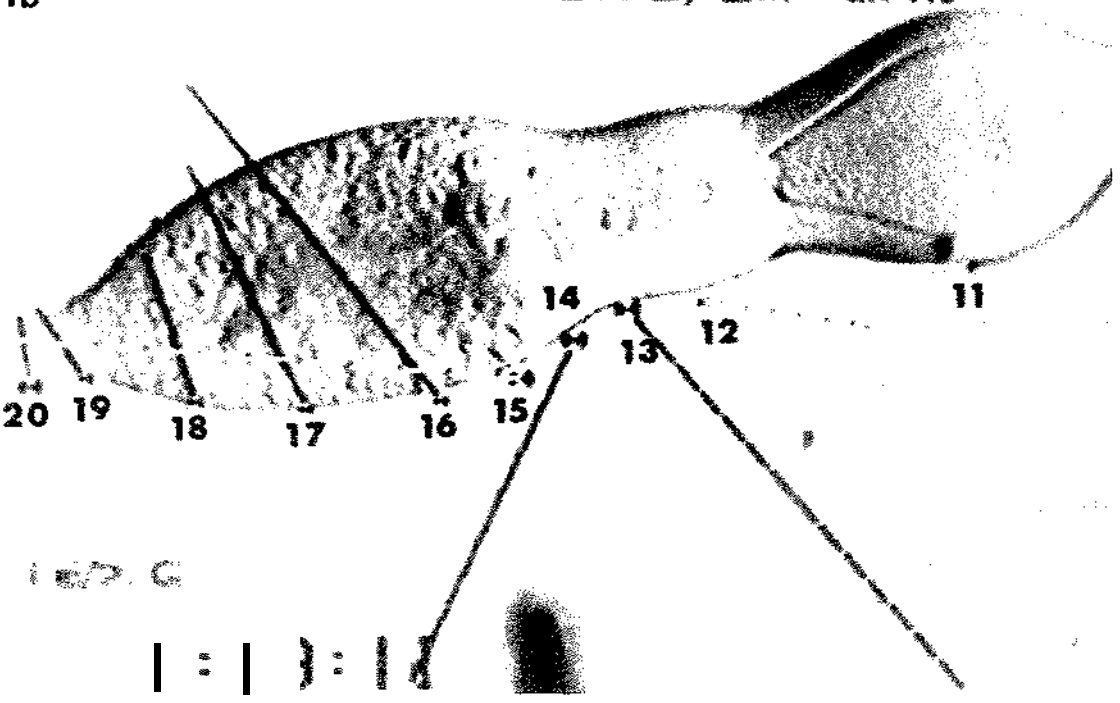

Figure 2

Extracellular current density and direction around class 1 ovarioles. Mean current density (± SEM) are indicated over 4 locations (quadrants) around the circumference of each ovariole at 20 positions per quadrant. Differences are significant between quadrants 0 and 180, position 14. Currents are not represented at postions 4 and 7. The bottom three-dimensional spline plot illustrates mean current fluctuations; the z axis scale is plotted with 16 divisions for graphical purposes only. N=9.

ODegree.

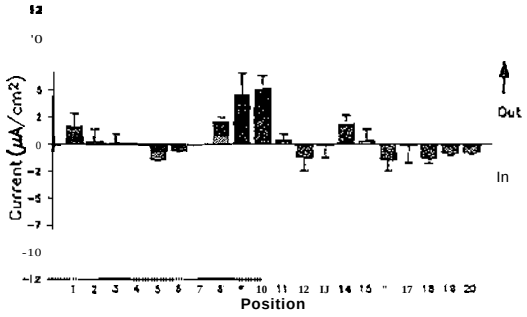

90 Degrees

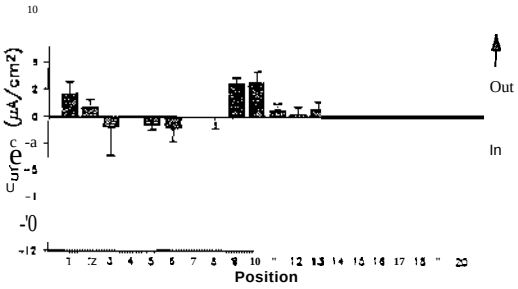

180 Degree.

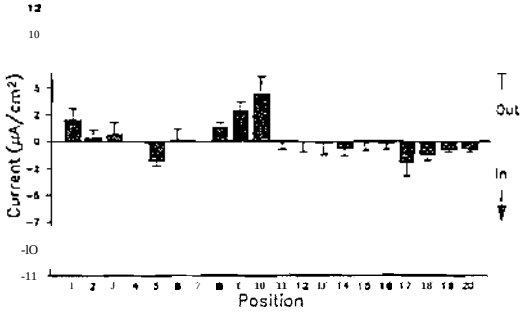

270 Degrees

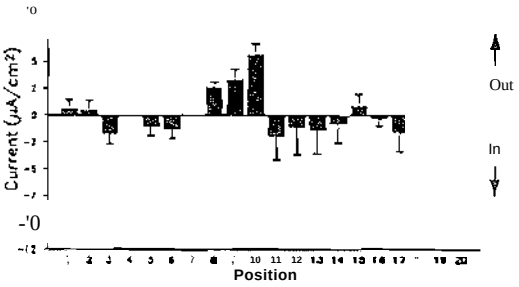

Mean Current Density Around Class 1 Ovarioles

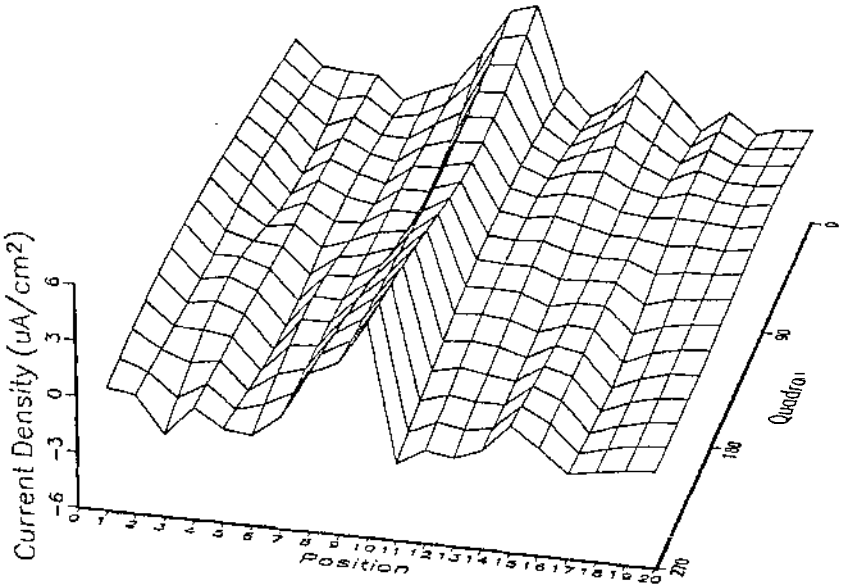

Figure 3

Extracellular current density and direction around class 2 ovarioles. Differences are significant between quadrants 0 and 180, position 2, and between quadrants 0 and 90, position 4. The bottom three-dimensional spline plot illustrates mean current fluctuations. N=7.

O Deqrees

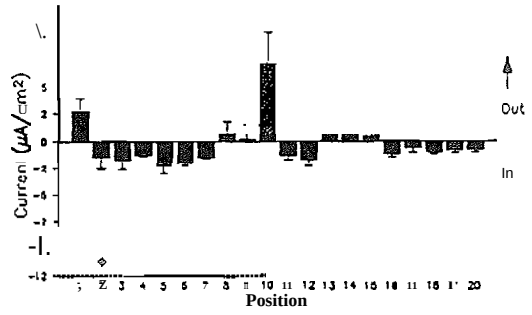

900egrees

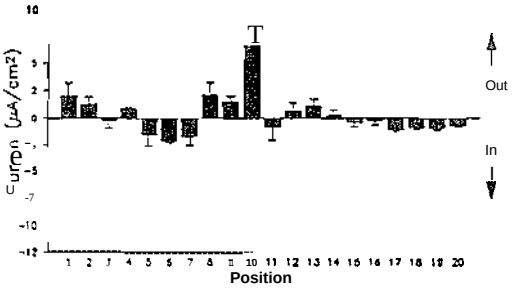

180 Degrees

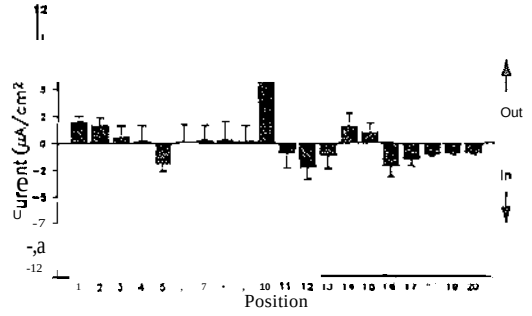

270 Degrees

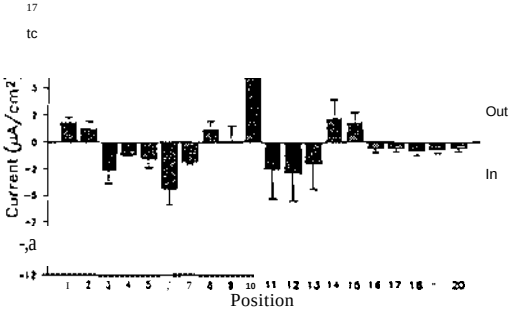

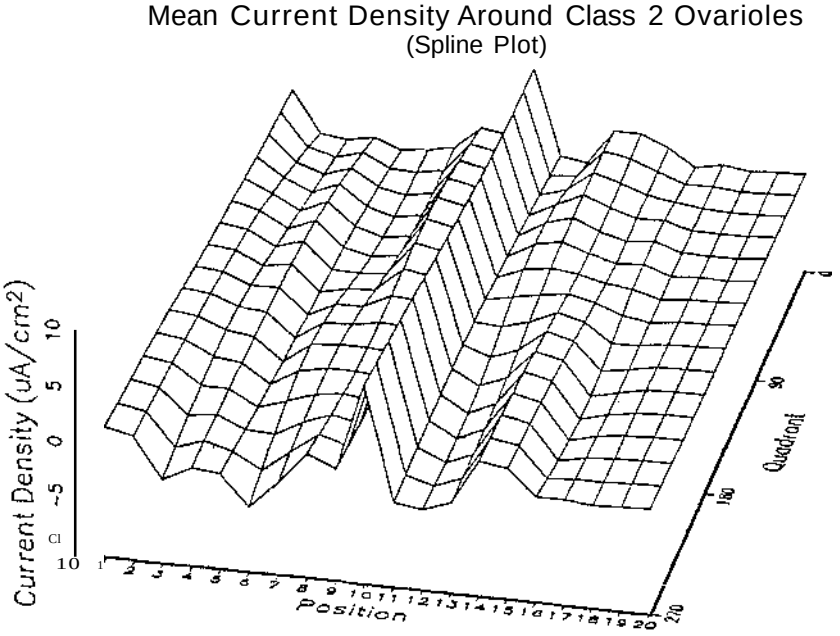

Figure 4

Extracellular current density and direction around class 3 ovarioles. Differences are significant between quadrants 180 and 270, position 2. The bottom three-dimensional spline plot illustrates mean current fluctuations. N=9.

ODegree.

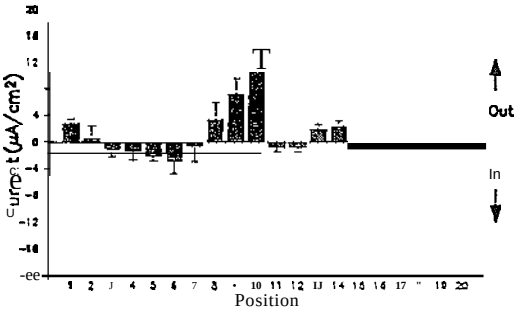

90 Degree.

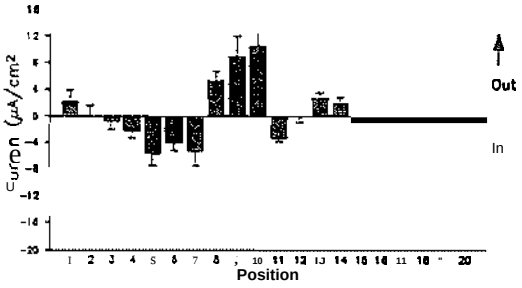

180 Degrees

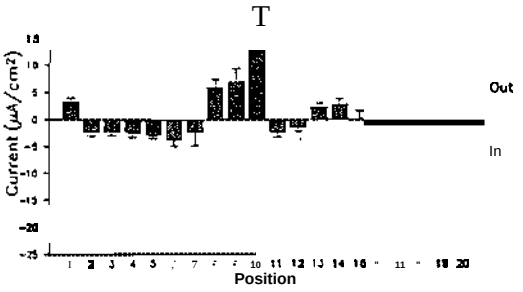

270 Degrees

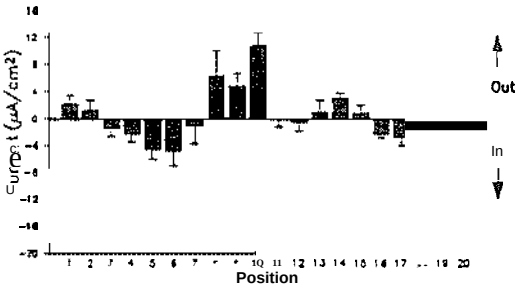

Mean Current Density Around Class 3 Ovarioles

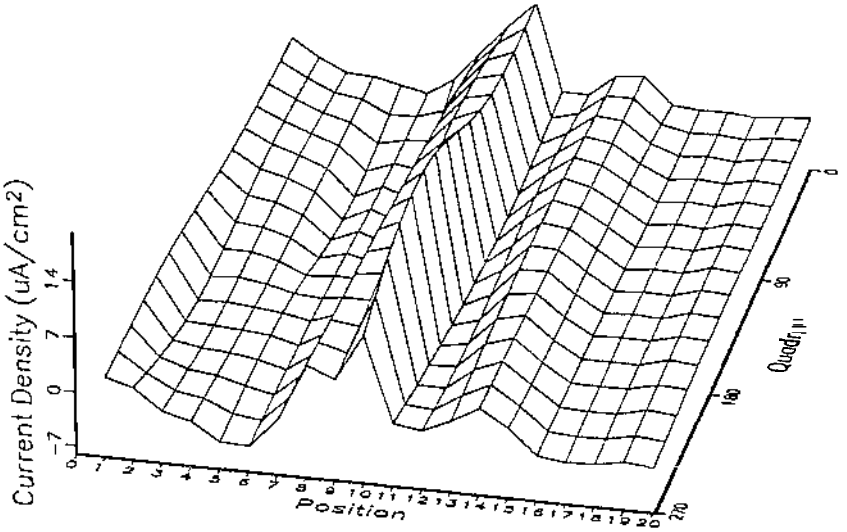

Figure 5

Extracellular current density and direction around class 4 ovarioles. Differences are significant between all quadrants at position 7/ except between quadrants 0 and 270. There are also significant differences between quadrants 0 and 180/ and 0 and 270/ position 10. The bottom three-dimensional spline plot illustrates mean current fluctuations. N=7.

O Degrees

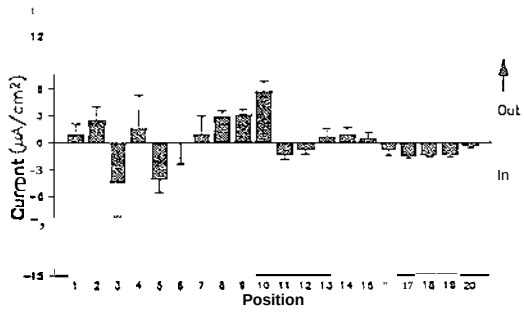

90 Degrees

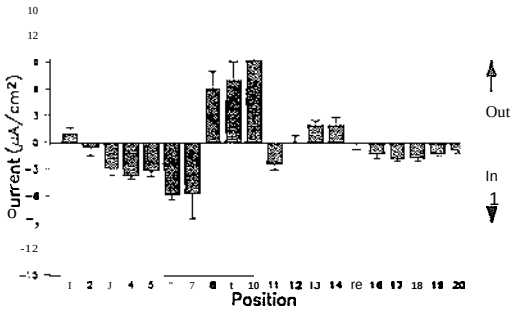

180 Degrees

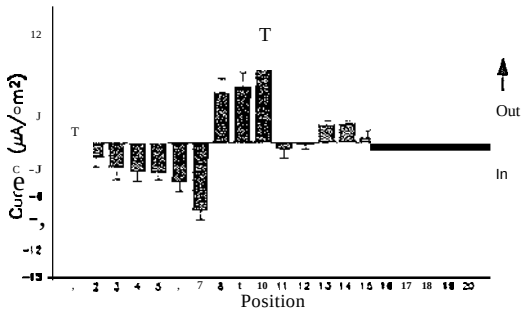

270 Degrees

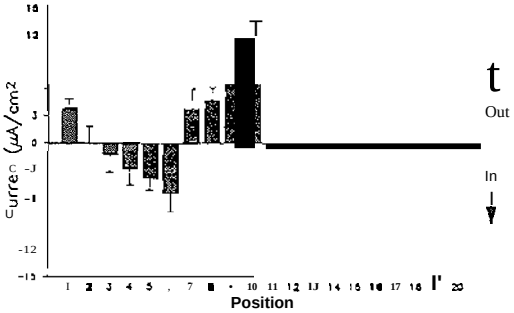

Mean Current Density Around Class 40varioles

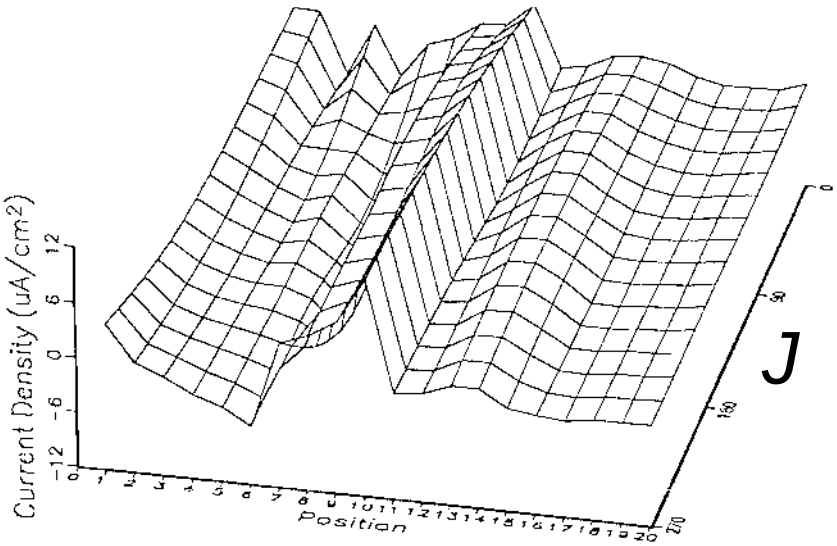

Figure 6

Extracellular current density and direction around class 5 ovarioles. There are marginally significant differences between some quadrants at the same longitudinal position. The bottom three-dimensional spline plot illustrates mean current fluctuations. N=7.

O Degrees

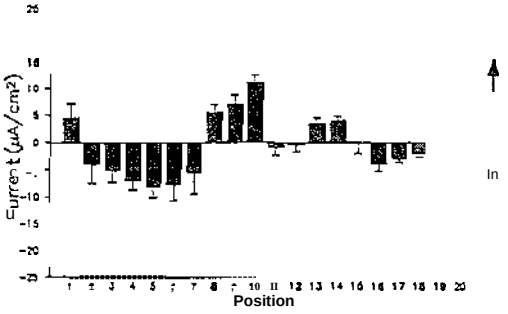

90 Degrees

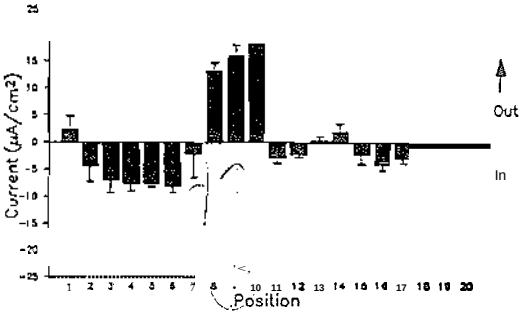

180 Degrees

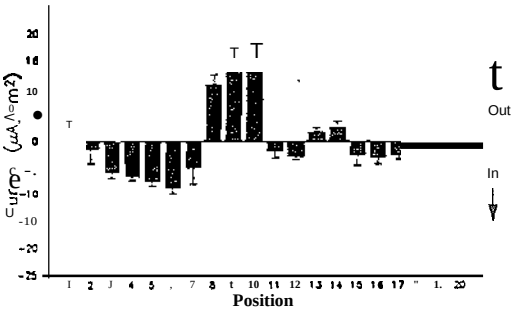

180 Degrees

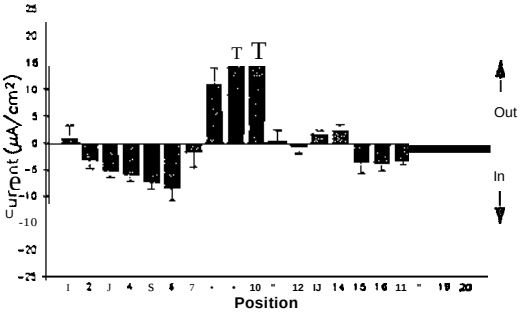

Mean Current Density Around Class 50varioles

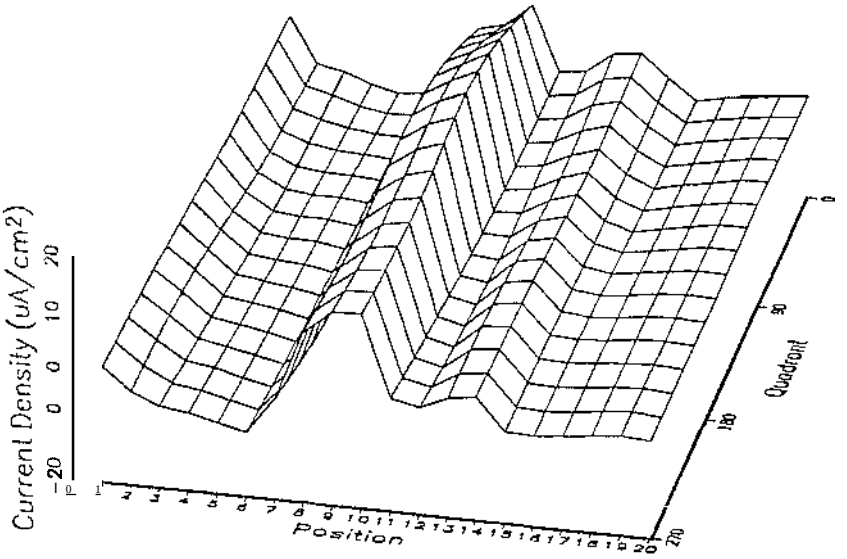

Figure 7

Extracellular current density and direction around class 6 ovarioles. There are marginally significant differences between some quadrants at the same longitudinal position. Only 3 replicates were obtained at each of positions 2, 4, 6 and 7. The bottom three-dimensional spline plot illustrates mean current fluctuations. N=9.

OOegrees

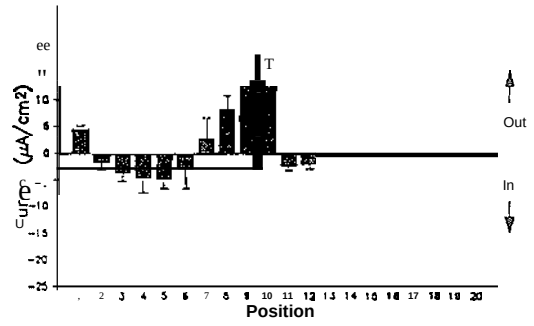

90 Degree.

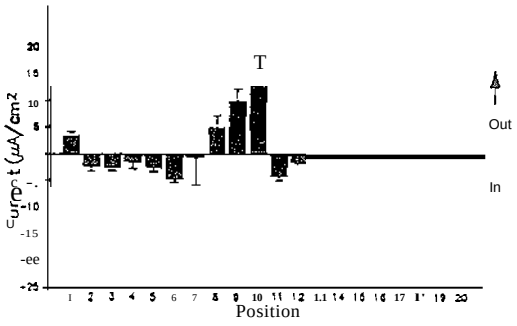

180 Degree.

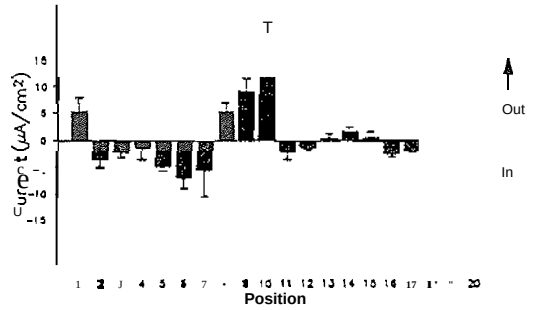

270 Degree.

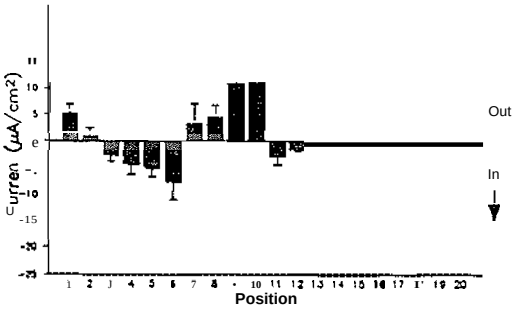

Mean Current Density Around Class 60varioles

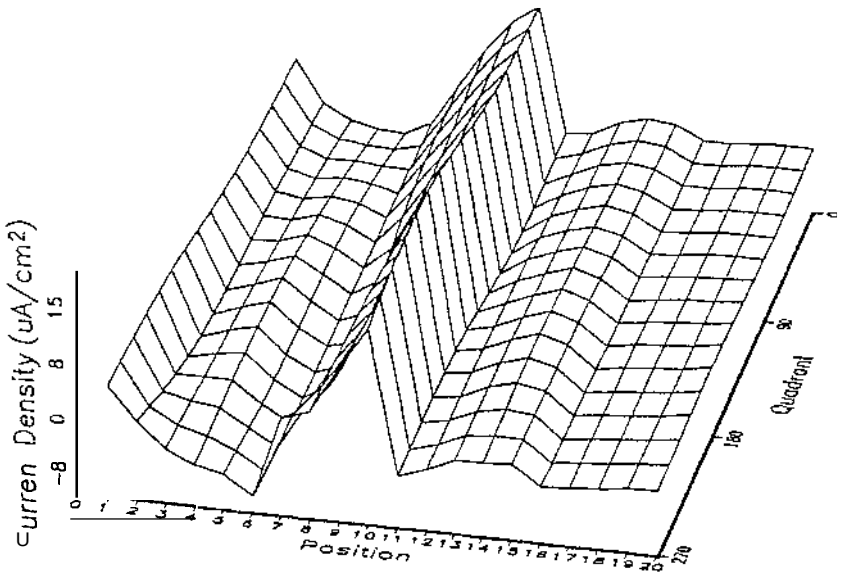

Figure 8

Extracellular current density and direction around class 7 ovarioles. There are marginally significant differences between some quadrants at the same longitudinal position. Only 3 replicates were obtained at each of positions 2, 4, 6 and 7. The bottom three-dimensional spline plot illustrates mean current fluctuations. N=5.

0 Degrees

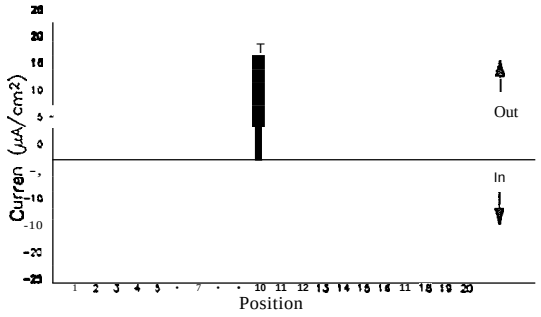

900.greea

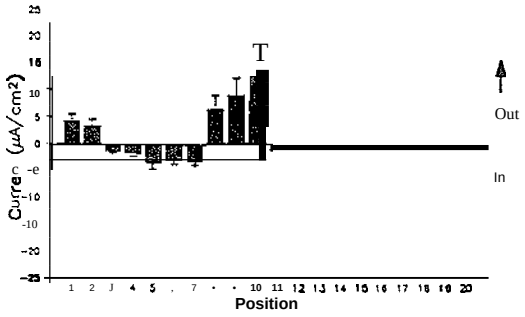

180 Degree.

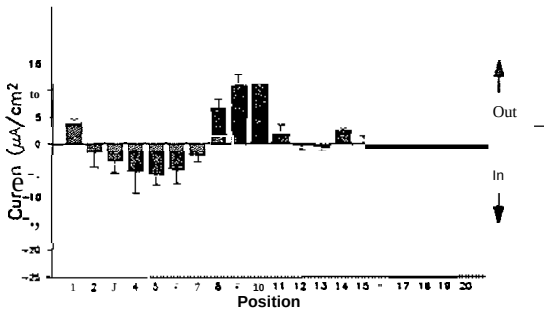

270 Degree.

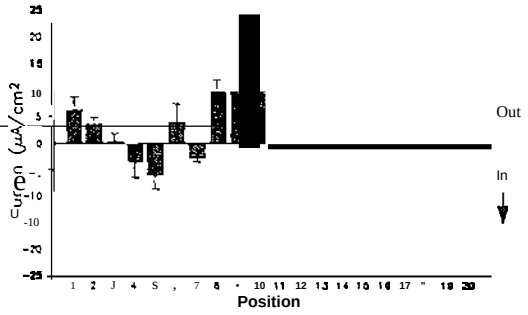

Mean Current Density Around Class 70varioles

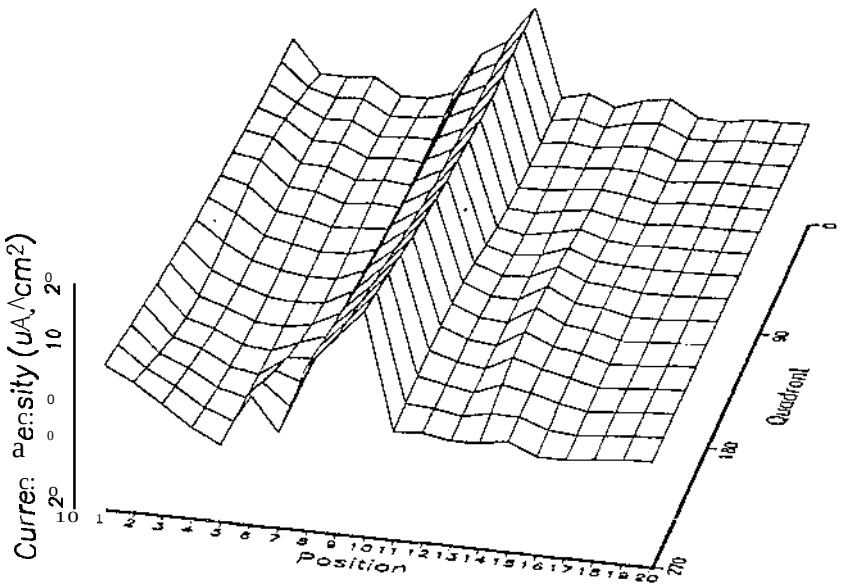

Figure 9

Extracellular current density and direction around class 8 ovarioles. Differences are significant between quadrants 0 and 270, position 7. Only 2 replicates were obtained at each of positions 2 and 7. The bottom three-dimensional spline plot illustrates mean current fluctuations. N=5.

ODegrees

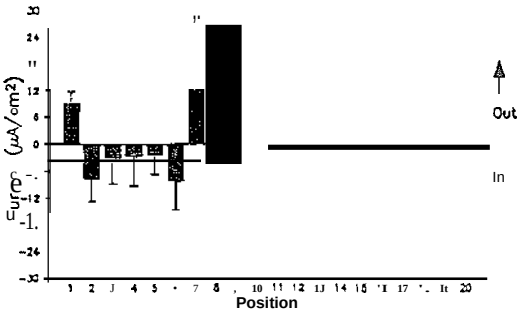

90 Degrees

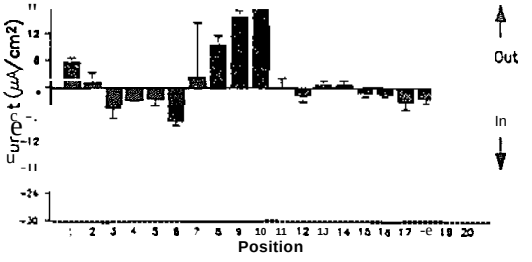

180 Degrees

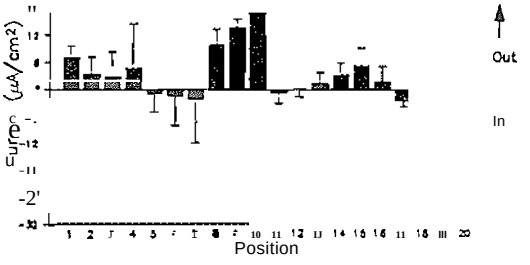

270 Degrees

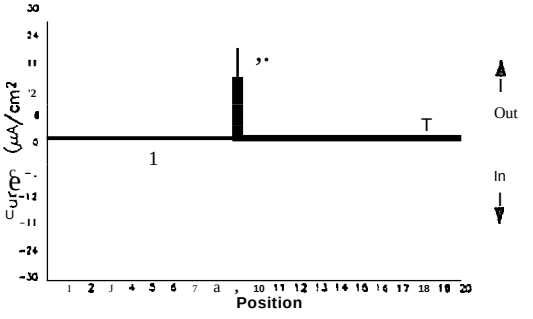

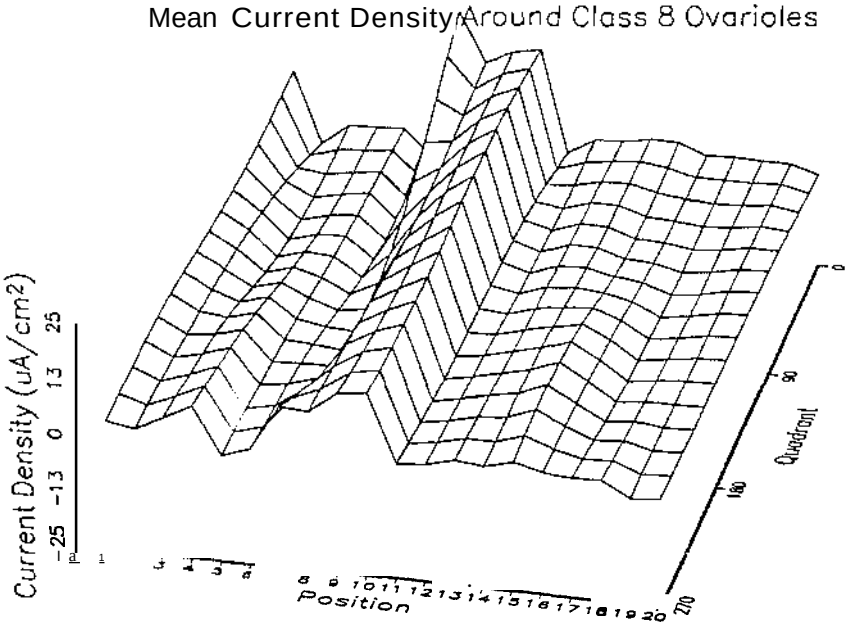

Figure 10

Extracellular current density and direction around class 9 ovarioles. There are no significant differences between quadrants at any positions. There are significant decreases in current flux between class 8 and class 9. N=5.

O Degree.

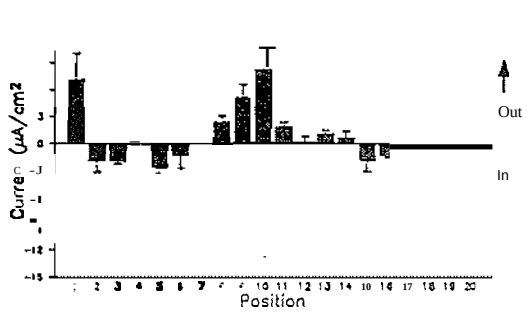

9D Degrees

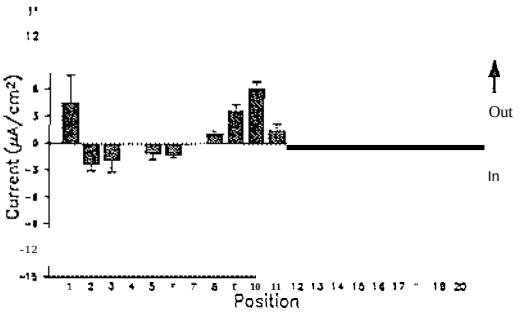

180 Degrees

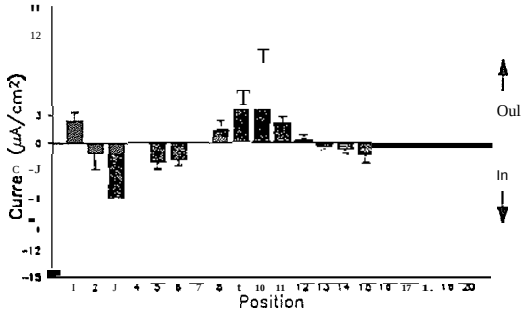

270 Degree.

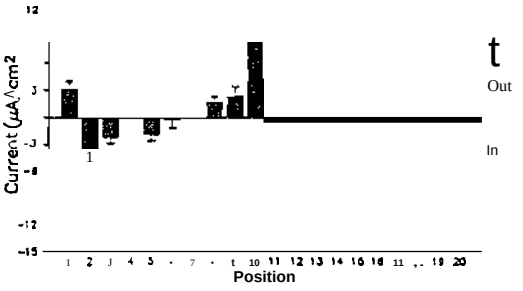

Mean Current Density Around Class 9 Ovarioles

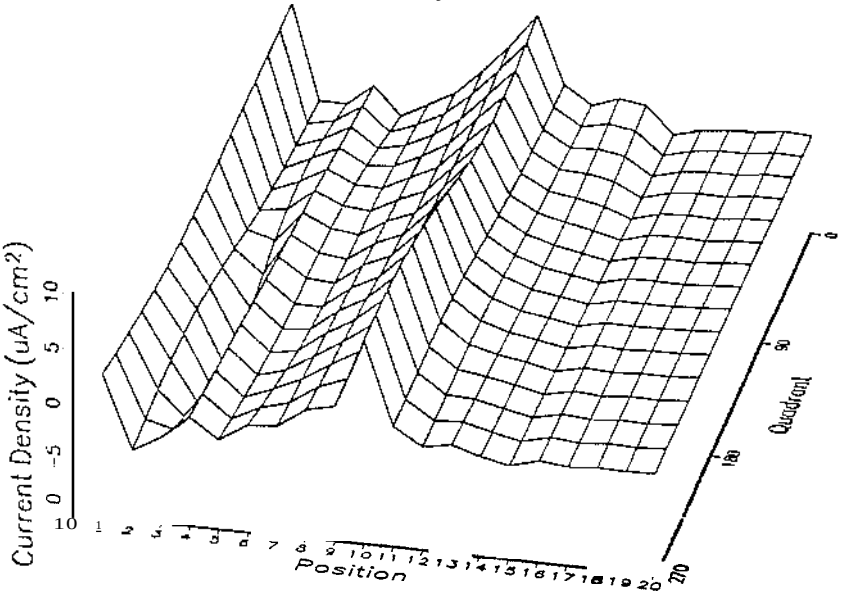

Figure 11

Extracellular current density and direction around denuded patches of early, mid-, and late vitellogenic ovarioles (T follicle lengths =400-500, 700-800, and 1500-2000 urn, respectively). Base T, Mid T, and Apex T = base, middle, and apex of the terminal oocyte. T-1 and T-2 refer to the preceding penultimate oocytes, while T-1C and T-2C refer to the trophic cords going to the repective oocytes. Number of replicates per measurement are indicated over the relevant bars. Note the reversal in current over the T-1 oocyte between mid- and late vitellogenesis.

Currents Around Denuded Ovorioles
(Early Vitellogenic)

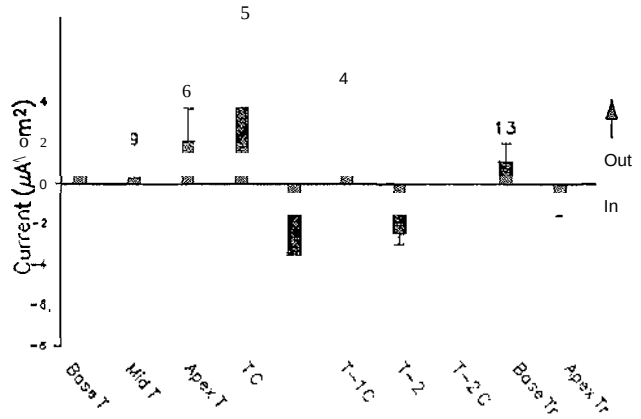

Currents Around Denuded Ovorioles
(Mid Vitellogenic)

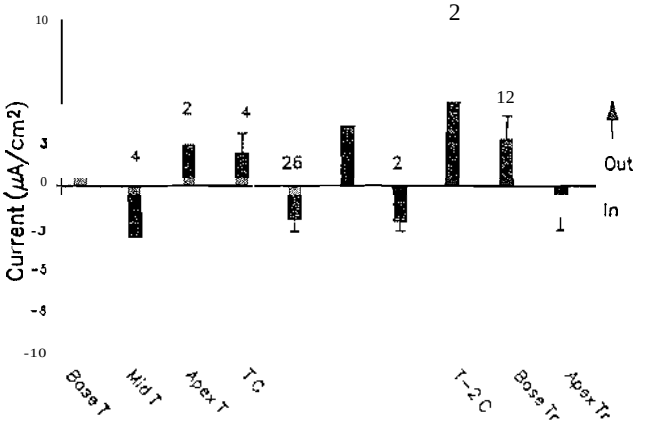

Currents Around Denuded Ovorioles
(Late Vitellogenic)

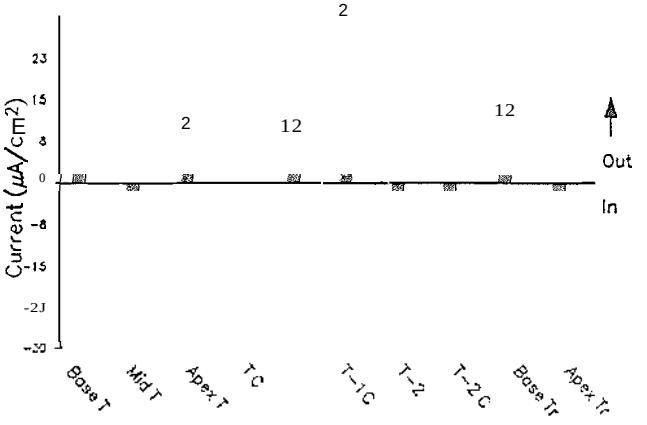

Figure 12

ab) Currents over partly denuded T-l oocytes from class 9 ovarioles (late vitellogenic/chorionating stages) exhibit outward currents. Mag. = 250X.

c) Currents over nearly completely denuded late-vitellogenic T oocyte. Note that current leaves the oocyte at the apex, near a few remaining follicle cells (FC). Lines represent direction and magnitude of current vectors. Mag. = 280X.

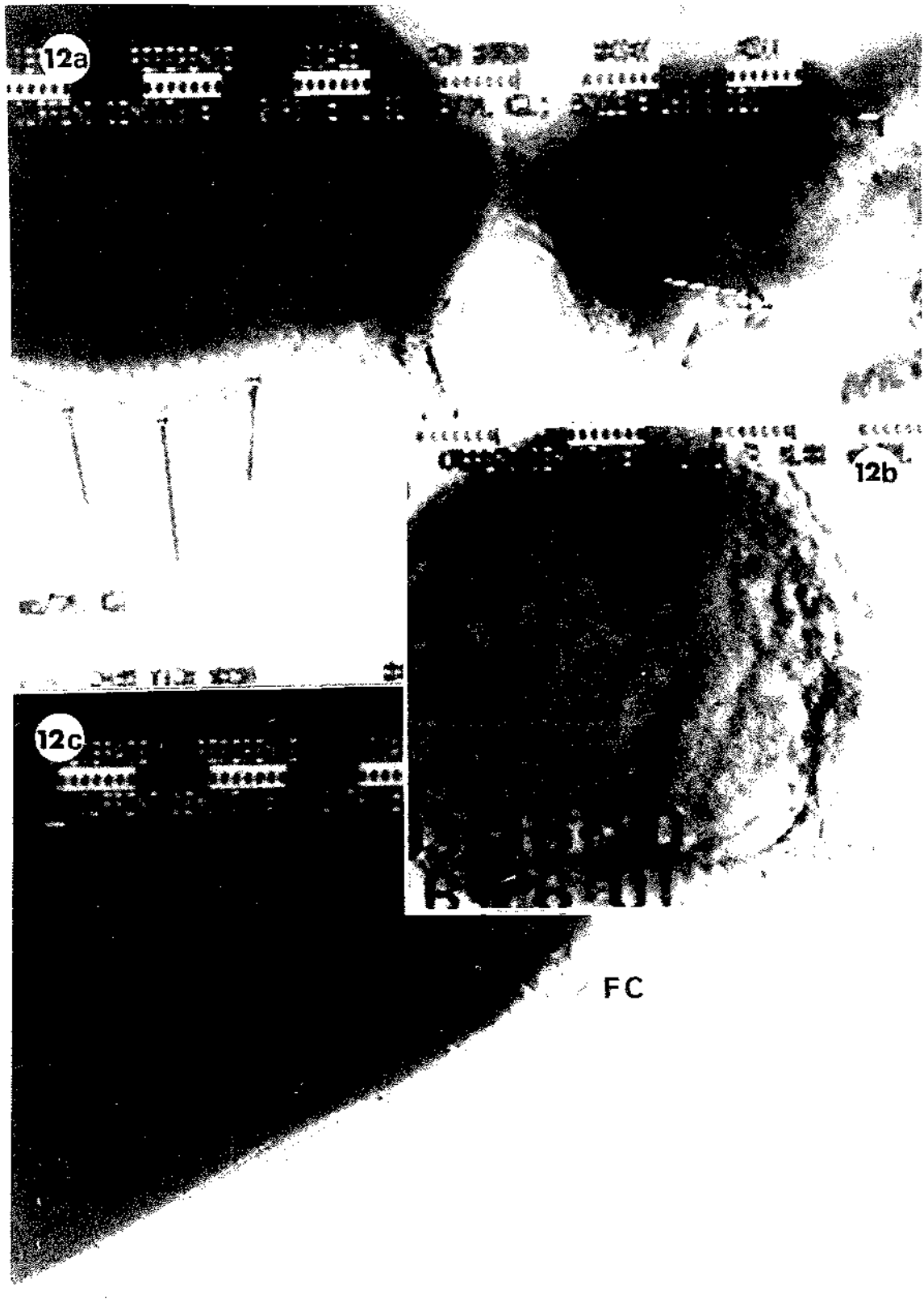
12a
12b
12c
FC

Figure 13

Current patterns over denuded subterminal oocytes. *a)* Current influx over a T-l oocyte in an early vitellogenic ovariole. *b)* Current influx over a mid-vitellogenic ovariole. c) Tangential current efflux from a trophic cord, directed towards the T oocyte. *d)* Current influx over a T-2 oocyte in a late vitellogenic ovariole. Tangential current influx is evident over the trophic cords. Mag. = 240X.

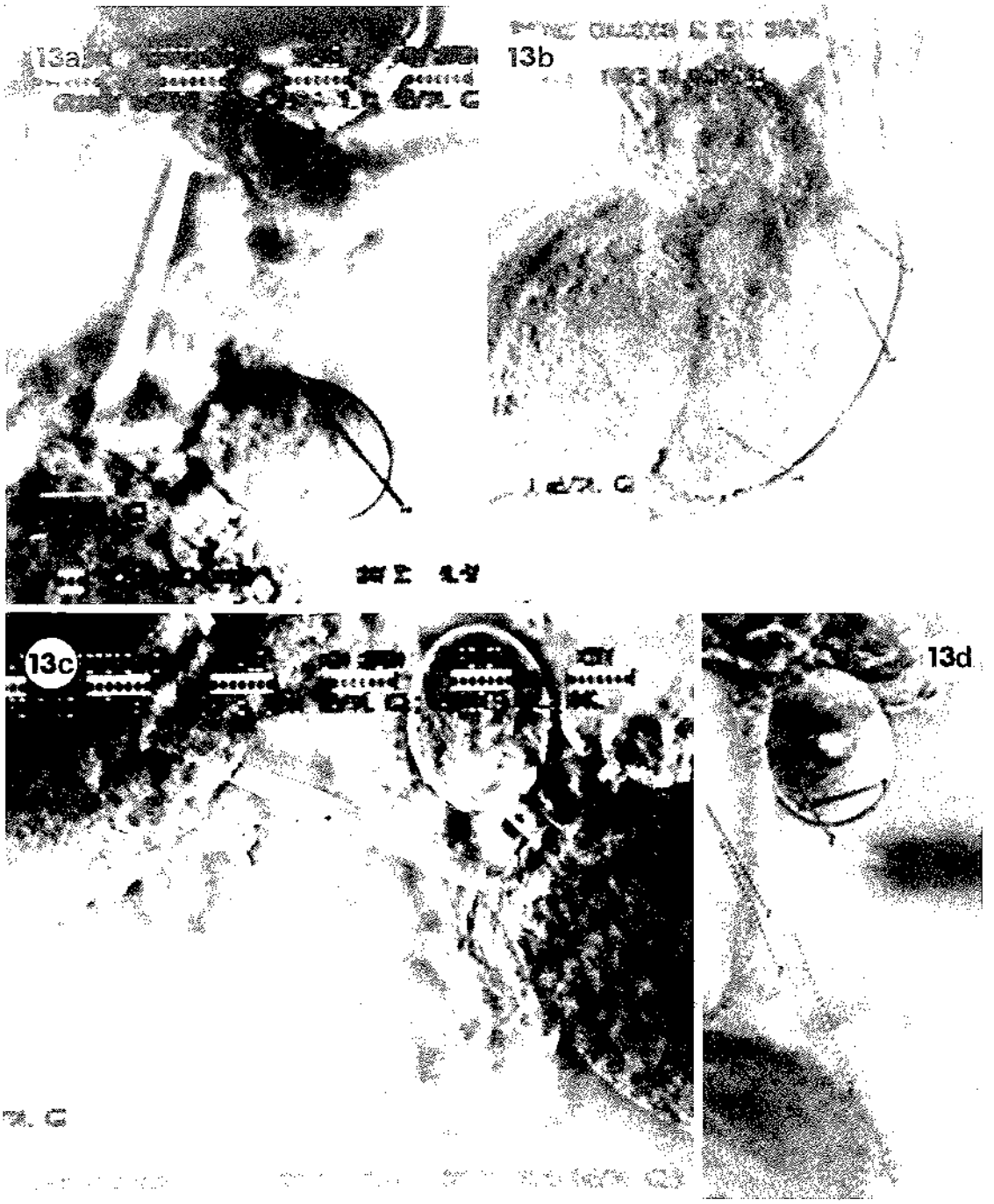
13a
13b
13c
13d

Figure 14

Currents patterns over partly denuded tropharia. *a)* All of the base and part of the apical half of the tropharium (Tr) has been denuded, as well as the T-2 and T-l oocytes. Current exits at the base of the tropharium and enters the apical half before it is enclosed by the remnants of the follicular epithelium. *b)* A wider area of current influx is evident over this partly denuded tropharium. Mag. = 200x.

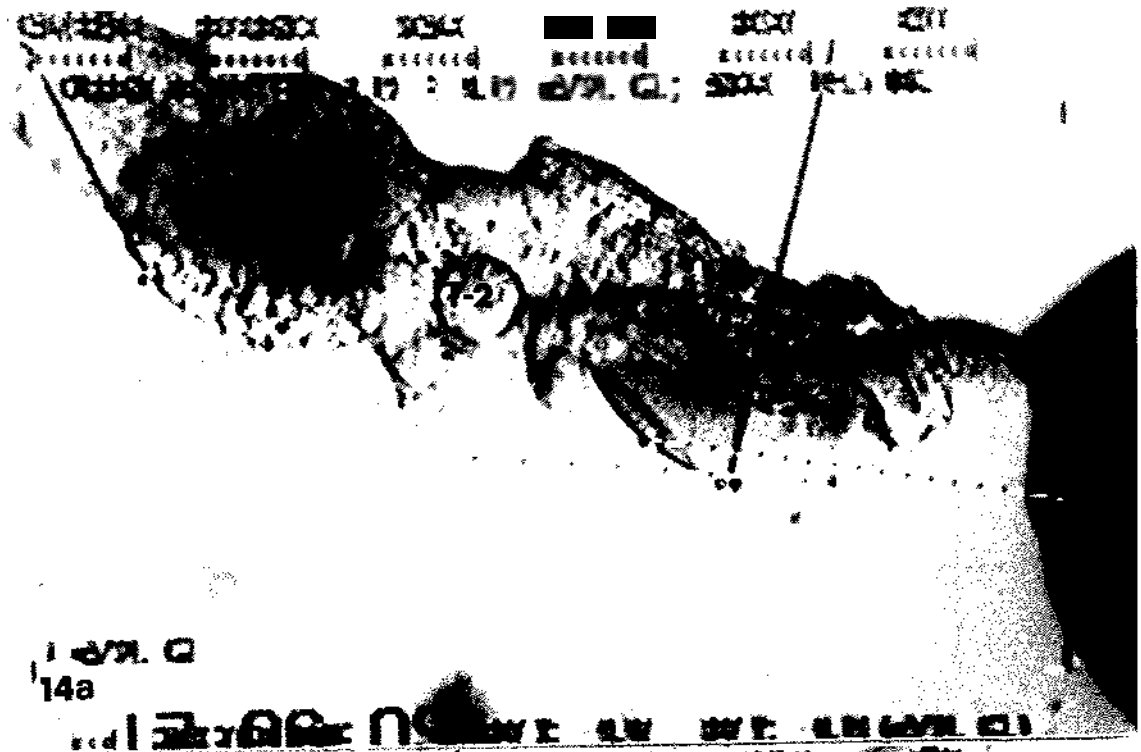

14a

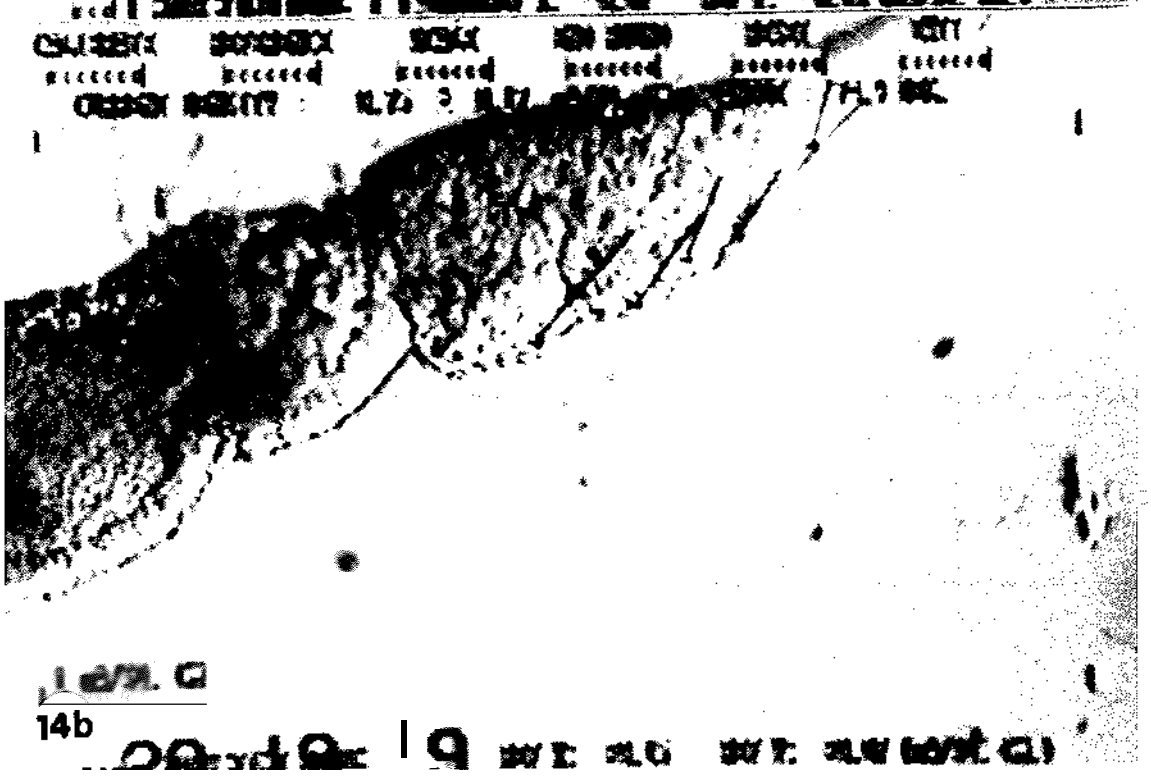

14b

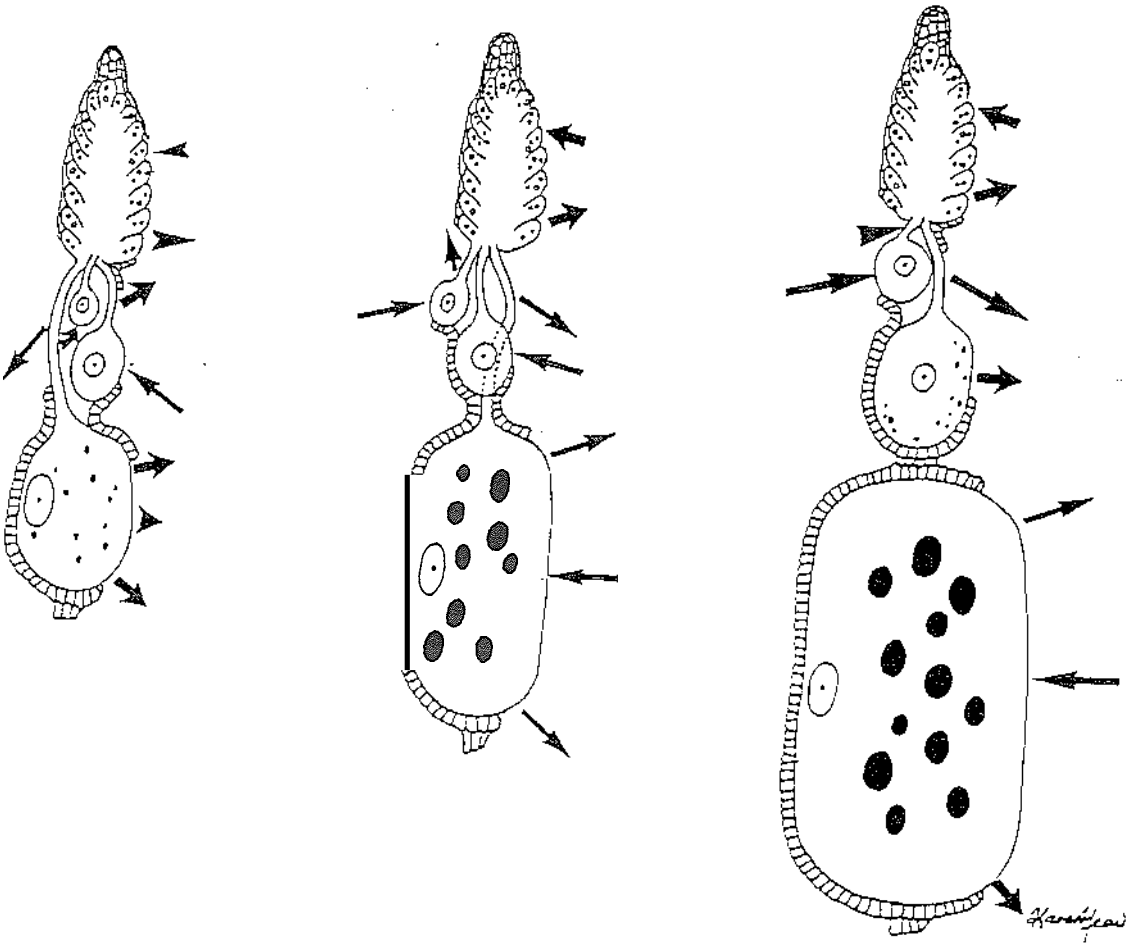

Figure 15

Schematic diagram representing the general directions of current efflux over denuded patches of early, mid- and late vitellogenic ovarioles (left to right). The magnitudes of current densities are not drawn to scale.

CHAPTER II

IONIC COMPOSITION OF TRANSCELLULAR CURRENTS AROUND *Rhodnius prolixus* OVARIOLES

INTRODUCTION

Transcellular ion currents are generated by a tremendous variety of developing organisms, from single and multicellular plant tissues (Nuccitelli and Jaffe, 1974; Weisenseel et al., 1975; Miller et al., 1986; Bjorkman, 1989; Hush and Overall, 1989) to invertebrate and vertebrate eggs (Jaffe and Woodruff, 1979; Robinson, 1979; Kline and Nuccitelli, 1985; Huebner and Sigurdson, 1986; Verachtert and DeLoof, 1986) and embryos (Jaffe and Stern, 1979; Stump and Robinson, 1986; Winkel and Nuccitelli, 1989). Inherent in all of these systems are spatially segregated ion transport processes. Two consequences of such currents can be internal voltage gradients and/or localized cytoplasmic ion gradients (Jaffe, 1981, 1986).

The onset and pattern of transcellular ion currents often correlate with events of developmental significance (Nuccitelli, 1990). Before causal links can be

established between ion currents and epigenesis, the identity of the current carrying ions must be established, as well as the associated transport mechanisms. With such information, in some cases it has been possible to perturb local ion fluxes and establish the physiological consequences. The least ambiguous example is the inward Ca^{+2} current over the algal Fucus egg, which precedes and predicts the future site of rhizoid elongation (Nuccitelli and Jaffe, 1974). If intracellular Ca^{+2} is chelated or external Ca^{+2} deleted, rhizoid growth does not occur (Robinson and Cone, 1980; Speksnijder et al., 1989). Conversely, local application of Ca^{+2} ionophore induces rhizoid growth (Brownlee and Wood, 1986). Recently, Zivkovic (1990) has shown that an inward Ca^{+2} current enters the animal pole of embryos of the freshwater mollusc, Lyrnnea; organic Ca^{+2} channel blockers abolish this current and prevent cleavage.

Extensive research has focused on the bioelectric properties of both panoistic and meroistic insect ovarioles, and the intracellular and extracellular electrical characteristics are generally believed to be an essential aspect of oocyte differentiation. The pioneering studies of Woodruff and Telfer (1973, 1980) showed that a standing voltage gradient between nurse cells and oocytes of H. cecropia was involved in unidirectional transport of charged proteins, thereby implicating intracellular electrophoresis. However, there have been only two published accounts of the ionic basis of transcellular current patterns around insect follicles (Overall and Jaffe, 1985; Diehl-lones and Huebner, 1989a), and there is currently no evidence linking possible cytoplasmic ion concentration

gradients with oocyte physiology or differentiation.

Diehl-lones and Huebner (1989a) applied ion substitutions and inhibitors and measurement of the extracellular currents at four locations along the telotrophic ovariole of R. prolixus. In the present study, I have extended this earlier work by examining other loci including positions along the terminal follicle. The aim of this work is to more completely delineate the composition of the extracellular currents and thereby provide an essential background necessary for further examination of the physiological relevance of transcellular currents. Several technical improvements have been made to avoid nonspecific ionic perturbations of the ovariole, and localized micropipette applications of inhibitors have been used to examine discrete positions and to avoid more global perturbations of this relatively complicated germ *celli*somatic cell complex. Results of this study are compared with the data from O'Donnell (1986) concerning the ionic basis of the resting potential of Rhodnius ovarioles, and O'Donnell's (1985) report of Ca^{+2} action potentials.

MATERIALS AND METHODS

Tissue

R. prolixus were reared as previously described (Huebner and Anderson, 1972a) and the ovarioles carefully dissected into fresh Rhodnius Ringers (Table

1). Mid-vitellogenic ovarioles (terminal oocyte length=600-750 urn) were used for most experiments and were desheathed just prior to vibrating probe measurements. Damaged or atretic ovarioles were discarded, and two ovarioles at most were used from each female. Occasionally ovarioles with clearly abnormal baseline current patterns were measured, and data from these ovarioles were not included. Ovarioles were immobilized in the recording chamber by allowing them to adhere to pieces of glass slides coated with 1% (wIv) high molecular weight poly-L lysine (Sigma).

Current Measurement

A Plexiglass flow-through recording chamber with built-in platinum/platinum-blacked ground and reference electrodes (previously described in Diehl-lones and Huebner, 1989a) was used for all experiments except for tetrodotoxin trials, when disposable 35x10 mm plastic Petri plates were used in conjunction with a bimorph-mounted reference electrode. Vibrating probe measurements were made with a modified two-dimensional vibrating probe purchased from the Vibrating Probe Co. (Davis, *CA);* outputs were digitized with a Labmaster A-D converter (Solon, Ohio) and were analyzed with an IBM PCXT. A current-injecting glass microelectrode was used for calibrating the vibrating probe with known current values (see General Introduction and Appendix for a complete description of equipment and procedures).

Ion Substitutions and Inhibitors

To examine the respective contributions of Na", K+, Ca^{+2}, Mg^{+2}, and H+ to the external current pattern, ion substitution media were made (Table 1). All media were adjusted to pH 6.8 with the exception of the proton exchange media, and corrected if necessary to 342 mOsmolar with a freezing-point micro osmometer (Precision Systems, Natick, Mass.). Ion transport inhibitors used are indicated in Table 2; all solutions except tetraethylammonium chloride (TEA) were prepared by direct addition to Rhodnius Ringers and used immediately. Ringers with TEA was prepared by equimolar substitution with NaCl. Three pharmacological agents used in this study -- 4-4'-diisothiocyano-2,2' disulfonic acid (DillS), ouabain, and verapamil -- are light sensitive and were therefore prepared in a darkened room. Ovarioles were exposed to these agents in the dark, and the microscope light source was turned on only during actual recordings.

In a preliminary analysis of the composition of ionic currents, flux changes were measured at four locations over late vitellogenic ovarioles: the T-connective; the middle of the penultimate follicle (T-l); the basal portion of the tropharium (Base Troph): and the middle of the tropharium (Mid Troph) (Diehl-Jones and Huebner, 1989a). Current measurements were made before and at 10,20, and 30 minutes post-exposure to ion substitutions and inhibitors, and recovery was measured at 10-minute intervals following replacement of the medium with normal Ringers (N=5 for each experiment).

As a result of a more in-depth analysis of the normal current pattern around Rhodnius ovarioles, the previous experimental protocol was modified. Mid-vitellogenic ovarioles were used for subsequent ion substitution and inhibitor experiments because: .(a) the trophic' cord to the terminal (T) oocyte is consistently still connected and (b) a key current efflux between the previtellogenic region at the base of the tropharium is invariably present at this stage (see Chapter 1). Eight locations covering the T-oocyte and tropharium were chosen for current measurements before (control), during (exposure), and after (recovery) treatment with inhibitors and substitutes. These locations correspond to positions 1, 5, 8, 10, 14, 16, and 17 illustrated in Fig. I, Chapter I, and are labelled Base T, Mid T, Apex T, TC, Base r-, Mid Tr, and Apex Tr, respectively. It should be noted that the Base Troph and Mid Troph recording positions in the previous study (Diehl-Jones and Huebner, 1989a) do not correspond with the Base Tr and Mid Tr positions. Mid Tr in the present study is actually more basal than the Mid Troph position, and represents a current efflux. Media were exchanged by flushing the recording chamber with 10ml of new solution (over 3 times the volume of the recording chamber) during a period up to 2 min. To separate direct effects of exposure to ion substituted media and inhibitors from secondary perturbations, media were exchanged over approximately two minutes with a push-pull syringe system and currents recorded in ion substituted media within approximately 2 minutes post-exposure (P.E.); currents around ovarioles exposed to various pharmacological agents were recorded within 5 min P.E. Early results

with ouabain, a specific inhibitor of the Na"/K+ ATPase, were negative; to determine if this was due to an inability of the enzyme to permeate the basal lamina and the follicular epithelium, I briefly exposed ovarioles to 0.1% trypsin prior to the Ouabain experiments. A paired, two-tailed t-test was used to determine if currents in the experimental media were significantly different from control values (Kleinbaum et al., 1988). All current densities are reported as ± standard error of the mean.

Since intracellular Ca^{+2} (Ca^{+2}_{j}) is also known to either modulate or gate some ion conductances (Hille, 1984), I investigated the effect of an agent known to perturb Ca^{+2}_{j}, TMB-8 (8-(N,N-diethylamino)-octyl 3,4,5-tri-methoxybenzoate hydrochloride), which blocks intracellular Ca^{+2} release (Chiou and Malagodi, 1975; Owen and Villereal, 1982).

Micropipette Inhibitor Applications

A limitation of exposing entire ovarioles to inhibitors was that, in a complex syncytium, current inhibition in one location could indirectly alter current flux generated by different mechanisms in another area of the tissue. In an attempt to separate these effects, 30-sec pulses of various inhibitors were applied to separate areas of ovarioles by means of a micropipette (outer diameter < 10μm), and recordings were made within 15 seconds post-application. Ovarioles were oriented in the recording chamber such that a continuous flow of fresh Ringers directed drugs away from the rest of the ovariole.

RESULTS

Preliminary Results

The results of initial experiments over longer time course are indicated in Fig. 1 (from Diehl-lones and Huebner, 1989a). Briefly, replacement of Na" with choline resulted in significant decreases in current efflux at the T connective and swelling of tissue by 10 min post-exposure (P.E.). Replacement of K^+ in the media had no significant effect on current influx or efflux, and addition of Co^{+2} resulted in a significant decrease in current efflux but did not alter current influx. Ethacrynic acid caused significant decreases in current efflux and influx, by 10 min P.E., and ouabain had no discernable effect. TEA caused a significant decrease in current efflux by 10 min P.E., whereas 4-aminopyridine (4AP) caused a significant reduction in current efflux only by 30 min P.E. Furosemide, an inhibitor of active chloride transport, had no significant effect at the positions measured.

Effects of Ion Substitutions

Replacement of Na" with the impermeant cation choline (Table I, substitution 2) was earlier shown to cause a significant change in current efflux but not in influx (Diehl-lones and Huebner, 1989a). Clearly, a decrease in current efflux must be mirrored by a similar decrease in current influx if Kirchoff's Laws are to be obeyed. In the present study, significant decreases in current influx

were observed at the Mid T (P=0.048), Mid Tr (P=0.013) and Apex Tr (P=O.OOl) positions (Fig. 2; N=l1). Significant decreases in current efflux were observed at three locations: the apex of the T follicle (P=0.035), the T connective (P=0.053), and at the base of the tropharium (P=0.003); there was no significant change in current at the base of the T follicle. All currents returned to near control values by 2 min recovery, except at the Apex T and T Con positions; earlier published results have shown that current efflux at the T connective returns to normal after 10 min recovery (Fig. 1).

Replacement of K^+ with equimolar Na" (Table 1, substitution l)had no effect on current direction or magnitude at the positions measured (Fig. 3a; N=5). Marked changes in current density occurred around ovarioles in high K^+ Ringers, however; significant decreases in current efflux occurred at the apex of the T follicle (P=0.032) and T connective (P=0.024), and at the base of the tropharium (P=O.OOOl), where current direction reversed from 4.75 (± 0.72) $\mu A/cm^2$ to -1.10 (±0.55) $\mu A/crrr'$ (Fig. 3b). A nonsignificant decrease in efflux occurred at the base of the T follicle. Current influx significantly decreased over the middle of the tropharium (P=0.016); current influx also decreased over the apex of the tropharium from -3.58 (±1.51) $\mu A/crrr'$ to -1.69 (±0.37) $\mu A/crrr'$, although this was not statistically significant. A marginally significant decrease in current influx also occurred over the middle of the T follicle (P=0.068; Fig. 3b).

The different strategies used for replacement of divalent cations yielded mixed results. Replacement of Ca^{+2} with Ba^{+2} (Table I, substitution 4), which has

a similar hydrated radius, was earlier shown to cause significant increases in current influx over the tropharium by 10 min P.E. (Fig. 1). However, within two minutes exposure to Ba^{+2} substituted Ringers, a different pattern emerged (Fig. 4a). Although there were no significant changes in current pattern over the terminal follicle, current efflux at the base of the tropharium significantly reversed from 5.21 (±O.5S) p.Amp/ crrr' in control Ringers to -2.71 (±0.43) uAmp/crrr' in the ion substituted media (P<O.OOOl). Correspondingly, current influx over the middle of the tropharium significantly decreased (P=0.023). Current over the apex of the tropharium also decreased, although not significantly. Currents did not recover within 2 min recovery in control Ringers. When Ca^{+2} is replaced with equimolar Co^{+2}, however, there are no significant differences in current magnitude or direction by either 2 or 10 min P.E. (Figs. 1, 4b).

Replacement of both Ca^{+2} and Mg^{+2} with Mn^{+2} (Table 1, substitution 3), which is a potent blocker of divalent cation channels, resulted in a change in current patterns similar to that observed in the $Ba^{+2\text{-substituted}}$ medium, but also with notable differences. Current efflux at the base of the tropharium significantly reversed from 5.23 (±0.97) μA/cnf to -0.47 (±1.40) μA/em? (P=O.OOI), and current influx significantly decreased over the middle and the apex of the tropharium (P=O.OOS and 0.004, respectively; Fig. 4c). Current influx and efflux recovered fully within 2 min. There were no significant changes in current magnitude or direction over the T follicle.

The effects of Cr substitution are indicated in Fig. 5a,b. Replacement with

Br' (Table I, substitution 6), which has a hydrated radius close to that CI", caused slight, but not significant increases in current density at all locations (Fig. 5a), with the exception of the base of the tropharium, where an increase in current efflux from 4.02 (±0.51) pAmp/crrf to 7.33 (±1.75) u.Amp/cm? was marginally significant (P=0.077). Replacement with SO_4^{-2} (Table I, substitution 7), which has a markedly larger hydrated radius than CI·, also yielded a general increase in current density, which was significant at the T connective (P=O.0003) and over the middle of the tropharium *(P=0.015)i* there was a slight, but not significant *decrease* in current efflux over the base of the tropharium (Fig. 5b).

To investigate any possible role of protons in extracellular currents, I manipulated H+ ion concentrations l,DOOO-fold. Ovarioles in pH 5 media (Fig. 6a) and in pH 9 media (Fig.6b) did not show any significant differences in current magnitude or direction. Equiosmolar substitution of glucose with sucrose also did not cause any significant changes in extracellular current patterns (Fig. 7).

Effects of Channel Blockers and Transport Inhibitors

Sodium and potassium channel blockers

Two pharmacologically distinct agents -- amiloride and tetrodotoxin -- induced different responses. Amiloride exposure resulted in a significant increase in current efflux at the T connective, from 13.77 (±2.56) p.Amp/crrr' in control Ringers to 23.2 (±2.03) pAmp / cm^2 in Ringers with amiloride (P=O.002). Current

influx over the middle of the T follicle showed a corresponding increase from -5.4 (±1.20) µAmp/crrr' to -8.61 (±1.72) µAmp/crrr', although this was not statistically significant (P=O.l44). Both of these increases remained stable after 5 min recovery in normalRingers. There were no obvious differences in current magnitude or direction at the other locations measured (Fig. Sa).

Ovarioles exposed to tetrodotoxin showed marked swelling and significant changes in current density (Fig. 8b). Significant decreases in current efflux occurred at the T connective (P=0.018), and marginally significant decreases in current influx occurred over the middle of the T follicle and the middle of the tropharium (P=0.098 and 0.086, respectively). A non-significant decrease in current efflux also occurred over the apex of the T follicle.

Exposure of ovarioles to TEA, a blocker of voltage- and $Ca^{+2\text{-gated}}$ K^{+} channels (Hermann and Gorman, 1981), resulted in a significant reversal in current influx over the middle of the T follicle; extracellular current changed from -7.21 (±1.77) µAmp/crrr' to 3.19 (±2.33) µAmp/crrr' (P=0.003). There was a corresponding decrease in current efflux from 10.08 (±2.67) µAmp/em" to 0.87 (±4.26) uAmp/crrr' over the base of the T follicle. There were no significant changes in current magnitude or direction at any of the other recording positions (Fig. 9).

Organic calcium channel blockers

Two distinct organic Ca^{+2} channel blockers perturbed the extracellular

current pattern in strikingly similar patterns. When ovarioles were exposed to a standard micromolar concentration of Diltiazem, there were no significant changes over the T oocyte (Fig. lOa); however, there was a significant reversal in current efflux at the base of the tropharium, from 3.47 (±0.52) p.Amp/cm? in control Ringers to -1.21 (±0.26) p.Amp/ em? in Ringers with Diltiazem (P=0.0004). Correspondingly, there was a significant decrease in current influx over the middle of the tropharium, from -2.47 (±0.33) u.Amp/rrrf in control Ringers to -1.21 (±0.26) p.Amp/ em' (P=0.018). There was also a slight but nonsignificant decrease in current influx over the apex of the tropharium. Current efflux at the base of the tropharium by 5 min recovery in normal Ringers was not significantly different form control values.

Exposure to verapamil similarly altered the extracellular current pattern (Fig. lOb). Current efflux over the base of the tropharium significantly decreased from 3.25 (±0.69) $\mu A/cm^2$ to -1.6 (±0.19) $\mu A/cm^2$ (P=0.002). There was a corresponding decrease in current influx over the middle of the tropharium, from -2.91 (±0.42) μA/crr' to -1.36 (±0.19) μA/crrr' (P=0.023), and a marginally significant influx decrease over the apex of the tropharium from -2.56 (±0.35) $\mu A/cm^2$ to -1.56 (±0.17) $\mu A/cm^2$ (P=0.057). There were no significant differences in current magnitude or direction over the rest of the ovariole, although current efflux at the T connective showed considerable variation. Unlike ovarioles treated with diltiazem, current efflux over the base of the tropharium did not recover significantly within 5 min in normal Ringers. Current densities over the middle

and apex of the T follicle, as well as at the T connective, increased during recovery, although not significantly.

Treatment with TMB8, an inhibitor of intracellular Ca^{+2} release, yielded equivocal results. A total of 7 ovarioles were treated, 4 of which had inward Ca^{+2} currents over the apex of the T follicle. Neither the combined data (aggregate) nor the data from ovarioles with $Ca^{+2\text{-in}}$ currents reveal significant differences in current magnitude or direction after exposure to TMB8 (Fig. 11a and b, respectively), although in the latter group there was considerable variation in current density at the middle of the tropharium during TMB8 exposure (Fig. 11b). In ovarioles without inward currents over the apex of the T follicle, marginally significant increases in current density over the base (P=0.0633), middle (P=0.0741), and apex (P=0.050) of the tropharium, which persisted up to 5 min recovery (Fig. 11c).

Chloride channel blockers

Ovarioles exposed to the chloride channel blocker 9-AC showed a significant decrease in current efflux over the middle of the T follicle, from -9.30 (±1.95) $\mu A/cm^2$ in normal Ringers to -3.00 (±1.64) pA/cm^2 after 2 min exposure (P=0.009), and recovered after 5 min in normal Ringers (Fig. 12a). Current efflux also decreased over the base (from 10.15 (±2.07) pA/cm^2 to 6.56 (±1.76) pA/cm^2) and apex (from 8.89 (±1.18) pA/cm^2 to 4.38 (±2.45) pA/cm^2) of the T follicle, although neither decrease was statistically significant. There were

slight, but not significant decreases in current efflux and influx over the tropharium.

DillS, an inhibitor of Cl' efflux and anion exchange (Komukai et al., 1985), did not cause any significant changes in extracellular current magnitude or direction at any of the locations tested (Fig. 12b). Current densities declined markedly during the Iecovery period, and this was likely due to a visible fouling of the probe by this particular inhibitor; calibration after each experiment revealed a significant loss of probe sensitivity to the calibration current.

ATPase inhibitors

Three inhibitors of ATP-dependent transport provoked significant, yet varied, changes in current patterns. Ethacrynic acid exposure resulted in significant reversals in current efflux over the base (P=O.034) and apex (P=0.045) of the T follicle, at the T connective (P=O.049), and at the base of the tropharium (P=O.043; Fig. 13a). There was a significant reversal in current influx over the middle of the T follicle (P=O.020) and a marginally significant reversal over the apex of the tropharium (P=O.057). The obvious reversal in current influx over the middle of the tropharium was not statistically significant.

Initially, we reported that ouabain had no effect on the current pattern (Diehl-Jones and Huebner, 1989a). However, after a very brief exposure to 0.1% trypsin, which is effective in weakening the basal lamina (see Chapter I), oubain exposure resulted in significant decreases in current efflux at the apex of the T

follicle (P=0.045) and at the base of the tropharium *(P=0.025i* Fig. 13b). Marginally significant decreases in current efflux were evident at the middle (P=0.070) and apex (P=0.055) of the tropharium. There were also insignificant decreases in current efflux and influx at the base and middle of the T-follicle, respectively.

Exposure to sodium orthovanadate induced two distinct responses. These are best demonstrated by presenting the data in aggregate and in separate groups. The aggregate data (Fig. 14a) indicates significant changes in current efflux at three positions: the apex of the T follicle, the T connective, and the base of the tropharium. Current efflux at the apex of the T follicle *increased* from 4.62 (±1.28) μA/crrr' to 27.76 (±2.00) μA/cm^2 *(P<O.OOOl)i* in marked contrast, current efflux at the T connective *reversed* from 12.39 (±2.39) μA/crrr' to -10.52 (±2.93) μA/crrr' (P=0.002). Current efflux from the base of the tropharium also reversed from 4.29 (±0.52) μA/crrr' to -5.48 (±4.11) μA/crrr', although this was only marginally significant (P=0.065). Reversals in current flux were evident at all other positions measured, but were not statistically significant due to high variances in current densities during drug exposure.

Of 8 ovarioles tested, 6 showed significant differences in current density only at the base and apex of the T follicle, and at the T connective (Fig. 14b). Current efflux at the base of the T follicle significantly reversed, from 4.56 (±2.11) μA/cm^2 to -17.03 (±3.54) μA/cm^2 (P=0.010); current efflux also reversed at the T connective from 11.028 (±2.8) μA/ern? to -6.99 (±2.46) μA/em? (P=O.009). The

apparent reversal in current at the middle of the T follicle was not statistically significant. There were no significant differences in current density over the tropharium, although current efflux at the base of the tropharium decreased from 3.83 (±0.54) μA/em? to 0.53 (±1.62) μA/em",

Two ovarioles exhibited statistically significant changes, despite a sample size of 2, in current flux over the base of the tropharium, the T connective, and the base of the tropharium (Fig. 14c). Current efflux at the base of the tropharium reversed, from 5.57 (±0.98) μA/crrr' to -23.52 (±3.04) μA/crrr', and current influx at the middle of the tropharium reversed, from -2.08 (±2.32) μA/cnf to 21.99 (±3.04) μA/crrr'. In contrast to the previous group, there was a marginally significant increase in current efflux at the base of the T follicle, from 2.43 (±0.68) $\mu A/cm^2$ to 24.05 (±3.06) $\mu A/cm^2$ (P=O.075), and an obvious but not statistically significant increase in current efflux at the apex of the T follicle, from 5.26 (±1.03) μA/crrr' to 28.26 (±3.42) μA/crrr',

Micropipette Applications

The method of micropipette applications of inhibitors is shown in Fig. 15a and b, with the results summarized in Fig. 16. Ouabain application reversed current efflux at the base of the T follicle, and had no effect on current efflux at the base of the tropharium. Both 4AP and TEA reversed current influx over the middle of the T follicle (P=0.056 and 0.001, respectively). Ethacrynic acid reversed current efflux at all the base and apex of the T follicle, and the base of the

tropharium, although statistical significance could not be shown. Both ethacrynic acid and verapamil significantly reversed current influx over the middle of the tropharium (P=0.032 and 0.011, respectively). Vanadate was not tested via micropippette application.

Effects of Inhibitors and Ion Substitution on Inward Apex T Currents

The effects of verapamil and Ca^{+2}/Mg^{+2}-free Ringers are summarized in Fig. 17a-c. Verapamil significantly reversed current influx at this location from 8.58 (±1.0) $\mu A/cm^2$ to 5.12 (±2.1) $\mu A/cm^2$ (P<O.OOOl). There was no significant difference after treatment with TEA. Exposure of whole ovarioles to Ca^{+2}/Mg^{+2}-free Ringers caused a marginally significant decrease the Apex Tin current, from -14.3 (±4.4) $\mu A/cm^2$ to 5.0 (±3.5) $\mu A/cm^2$ (P=0.071). Of 10 ovarioles placed in high K+ Ringers, 4 ovarioles showed significant reversals of current efflux at the Apex T position, from 7.53 (±3.1) $\mu A/cm^2$ to -6.33 (±3.7) $\mu A/cm^2$ (P=0.033).

DISCUSSION

Current Efflux Involves Active Na' Transport

The effects of two inhibitors of Na+transport, ouabain and ethacrynic acid, as well as Na" substitution experiments, indicates that a major component of the current efflux around Rhodnius ovarioles is carried by active Na" transport.

Marked differences in the relative effects of these inhibitors on the current pattern raise questions as to the actual mechanismts) of transport. To interpret these findings it is useful to review the possible modes of action of oubain and ethacrynic acid.

Oubain is a well-characterized cardiac glycoside and is a specific inhibitor of the ubiquitous Na'/K+ ATPase (Schwartz et a1., 1975; Skou, 1969). The glycoside receptor is on the beta subunit, and site-specific allosteric binding of ouabain inhibits K+ interaction at the same site. The Na"/K+ ATPase requires K+ at the external surface of the plasma membrane, and in some tissues is partly inhibited by furosemide and ethacrynic acid (Del Castillo and Robinson, 1985).

Ethacrynic acid is a diuretic agent which has been reported to inhibit Na"/K+ ATPases in a variety of mammalian systems (Davis, 1970; Duggon and Noll, 1965; Schwartz et a1., 1975), albeit with a somewhat broad spectrum of effects. Its main mode of action on Na"/K+ ATPase appears to be via interaction with the enzyme sulfhydryl groups, which are known to be required for enzyme activity (Davis, 1970; Duggon and Noll, 1965). Ethacrynic acid blocks phosphorylation of Na"/K+ ATPase while not inhibiting Nat-dependent phosphorylation (Charnock et a1., 1970), prevents the ADP-ATP exchange reaction and stabilizes phosphorylated intermediates (Schwartz et a1., 1975). Additionally, Perez-Gonzalez De La Manna et a1. (1980) have reported that ethacrynic acid can also affect a variety of other cellular processes, including glycolytic and mitochondrial ATP production.

Invertebrate Na"/K+ ATPases are known to vary in sensitivity to oubain (Anstee and Bowler, 1979), and ethacrynic acid has been used as an alternative to oubain to elucidate ion transport mechanisms. Fathpour et al. (1983) were able to show that both oubain and ethacrynic acid affected transepithelial potentials and fluid secretion in Locusta malphigian tubules; however, Berridge et al. (1976) found that ethacrynic acid but not ouabain could inhibit putative Na"/K+ATPase activity in Calliphora salivary glands.

Three lines of evidence support the existence of both Na"/K+-dependent and Nat-dependent ATPases in Rhodnius ovarioles. First, in support of the Na"/K+ ATPase involvement, ouabain had a significant, although relatively lesser, effect on current efflux than ethacrynic acid. There are no other known ATPases with which ouabain binds (Schwartz et al., 1975), and the results of this study are consistent with O'Donnell's (1986) report that Na"/K+ ATPase contributes to the oocyte resting membrane potential: when exposed to ouabain, the Rhodnius oocyte membrane potential is depressed. Suppression of current efflux by ouabain is consistent with the Na"/K+ pump location on the base-lateral membrane of epithelial cells (Davis, 1970; Fathpour et al., 1983), and with the 3:2 stoichiometry of Na"/K+ exchange.

Secondly, consistent with existence of either pump, Na" substitution experiments showed that at least a portion of current influx is due to Na+ entry. Suppression of Na" influx could depress the amount of intracellular Na" available for binding with either ATPase, thereby inhibiting current efflux (O'Donnell,

1986). Again, this is consistent with O'Donnell's (1986) report that Nat-free media depress (or depolarize) the membrane potential of Rhodnius oocytes. Thirdly, the fact that Kt-free Ringers did not cause a significant change in current, strongly argues for the presence of another ion motive force in addition to Na"/K+ ATPase. The existence of a Nat-dependent ATPase is suggested by the results of inhibitor and ion substitution experiments, although the results of the ethacrynic acid experiments must be viewed with caution. Since ethacrynic acid can also inhibit glycolytic and mitochondrial ATP production (Davis, 1970), the possibility exists that other ATP-driven transporters are present in this tissue.

There are at least two possible interpretations of the differential effects of ethacrynic acid and oubain on ionic currents around Rhodnius ovarioles. First, both of these agents may be inhibiting the same membrane-bound ATPase. In this case, the more marked effect of ethacrynic acid may be due to either i) its higher affinity for Na"/K+ ATPase, or ii) better permeation of ethacrynic acid. The initial difficulty in attaining a response to ouabain may have been due to an inability of this molecule to traverse the basal lamina and interact with pump sites. Nuccitelli and Wiley (1985) suggest that Reissner's membrane acts a barrier between ouabain and Na"/K+ ATPases in the developing mouse embryo, and Strange and Phillips (1985) postulate that the basal lamina of the insect salt gland also can prevent permeation of ouabain. The fact that ouabain applied by micropipette also alters currents at the base and apex of the T follicle further supports the idea that the basal lamina acts as a barrier.

The second interpretation is that ethacrynic acid inhibits other, distinct ATPases as well as Na"/K+ ATPase; Fathpour et al. (1983) suggest this as a plausible explanation for the more dramatic effects of ethacrynic acid on transepithelial potentials across Locusta epithelial cells. It seems likely that other ATP-dependent pumpts) is/are highly electrogenic and account for most of the transcellular current. . Gee (1976) shows that a Nat-dependent ATPase is present in the plasma membranes of epithelial cells of Glossina malphigian tubules, in addition to the Na"/K+-dependent ATPase. A Nat-stimulated ATPase in the renal proximal tubule, which is not dependent on K+ and which has a different Na" affinity and a different pH optimum has also been characterized (see Fathpour et al., 1983). Del Castillo and Robinson (1985) also demonstrate a pump with similar characteristics in the basolateral plasma membrane of guinea-pig intestinal cells; this pump has a very low affinity for ouabain, a high binding affinity for ethacrynic acid, and was secondarily inhibited by furosemide.

Other Mechanisms of Current Efflux

ATP-dependent transport

One possible active-transport candidate which cannot be excluded is the Ca^{+2} ATPase. Significant reversals in current efflux over the T oocyte and at the base of the tropharium are induced by vanadate and could be a result of the

inhibition of this pump. The pentavalent vanadate ion is capable, under certain conditions, of inhibiting Ca^{+2} ATPases in the plasma membrane of erythrocytes (Bond and Hudgins, 1980) and in the sarcoplamsic reticulum (Highsmith et al., 1985); this is probably a result of competition with Ca^{+2} for the high-affinity Ca^{+2} binding site (Dux and Martonosi, 1983).

As with any pharmacological agent, one must be aware of dosage-dependent effects and differences in tissue specifity. Hajjar et al. (1986) have demonstrated that at low concentrations (10^{-4} M), vanadate causes Cl, Na", and water secretion in the rat jejunum by stimulation of adenylate cyclase. At higher concentrations (10^{-3}-10^{-2} M), vanadate inhibits absorption of Na" and Cl- by inhibition of Na"/K+ ATPase (Hajjar et al., 1986). At the concentration range used in my study, it is possible that vanadate could have inhibited Ca^{+2} ATPase and/or Na+/K+ ATPase. If vanadate inhibits the same pump as ethacrynic acid and/or ouabain, differences in the effects of these inhibitors could have been due to: (i) differential permeability and access to pump binding sites; (ii) differences in ATPase affinity; or (iii) inhibitor-specific secondary effects, especially in the case of both ethacrynic acid and vanadate.

Unlike ouabain or ethacrynic acid, vanadate induces a highly significant increase in current efflux at the apex of the T follicle. It is plausible that vanadate increases an existing ion conductance or uncovers a previously electrically silent one through an effect on adenylate cyclase. By contrast, this differential effect on current efflux at the apex of the T follicle may indicate that a vanadate-specific

pump is not located at this location.

The reason for the variation in responsiveness of current efflux at the base of the tropharium to vanadate is unclear, although it may be indicate that within ovarioles of the same size group there are different transport mechanisms at the base of the tropharium. A more credible explanation is that these differences are the result of variations in ovariole physiology *(e.g.,* intracellular energy levels, phosphoenzyme concentrations) which make them less susceptible to vanadate inhibition. Whatever the mechanism behind these heterogeneities in sensitivity, data from the vanadate experiments underscore the fact that the local current circuit around the tropharium can persist despite global changes in extracellular currents around the T follicle. Although it has been clearly shown that the T follicle is electrically coupled to the tropharium via the trophic cord and that injury to the T follicle is reflected in changes in current patterns around the tropharium (Chapter I), substantial changes in current efflux over the T follicle do not necessarily disrupt extracellular currents around the tropharium (Fig. 14b). This is further evidence that the tropharium and T follicle may be setting their own resting potentials, and that extracellular current patterns around intact ovarioles are not necessarily contradictory, at least in Rhodnius, with oocyte/tropharium intracellular potentials.

Passive transport

Another possibility is that current efflux is carried by K^+ ions. O'Donnell

(1986) has shown pharmacologically the presence of voltage-gated K^+ channels in the oocyte membrane; exposure of Rhodnius oocytes to 5 rnrnol l^{-1} 4-AP potentiates Ca'<based action potentials and higher concentrations depolarize the oocyte resting potential by several millivolts, suggesting that there is a nominal resting K^+ conductance. There is also precedence to suggest K^+ as a major carrier of current efflux: outward current flux leaving the first cleavage furrow of Xenopus eggs is carried mainly by K^+ ions (Kline et al., 1983).

It is not possible to resolve, on the basis of anyone experiment, whether K^+ efflux carries part of the extracellular current. The results of the K^+ replacement experiment are difficult to interpret, since in almost all cells, a change in extracellular K^+ will change both the resting membrane potential and the K^+ concentration gradient (Kline et al., 1983; Kuffler et al., 1984). If K^+ efflux carries a major part of the extracellular current, I would expect K^+ replacement not to change the total electrochemical driving force on K^+; theoretically, there would be no change in the extracellular current pattern, which is in fact what was observed. High external K^+ depolarizes Rhodnius oocytes (O'Donnell, 1986), and would probably reduce or reverse transcellular currents, which also was observed. However, similar effects are also plausible even if K^+ efflux is not involved as a current carrier.

The results of TEA exposure and micropipette application are also not definitive. Both of these treatments significantly reduced extracellular currents over a short time-course, but at a totally unexpected location. The reversal in

current influx over the middle of the T follicle would be explained by a significant reduction or reversal of current efflux elsewhere over the T follicle. However, micropipette application of TEA over the apex and base of the T follicle had no significant effect, and exposure of entire ovarioles to this K^+ channel blocker did not cause a statistically significant decrease in current efflux (Figs. 16 and 10, respectively).

Diehl-lones and Huebner (1989a) earlier show that, by 10 min post-exposure there is a significant decline in current (Diehl-lones and Huebner, 1989a). Besides the difference in time course, the present study also differed from the previous one in that Ringers with TEA was prepared by equimolar substitution with Na". The longer-term effect on transcellular currents could have been due to secondary or cumulative of TEA on currents, or it may have been due to osmotic effects. Unlike the previous study, all salines in the present study were osmotically balanced. Within a short time course, however, TEA does not substantially affect current efflux, and this is consistent with O'Donnell (1986) who showed that TEA does not significantly affect the resting membrane potential of Rhodnius oocytes exposed to the same concentrations of TEA. One explanation of the TEA-induced perturbation is that, while K^+ may not be a major current efflux carrier, there are likely some K^+ channels in the plasma membrane in the middle of the T follicle which are in an open state at resting membrane potentials. Potassium efflux would be masked by the larger current influx; perturbation of K^+ channels in this region may then have a local effect on the labile, passive ion

flux that *carries* the inward current. The apparent imbalance in current flux created by application of TEA (or of 9AC) more likely is indicative of the fact that current flux over all areas of the ovariole could not be monitored. When only local current perturbations are involved, fluctuations in current flow which must occur to balance electroneutrality are either not detected or are evident only in terms of the total trans-ovariole current fluctuations.

Externally-applied Ba^{+2} has been shown to decrease K^+ conductance in several different cell types (Hermsmeyer and Sperelakis 1970; Standen and Stanfield, 1978; Nielsen, 1979). Externally-applied Ba^{+2} has no effect on currents around the T follicle. The situation is different around the tropharium; Ringers with Ba^{+2} substituted for Ca^{+2} has a marked effect on current efflux at the base of the tropharium, and this will be discussed in a later section. Taken together, however, the data suggest that K^+ does not carry a significant portion of the current efflux around the T follicle, although there is likely a resting K^+ conductance.

Current Influx Over the T *Follicle Involves Na: Influx and* Cl^- *Efflux*

The results of Na" substitution and tetrodotoxin experiments suggest that part of the current influx over both the T follicle and the tropharium is carried by Na" influx. Significant decreases in current influx occur at all positions measured, and are reflected by corresponding decreases in current efflux. Inward current is not associated with either Na"/glucose or Na"/amino acid symport, as

demonstrated by the glucose substitution experiments and the lack of amino acids in the recording medium. A Na" influx is also consistent with O'Donnell's (1986) report that replacement of Na" with choline reduces the resting membrane potential of Rhodnius oocytes. Reduction of Na" influx and subsequent lowering of cortical intracellular Na" levels could inhibit electrogenic Na"/K+ or Na" ATPases. The Nat-based influx is a common motif in several animal systems. Current influx over the anterior or nurse cell end of Drosophila follicles is carried by Na" (Overall and Jaffe, 1985), and current entering the pigmented membrane of cleaving Xenopus eggs is carried in part by Na" (Kline et al., 1983). Sodium also carries current influx in regenerating amphibian limbs (Borgens et a1., 1979).

A portion of current influx is probably also carried by Cl efflux. This is strongly suggested by the results of 9AC exposure. The Cl substitution experiments suggest a more general involvement of Cl' in current influx. Replacement of cr with SO_4^{-2} would have increased the concentration gradient of Cl' within the ovariole, thereby increasing the outward driving force on Cl', Current influx in the S04-2-substitution media increases at all locations measured, although this is significant only over the middle of the tropharium; current efflux significantly increased at the T connective, which would enable maintenance of electroneutrality. Bromide-substituted media do not in general produce increases in current flux as large as those in SO_4^{-2}-substituted media, which is consistent with our earlier findings (Diehl-lones and Huebner, 1989). This may be due to the fact that Br- ions have a hydrated radius similar to that of Cl ions. The

change in intracellular Cl' activity would not be as great as that in SO_4^{-2}-substituted media. Considering both the inhibitor and the substitution data, it is likely that CI- efflux is involved in current influx over the middle of the T oocyte. Again, this pattern is similar to one suggested by Overall and Jaffe (1985) for Drosophila ovarioles. During chorion formation, basal current influx is thought to be carried by CI- efflux. Current influx over the tropharium of Rhodnius could also be carried CI- efflux, but this is not confirmed by the 9AC experiments. The data do, however, definitively show that active Cl transport is not involved in current efflux, which differs from 5arcophaga follicles (Verachtert, 1988).

Current Influx Over the Tropharium Involves Ca^{+2}

Experiments with organic Ca^{+2} channel blockers strongly implicate Ca^{+2} ion influx over the tropharium, but not over the T follicle. Diltiazem and verapamil, which are from distinct classes of organic compounds (Lee and Tsien, 1983) produced very similar changes in the extracellular current pattern. In both series of experiments, current influx over the middle of the tropharium is significantly reduced, and current efflux at the base of the tropharium is abolished or reversed. There are no significant changes in the current pattern around the T follicle (Fig. 10a,b).

The fact that Mn^{+2} substitution, an inorganic channel blocker with a different mode of action, produces a very similar change in current pattern (Fig. 4c) further increases confidence that Ca^{+2} carries part of the inward current over

the tropharium. Inorganic blockers such as Mn^{+2} and Cd^{+2} are believed to compete with Ca^{+2} for a metal cation coordination site within Ca^{+2} channels (Hagiwara and Byerly, 1983), whereas organic blockers such as verapamil and diltiazem are hypothesized to bind to another cation binding site closer to the inside of the membrane (Lee and Tsien, 1983).

Diehl-lones and Huebner (1989a) report that Co^{+2} substitution does not significantly affect inward currents over the tropharium was confirmed over a shorter time course (Fig. 14b). This seems at first contradictory to the effects of Mn^{+2}, but is probably due to the fact that a Ca^{+2} chelator such as EGTA was not used, and that Co^{+2} was in relatively low concentrations (2 mM). There may have been sufficient Ca^{+2} present around the ovariole to carry the current and out-compete the Co^{+2}. Zivkovic (1990) suggests that by not using a Ca^{+2} chelator in substitution media there may be enough Ca^{+2} left in the medium to support inward Ca^{+2} currents over Lyrnnea embryos. Furthermore, by replacing both Ca^{+2} and Mg^{+2} with Mn^{+2}, the final concentration of Mn^{+2} is 10.5 mM, which likely produces a more complete blockage of inward Ca^{+2} flux.

When Ba^{+2} was substituted for Ca^{+2} (Fig. 4), a familiar pattern of current disruption was evident (Fig. 18a,b): significant reductions in current flux were observed at the base and middle of the tropharium. In view of the previous results with Ca^{+2} channel blockers, I hypothesize that Ba^{+2} inhibits, either directly or indirectly, the current efflux at the base of the tropharium. By decreasing ion conductance at the base of the tropharium, a current loop between the base and

the rest of the tropharium is essentially uncoupled, resulting in a decrease in the inward driving force on Ca^{+2} and Na" ions. Barium could exert its effects via either intracellular or extracellular mechanisms, since Ba^{+2} ions are known to pass through L-type calcium channels more easily than Ca^{+2} (Bean,1985). Thus, in this model, Ba^{+2} could either displace intracellular Ca^{+2} as the dominant divalent cation and thereby inhibit $Ca^{+2\text{-gated}}$ conductances, or could itself negatively gate current efflux. Within this model, Ba^{+2} substitution and Ca^{+2} channel blockade would have the same effect of uncoupling the "trans-tropharium" current.

An obvious candidate for negative-gating is the K^+ channel. Calcium-gated K^+ channels have been well established, and play an important role in cell metabolism (Kuffler et al., 1984). Such channels could also play an important role in the nominal functioning of a Na"/K^+ pump at the base of the tropharium. If K^+ efflux is blocked, net Na" outward flux would have to be reduced to maintain electroneutrality. Barium ions are known in a number of systems to block K^+ conductance (Hermsmeyer and Sperelakis, 1970; Standen and Stanfield, 1978; Nielsen, 1979), and according to this hypothesis could inhibit the putative Na"/K^+ pump.

Figure 18a,b shows the effect of barium exposure on the tropharium; the same basic pattern results after exposure to manganese and high potassium as well (Fig. 19a-c). In Fig. 19a, a current loop is maintained by inward Ca^{+2} and Na" flux over the middle of the tropharium and outward current flux generated mainly by a Na"/K^+ ATPase. Potassium channels, which do not contribute

significantly to the outward current flux at the base of the tropharium, are required for efflux of intracellular K^+ ions pumped in by the ATPase. In Fig. 19b, uncoupling of the current loop is brought about by a Mn'<induced decrease in Ca^{+2} conductance. Not depicted in this figure is the possibility that intracellular Ca^{+2} positively gates ion conductances; a reduction in intracellular Ca^{+2}, in this case, would further uncouple the circuit. In Fig. 19c, inhibition by either intracellular and/or extracellular Ba^{+2} is represented. If K^+ efflux is blocked, the Na"/K+ pump would necessarily be inhibited to maintain electroneutrality. Also depicted in Fig. 19a-c is a conductance at the base of the tropharium which is normally masked by the electrically larger Na"/K+ pump and K^+ efflux. As shown, this could be either an influx of positive ions or efflux of negative ions (represented by X^+ and X^-, respectively). When the current loop is uncoupled, the inward current usually seen is hypothetically carried via this channel. A further possibility is that this conductance is very low during normal functioning, and is increased during uncoupling, either by a more favourable electrochemical gradient or an unknown gating mechanism.

This model is also consistent with the observed effects of high external K^+ (Fig. 3b). This treatment would also uncouple the tropharium current loop by reversing the outward-driving chemical gradient on K^+ and inhibiting the Na"/K+ ATPase. The change in current pattern in high K^+ Ringers is striking similar to the that observed after treatment with organic and inorganic Ca^{+2} channel blockers and Ba^{+2}. TEA treatment might have been expected to produce similar

effects. As with ouabain treatments, it seems likely that K^+ channel sites were difficult to reach; the basal lamina thickens noticeably over the tropharium (Huebner and Anderson, 1972c) and this barrier and/or the long follicular epithelial cells at the base of the tropharium could have obstructed permeation. Alternatively, TEA may not be a pharmacologically compatible inhibitor for this particular channel. .

Finally, this model explains what initially was thought to be an inconsistency with our earlier observation that Ba^{+2} increases current influx over the tropharium 10 min P.E. (Fig. 1). In fact, the difference in response to Ba^{+2} probably reflects a time-dependent effect. Nielsen (1979) and Hermsmeyer and Sperelakis (1970) have shown in frog skin and cardiac muscle cells, respectively, that externally-applied Ba^{+2} has a biphasic effect on K^+ channels. The initial, or primary effect is to decrease K^+ conductance, and occurs almost immediately after Ba^{+2} exposure. The secondary effect is to increase K^+ conductance; this starts to occur 2 to 5 minutes after Ba^{+2} exposure (Nielsen, 1979). According to the model, alterations in K^+ channel conductance could well explain the decrease in current influx within two minutes post-exposure, followed by the significant increase by 10 min P.E. The increase in current influx measured over the tropharium could be due to the relatively higher Ba^{+2} conductance through Ca^{+2} channels once the K^+ channel conductance is restored.

It is difficult to interpret the marginally significant increase in current flux induced by TMB8 over both the base and the middle of the tropharium. Since

this agent is known to prevent the release of Ca^{+2} from the endoplasmic reticulum (Chiou and Malagodi, 1975; Owen and Villereal, 1982), it is possible that the free intracellular Ca" concentration decreased. This conceivably would increase the inward driving force on extracellular Ca^{+2}, resulting in increased current influx. Since this latter result is based on a sample size of 3, these results must be viewed with caution, although the finding that ovarioles with inward Ca^{+2} currents (N=4) do not respond in a measurable way to TMB8 is consistent with this interpretation. More definitive tests should include microinjection of a Ca^{+2} chelating buffer such as BAPTA (see Kropf, 1989; Speksnijder et al., 1989). This could possibly shed light on both the physiological rolets) of intracellular Ca^{+2} in Rhodnius ovarioles and whether or not Ca^{+2} is either positively or negatively gating ion conductances in the tropharium.

Ca^{+2}-Inward Currents Correlate with Ca^{+2} Ion Localization

The inward Ca^{+2} currents described over the middle of the tropharium correlate with elemental analysis using Electron Spectroscopic Imaging (ESI) (Huebner and Heinrich, *in prep.)* With this technique, Ca'<rich precipitates were localized in follicle cells and in some nurse cells coinciding with the general area of Ca^{+2} ion influx. It is not known whether this represents free or bound Ca^{+2}.

Influx Over the Apex of the T Follicle Is *a Ca^{+2} Current*

Based on both the micropipette applications and on ion substitution

experiments, it is clear that the inward currents over the Apex T position is carried by Ca^{+2} ions. The spatial and temporal timing of these currents have several physiologically relevant implications. First, the area of Ca^{+2} influx is close to the trophic cord, and could represent a possible signal or mechanism by which the trophic cord closure is effected. Since intracellular Ca^{+2} is well known to influence cytoskeletal dynamics via interaction with cytoskeletal-associated protein (Forscher, 1989), Ca^{+2} influx could promote changes in both the microtubules and F-actin of the trophic cord, thereby initiating trophic cord closure, a mechanism not well understood. Second, Ca^{+2} influx may regulate the development of the oocyte apical cortical cytoskeleton, which is markedly different from the rest of the oocyte (Graham-McPherson and Huebner, *in prep.).* Third, Ca^{+2} may gate yet other ion conductances which contribute to regulating oocyte physiology and development. Finally, the influence of intracellular Ca^{+2} on the oocyte could be mediated via $Ca^{+2\text{-binding}}$ proteins such as calmodulin (Alberts et al., 1990; Kakiuchi and Sobue, 1983; Dinsmore and Sloboda, 1988).

It is unlikely that the Ca^{+2} influx at the apex of the T follicle is the same Ca^{+2} action potential described by O'Donnell (1985, 1986) in Rhodnius oocytes. The mean duration of evoked action potentials was 2.6s in normal Ringers and as long as 120s in $Ba^{+2\text{-supplemented}}$ Ringers. By contrast, the inward current over the apex of the T follicle usually lasts several minutes (see Chapter 1). Transient current influxes were measured over the apex of the T follicle in high K^{+} Ringers which were probably the rising phase of Ca^{+2} action potentials;

however, the temporal resolution of the vibrating probe is much lower than that of standard intracellular electrodes, so it is difficult to measure action potentials with accuracy. However, depolarization of follicles with high K^+ Ringers showed that, in 4 out of 10 ovarioles, transient reversals in current occur in the same area where steady state Ca^{+2} can occur; whether this is in fact an action potential is unclear.

O'Donnell (1985) has suggested that Ca'<based action potentials in Rhodnius may be involved in developmental events at the time of fertilization, such as an electrical or fast block to polyspermy, or may serve to raise cytosolic Ca^{+2}levels. Alternately, such action potentials "may be present in preparation for future development into excitable cells" (O'Donnell, 1985). The presence of steady-state, temporally and spatially segregated Ca^{+2} currents supports the latter statement, and strongly suggests that an involvement in action potentials may not be the only function these Ca^{+2} channels. Simoncini et al. (1988) show that lineage-specific Ca^{+2} currents develop shortly after gastrulation in Boltenia villosa embryos; localized inward Ca^{+2} currents in Rhodnius oocytes may reflect one of the mechanisms by which a portion of the oocyte acquires a different developmental fate.

Summary of Ionic Basis of Transcellular Currents

An overview of the proposed ionic basis of transcellular currents around Rhodnius ovarioles is presented in Fig. 20. I propose that current efflux is

generated by Na+/K+ ATPase and possibly also by a Na" ATPase not dependent on K+; the return current loop is carried over the middle of the T follicle by Na+ influx and Cl- efflux. Given the direction of current efflux over the apex of the T follicle and the T connective, as well as the current pattern over denuded subterminal oocytes (see Chapter I), a portion of the current efflux probably returns via influx over the T-1 follicle and the tropharium. Current efflux at the base of the tropharium is also likely generated by a Na"/K+ A'TPase, and the return circuit over the tropharium is carried by Ca^{+2} and Na" influx.

The relative contributions of follicle cells versus germ cells is not explicitly indicated in this model. However, based on examination of current patterns around intact and denuded ovarioles (Chapter 1), it is likely that the germ cell membranes contribute at least part of the current. Since currents around denuded oocytes and tropharia are invariably weaker than in intact ovarioles (Chapter I), it is possible that follicle cells and germ cells both contribute to current generation. Regardless of the relative contributions of germ cell and follicle cell membranes, current entering the follicle cells must also enter the germ cells (Nuccitelli, 1990), since they are well-coupled via gap junctions (Huebner, 1981b). This is supported by electron spectroscopic imaging, which shows that there are $Ca^{+2\text{-rich}}$ follicle cells and nurse cells (Huebner and Heinrich, *in prep).*

Generation of current efflux by Na"/K+ ATPase is in agreement with earlier characterizations by Abu-Hakima and Davey (1979) and Ilenchuk and Davey (1982, 1983) of a juvenile hormone-sensitive Na"/K+ ATPase in vitellogenic

Rhodnius follicle cells. It is well known that cardiac glycoside-sensitive Na"/K+ ATPases and Na" ions are involved in regulation of cellular volume (MacKnight and Leaf, 1977). Huebner and Injeyan (1980) found that the degree of patency of follicle cells is increased by application of juvenile hormone (JH) and that this effect is inhibited by application of antigonadotropin. Abu-Hakima and Davey (1977) propose that follicle cell volume is differentially regulated by two populations of Na"/K+ ATPase, and that this is in turn mediated by Juvenile hormone (Ilenchuk and Davey, 1982). Furthermore, Sigurdson (1984) shows that current densities over the apex and base of T follicles, as well as the basal and mid-lateral surfaces of tropharium are significantly modulated by a JH analogue, Altosid. Sigurdson (1984) also proposes that an antigonadotropin prevents the appearance of the second group of JH sensitive sites - presumably Na"/K+ ATPase -- and therefore inhibits follicle cell volume changes in virgin female Rhodnius ovarioles, which have been previously shown to have a lower degree of follicle cell patency (Huebner and Davey, 1973). The Na"/K+ ATPase may not be the only target of insect hormones; Vilain et al. (1989) show that progesterone modulates outward Ca'<gated cr currents during meiosis in Xenopus oocytes, and Rodeau and Vilain (1987) show progesterone-induced changes in intracellular Na" and Cl" activities in the oocytes of other amphibians.

Modulation of follicle cell patency is one possible physiological role for a Na"/K+ ATPase in Rhodnius follicles. To correlate more definitively the spatial and temporal pattern of extracellular currents to a physiological response, it is

necessary to selectively inhibit these currents with ion substitutions and inhibitors and monitor the effects on oocyte physiology. This is the basis for the following chapter, in which I demonstrate that Na^{+}-free Ringers and ethacrynic acid markedly effect a dynamic cellular process, that of fluid phase endocytosis. Other possible functions of the transcellular currents, especially the role of Ca^{+2} influx over the tropharium and the apex of the T follicle, are not yet known, and offer challenging problems for future investigations. Finally, before conclusive identification of ion pumps and channels can be offered, patch clamp analysis of follicle cell and germ cell membranes are required. In this manner, it will be possible to fully characterize these membrane-bound proteins electrophysiologically, as well as the factors gating or regulating their activity.

Table 1 : Composition and Concentration (mM) of Ion-Substituted Media

Component	Control	Ion Substitutions						
		1	2	3	4	5	6	7
NaCl	129.0	137.6	-	129.0	129.0	129.0	-	-
KCl	8.6	-	8.6	8.6	8.6	8.6	-	-
$MgCl_2$	8.5	8.5	8.5	-	8.5	8.5	-	-
$CaCl_2$	2.0	2.0	2.0	-	-	-	-	-
Glucose	34.0	34.0	34.0	24.0	24.0	34.0	34.0	34.0
Bis-Tris	15.0	15.0	15.0	15.0	15.0	15.0	15.0	15.0
Choline Cl	-	-	129.0	-	-	-	-	-
$MnCl_2$	-	-	-	10.5	-	-	-	-
$BaCl_2$	-	-	-	-	2.0	-	-	-
$CoCl_2$	-	-	-	-	-	2.0	-	-
NaBr	-	-	-	-	-	-	129.0	-
KBr	-	-	-	-	-	-	8.6	-
$CaBr_2$	-	-	-	-	-	-	2.0	-
$MgBr_2$	-	-	-	-	-	-	8.5	-
Na_2SO_4	-	-	-	-	-	-	-	64.5
K_2SO_4	-	-	-	-	-	-	-	4.3
$CaSO_4$	-	-	-	-	-	-	-	2
$MgSO_4$	-	-	-	-	-	-	-	8.5

N.B. pH=6.8
Bis Tris=(bis[2-Hydroxyethyl]imino-tris[hydroxymethyl]methane)

Table 2: Channel Blockers, Inhibitors and Modes of Action

Agent	Mode of Action
Amiloride (2mM)	Blocks Na^+/H^+ countertransport
4-Aminopyridine (1mM)	K^+ channel blocker (does not affect Ca^{+2}-activated K^+ channels)
9-AC (100μM)	Cl^- channel blocker
Cobalt	Ca^{+2} channel blocker
DIDS (0.5mM)	Cl^-/HCO_3^- exchange inhibitor
Diltiazem (2mM)	Ca^{+2} channel blocker
Ethacrynic Acid (1mM)	Inhibits Na^+/K^+ ATPase and Na^+ transport not dependent on K^+
Furosemide (1mM)	Inhibits Cl^- transport
Manganese	Ca^{+2} channel blocker
Ouabain (0.1-1.0mM)	Inhibits Na^+/K^+ ATPase
TEA (100mM)	Blocks voltage-dependent K^+ channels
Tetrodotoxin (0.5mM)	Na^+ channel blocker
TMB-8 (0.2mM)	Blocks intracellular Ca^{+2} release
Vanadate (3mM)	Inhibits several ATPases
Verapamil (5mM)	Ca^{+2} channel blocker

9-AC=anthracene-9-carboxylic acid
DIDS=4-4'-diisothiocyano-2,2' disulfonic acid
TEA=tetraethylammonium chloride
TMB-8=8-(N,N-diethylamino)-octyl 3,4,5-tri-methoxybenzoate hydrochloride
Vanadate=sodium orthovanadate

Figure 1

Initial results of inhibitor and ion substitution experiments. T-Con = connective to the terminal oocyte; T-1 = T-1 follicle; Base Troph = basal portion of the tropharium; and Mid Troph = middle of the tropharium. Note that Base Troph and Mid Troph roughly correspond to Mid Tr and Apex Tr, respectively, in the present study. C = control medium. At times 10, 20, and 30 min post-exposure ovarioles were incubated in experimental media, after which the medium was replaced with normal Ringers. N = 5 replicates/experiment.

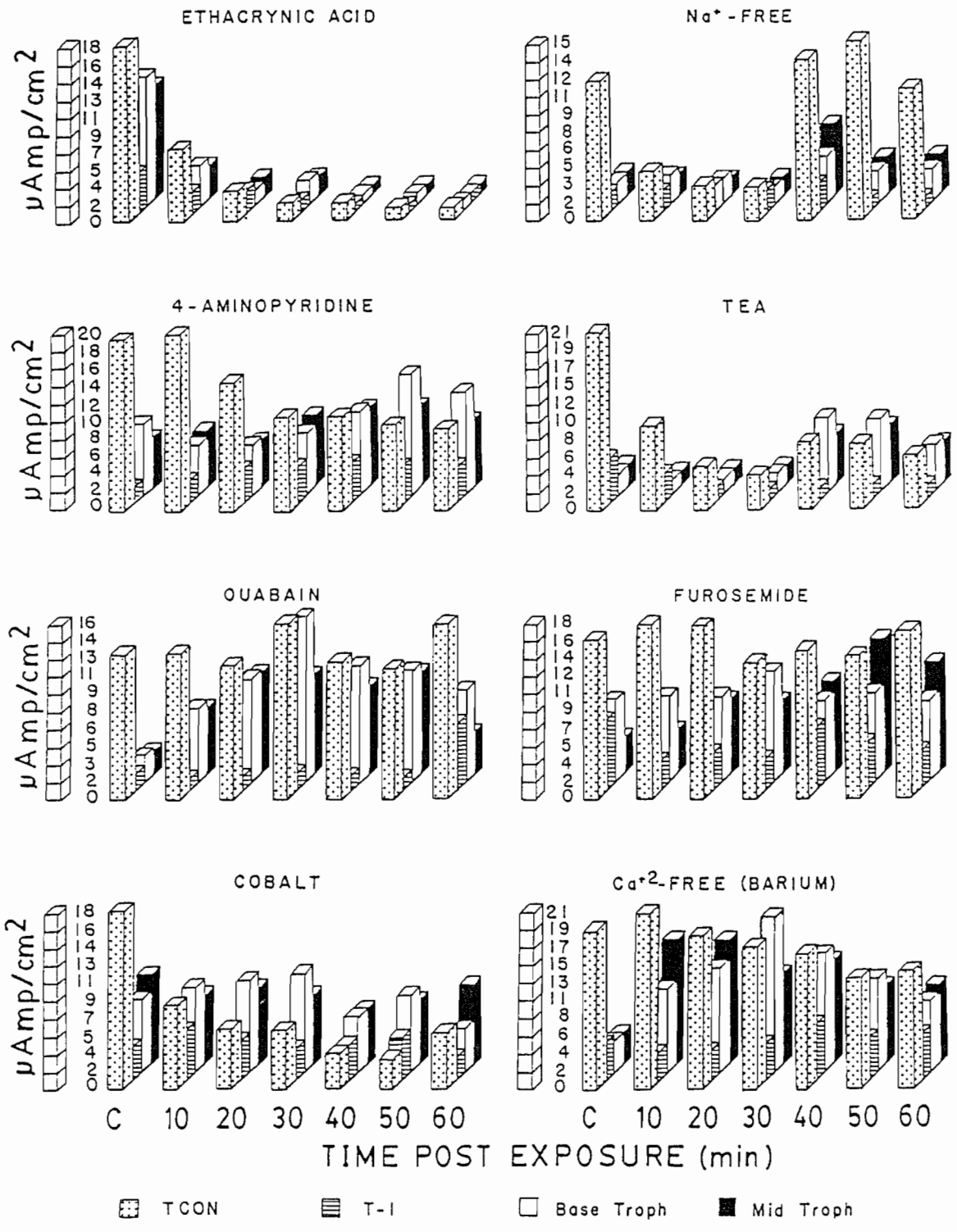
ETHACRYNIC ACID
Na+ - FREE
4 - AMINOPYRIDINE
TEA
OUABAIN
FUROSEMIDE
COBALT
Ca+2 - FREE (BARIUM)
μAmp/cm2
C 10 20 30 40 50 60
TIME POST EXPOSURE (min)
TCON
T-1
Base Troph
Mid Troph

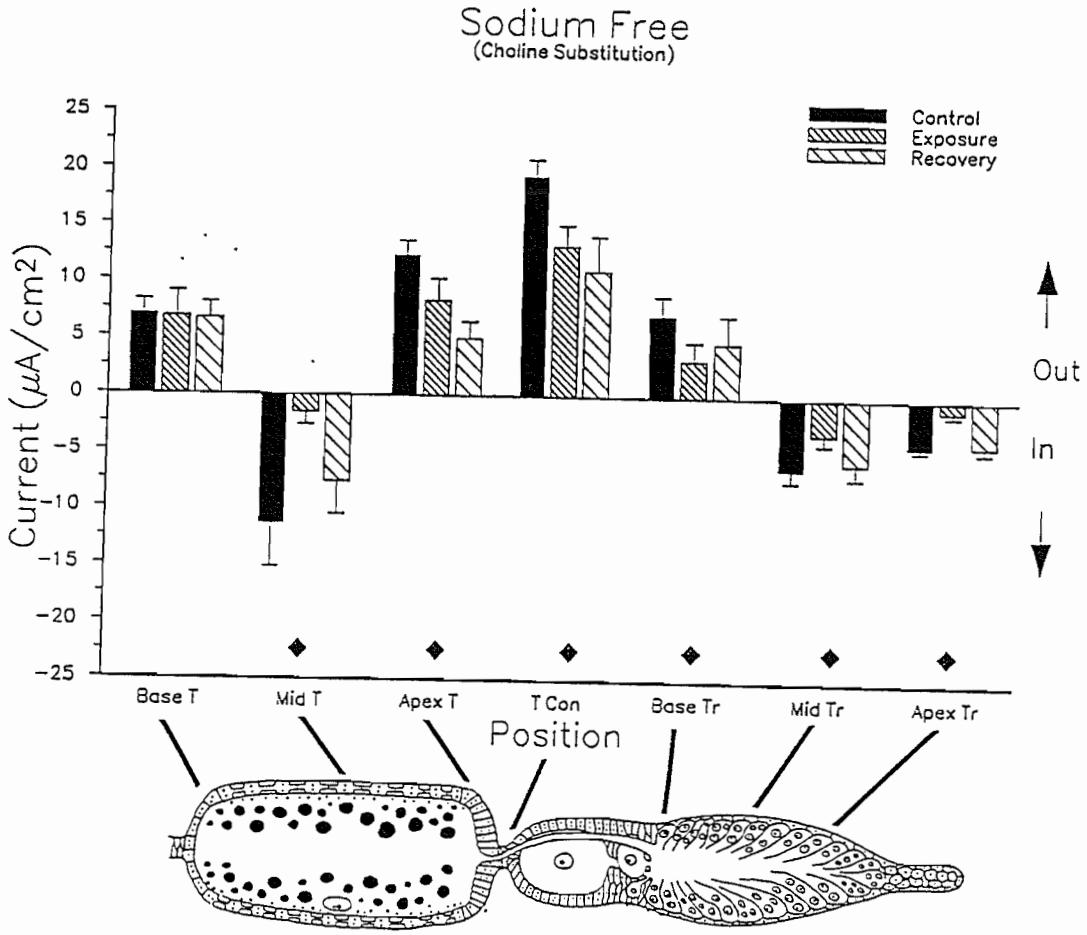

Figure 2

Changes in mean extracellular current density around ovarioles in sodium-free Ringers (±SEM). ♦ = significant difference ($P<0.05$); ◊ = marginally significant difference ($0.10>P>0.05$). Lines drawn to ovariole inset indicate recording positions. N=11.

Figure 3

Mean current densities around ovarioles in K^+-perturbed Ringers (±SEM). ♦ = significant difference ($P<0.05$); ◊ = marginally significant difference ($0.10>P>0.05$). *a)* K^+-free substitution) Ringers. Differences are not significant. N=5. *b)* High K^+ (120mM) Ringers. Current direction reverses at Base TR; current magnitude significantly decreases at all positions except Base T and Apex Tr. N=8.

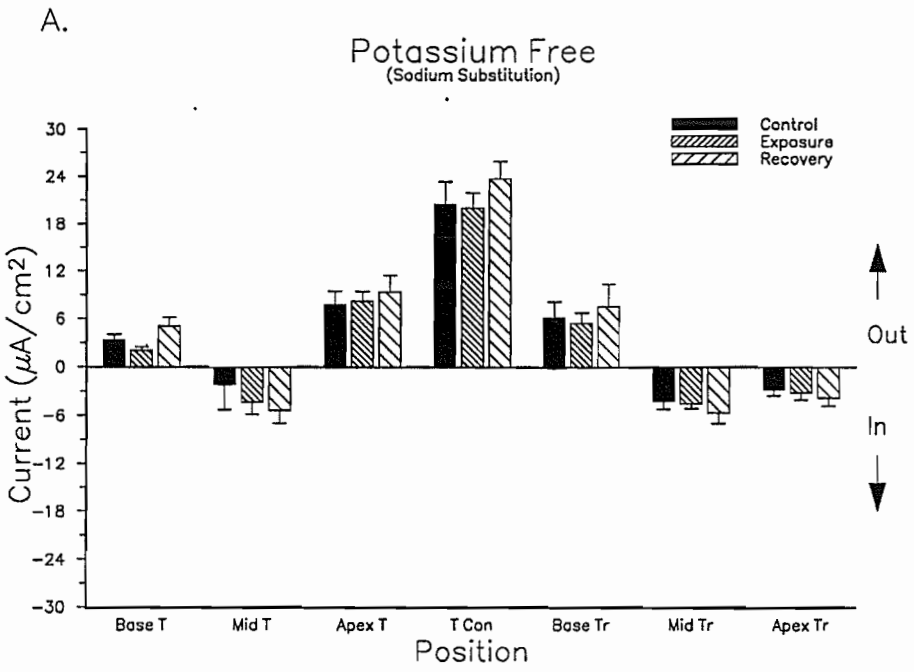
A.
Potassium Free
(Sodium Substitution)
Control
Exposure
Recovery
Current (μA/cm²)
30
24
18
12
6
0
−6
−12
−18
−24
−30
Out
In
Base T
Mid T
Apex T
T Con
Base Tr
Mid Tr
Apex Tr
Position

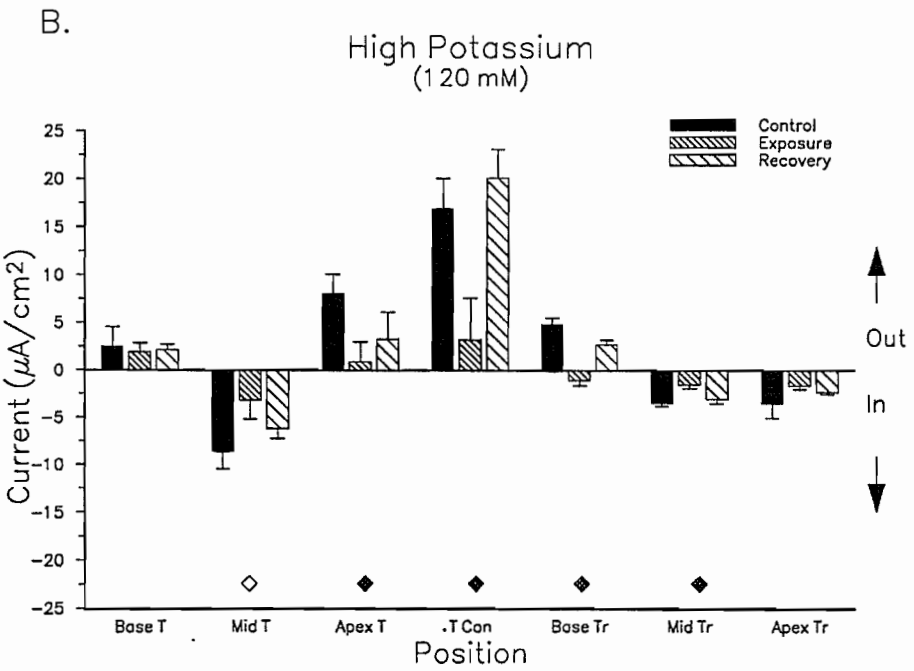
B.
High Potassium
(120 mM)
Control
Exposure
Recovery
Current (μA/cm²)
25
20
15
10
5
0
−5
−10
−15
−20
−25
Out
In
Base T
Mid T
Apex T
.T Con
Base Tr
Mid Tr
Apex Tr
Position

Figure 4

Mean extracellular current densities around ovarioles in Ca^{+2} or Ca^{+2}/Mg^{+2}-free Ringers. ♦ = significant difference ($P<0.05$). *a)* Ba^{+2} substituted for equimolar Ba^{+2}. Current direction reverses at Base Tr and decreases at Mid Tr. N=5. *b)* Co^{+2} substituted with equimolar Ca^{+2}. There are no significant differences in current magnitude or direction. N=5. *c)* Mn^{+2} substituted for equimolar Ca^{+2} and Mg^{+2}. Changes in current magnitude and direction are similar to Figure 5a, except for significant decrease at Apex Tr. N=10.

A.

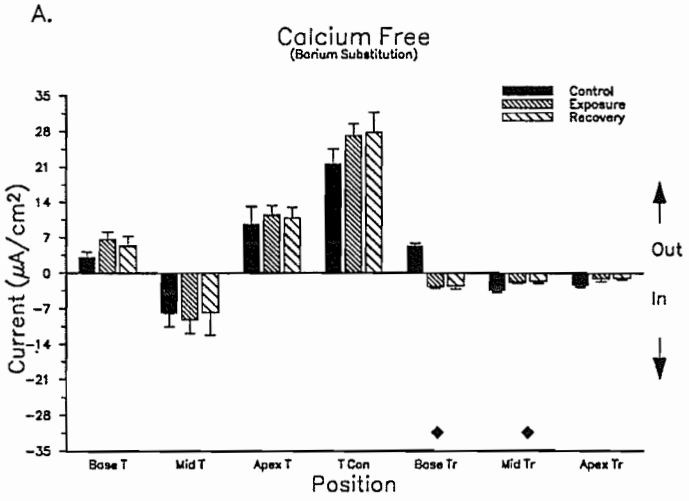
Calcium Free
(Barium Substitution)
Control
Exposure
Recovery
Current (μA/cm²)
35
28
21
14
7
0
-7
-14
-21
-28
-35
Out
In
Base T
Mid T
Apex T
T Con
Base Tr
Mid Tr
Apex Tr
Position

B.

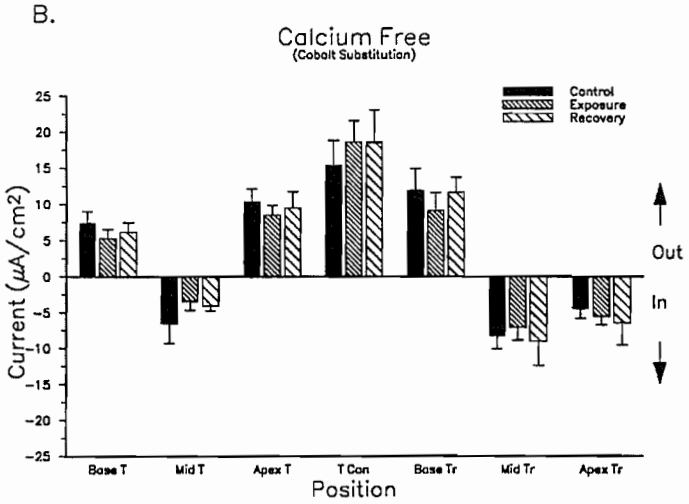
Calcium Free
(Cobalt Substitution)
Control
Exposure
Recovery
Current (μA/cm²)
25
20
15
10
5
0
-5
-10
-15
-20
-25
Out
In
Base T
Mid T
Apex T
T Con
Base Tr
Mid Tr
Apex Tr
Position

C.

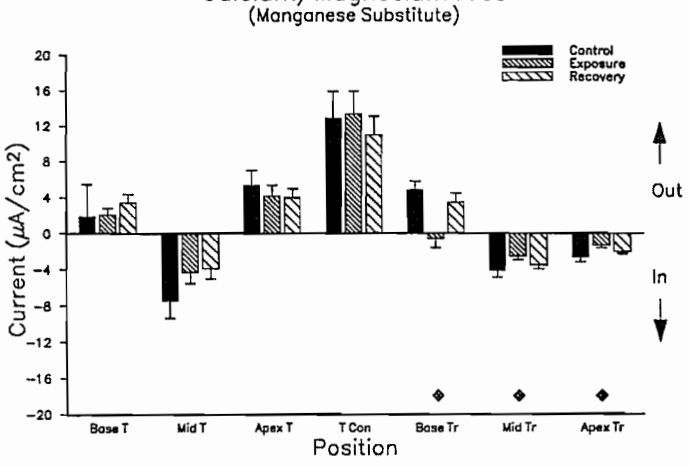
Calcium/Magnesium Free
(Manganese Substitute)
Control
Exposure
Recovery
Current (μA/cm²)
20
16
12
8
4
0
-4
-8
-12
-16
-20
Out
In
Base T
Mid T
Apex T
T Con
Base Tr
Mid Tr
Apex Tr
Position

Figure 5

Mean extracellular current densities around ovarioles in Cl^--free Ringers. ♦ = significant difference ($P<0.05$); ◊ = marginally significant decrease ($0.10>P>0.05$). *a)* Cl^- substituted with equimolar Br^-. There is a marginally significant increase in current magnitude at Base Tr. N=7. *b)* Cl^- substituted with equimolar SO_4^{-2}. There are significant decreases in current influx and efflux at T Con and Mid Tr, respectively. N=9.

A.

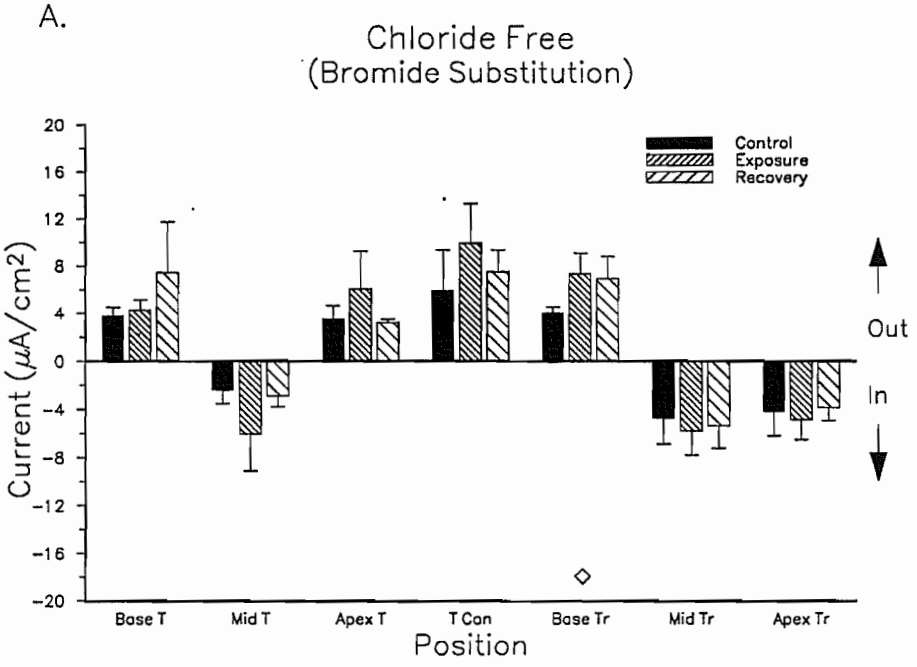
Chloride Free
(Bromide Substitution)
Control
Exposure
Recovery
Current (μA/cm²)
20
16
12
8
4
0
-4
-8
-12
-16
-20
Out
In
Base T
Mid T
Apex T
T Con
Base Tr
Mid Tr
Apex Tr
Position

B.

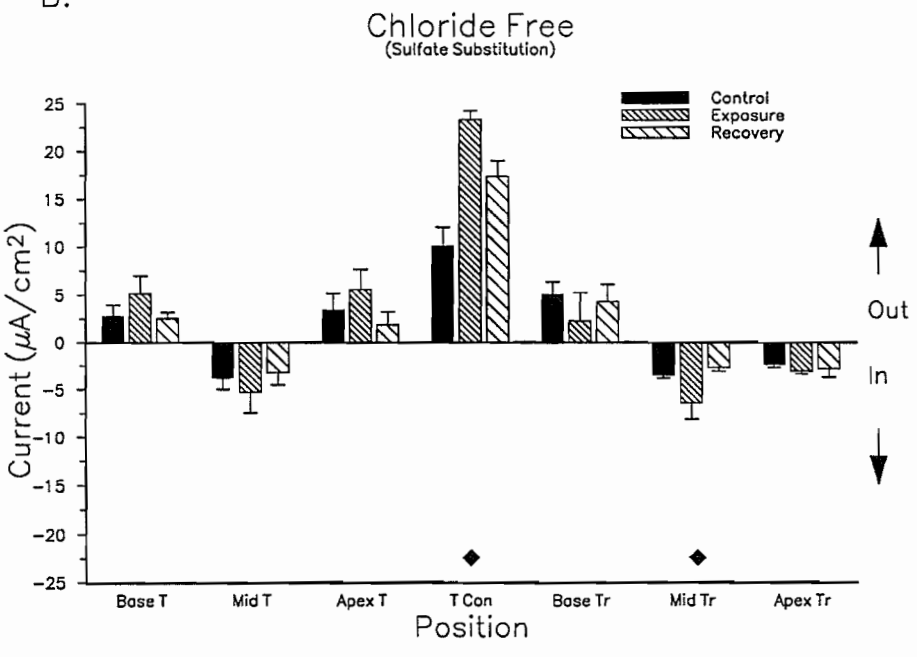
Chloride Free
(Sulfate Substitution)
Control
Exposure
Recovery
Current (μA/cm²)
25
20
15
10
5
0
-5
-10
-15
-20
-25
Out
In
Base T
Mid T
Apex T
T Con
Base Tr
Mid Tr
Apex Tr
Position

Figure 6

Mean extracellular current densities around ovarioles in proton-perturbed Ringers. *a)* pH 5. There are no significant differences. N=5. *b)* pH 9. There are no significant differences. N=6.

A.

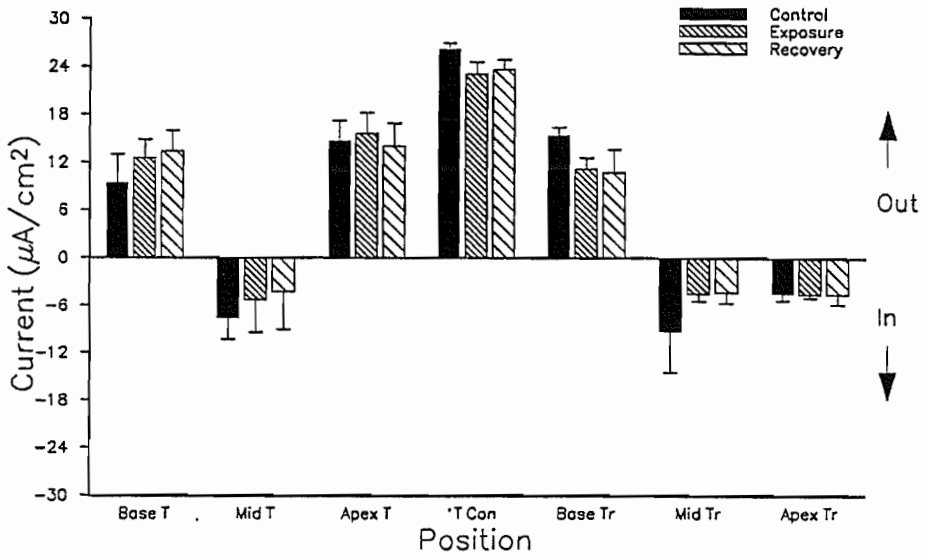
pH 5
Control
Exposure
Recovery
30
24
18
12
6
0
-6
-12
-18
-24
-30
Current (μA/cm²)
Out
In
Base T
Mid T
Apex T
T Con
Base Tr
Mid Tr
Apex Tr
Position

B.

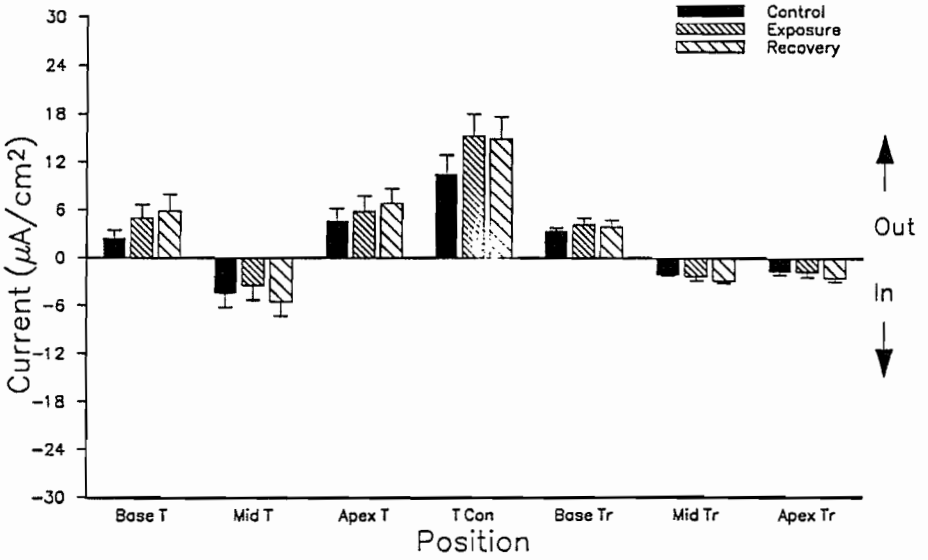
pH 9
Control
Exposure
Recovery
30
24
18
12
6
0
-6
-12
-18
-24
-30
Current (μA/cm²)
Out
In
Base T
Mid T
Apex T
T Con
Base Tr
Mid Tr
Apex Tr
Position

Figure 7

Mean extracellular current densities around ovarioles in glucose-free Ringers (sucrose substitution). There are no significant differences in current direction or magnitude. N=6.

Figure 8

Mean extracellular current densities around ovarioles in Ringers with Na^+ channel blockers. ♦ = significant difference ($P<0.05$); ◊ = marginally significant difference ($0.10>P>0.05$). *a)* Amiloride exposure. There is a significant increase in current efflux at T Con. N=5. *b)* Tetrodotoxin exposure. There are significant decreases at all position except Base T and Base Tr. N=5.

A.

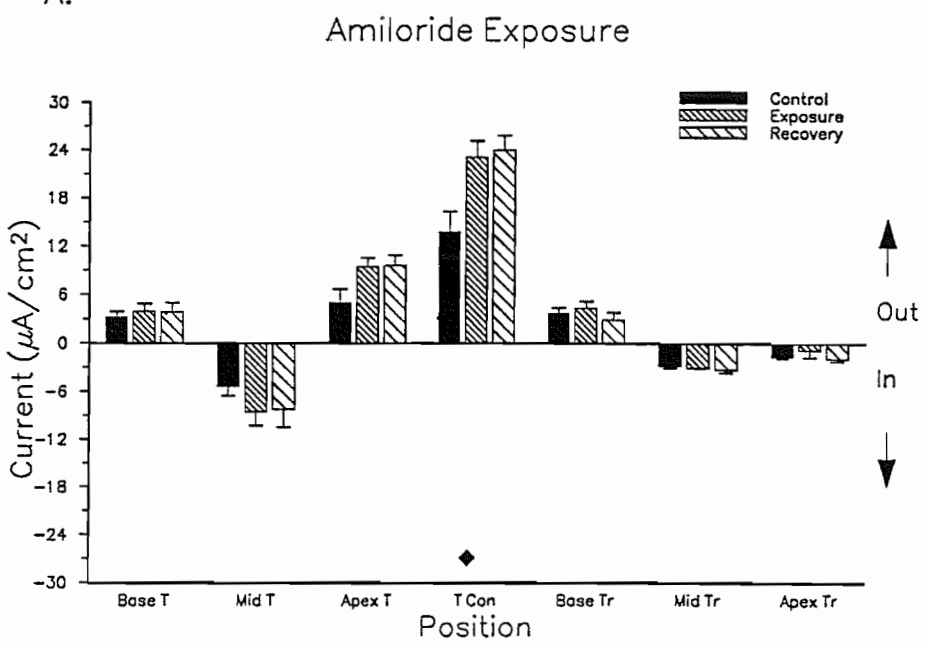
Amiloride Exposure
Control
Exposure
Recovery
Current (μA/cm²)
30
24
18
12
6
0
-6
-12
-18
-24
-30
Out
In
Base T
Mid T
Apex T
T Con
Base Tr
Mid Tr
Apex Tr
Position

B.

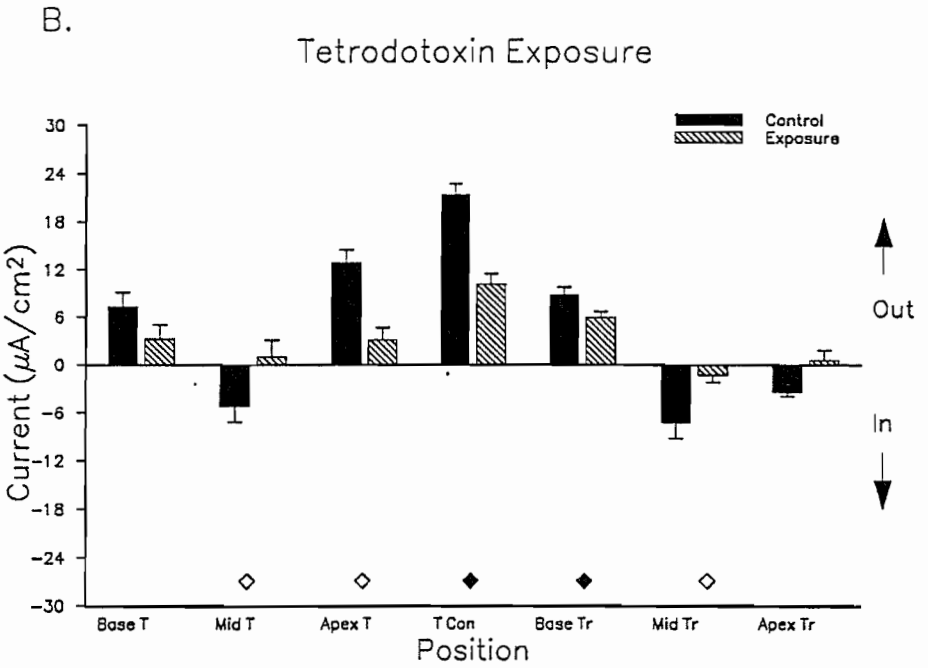
Tetrodotoxin Exposure
Control
Exposure
Current (μA/cm²)
30
24
18
12
6
0
-6
-12
-18
-24
-30
Out
In
Base T
Mid T
Apex T
T Con
Base Tr
Mid Tr
Apex Tr
Position

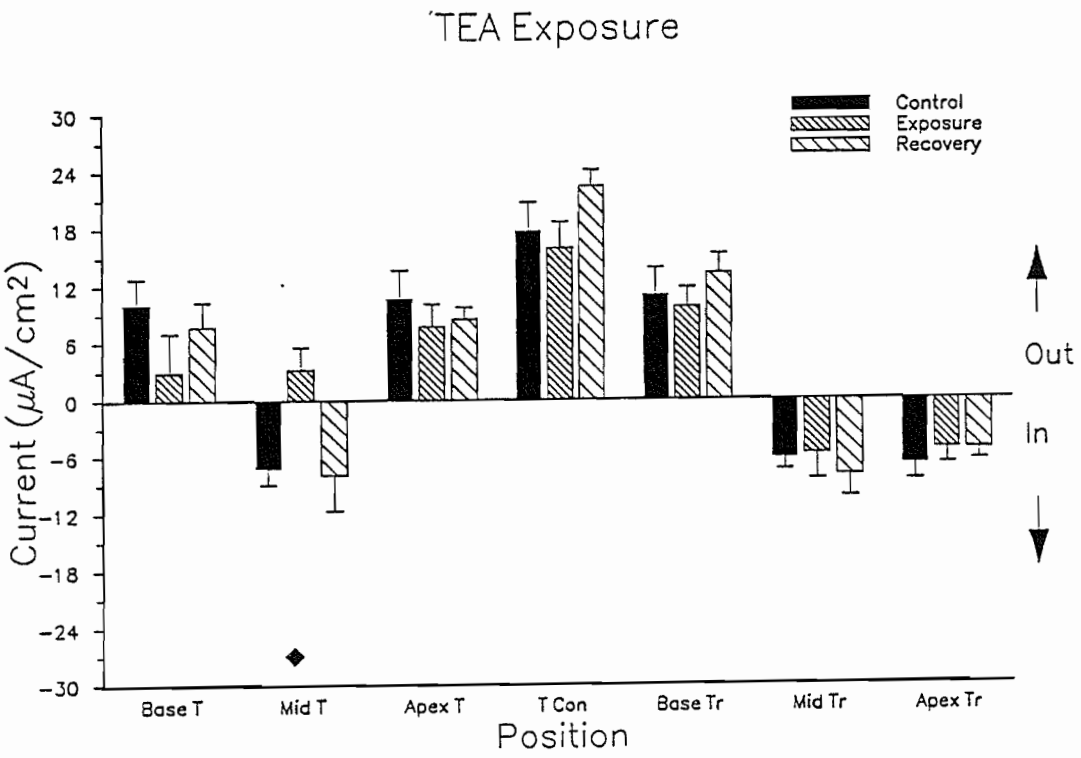

Figure 9

Mean extracellular current densities around ovarioles in Ringers with tetraethylammonium chloride. ♦ = significant difference ($P<0.05$). There is a significant change in current influx at Mid T, and noticeable but not significant decreases in current efflux at Base T and Apex T. N=6.

Figure 10

Mean extracellular current densities around ovarioles in Ringers with organic Ca^{+2}-channel blockers. ♦ = significant difference ($P<0.05$); ◊ = marginally significant difference ($0.10>P>0.05$). *a)* Diltiazem exposure. There is a significant reversal in current efflux at Base Tr, and a significant decrease in current influx at Mid Tr. N=4. *b)* Verapamil exposure. Changes in current magnitude and direction are similar to that in Diltiazem, with a marginally significant decrease at Apex Tr. N=7.

A.

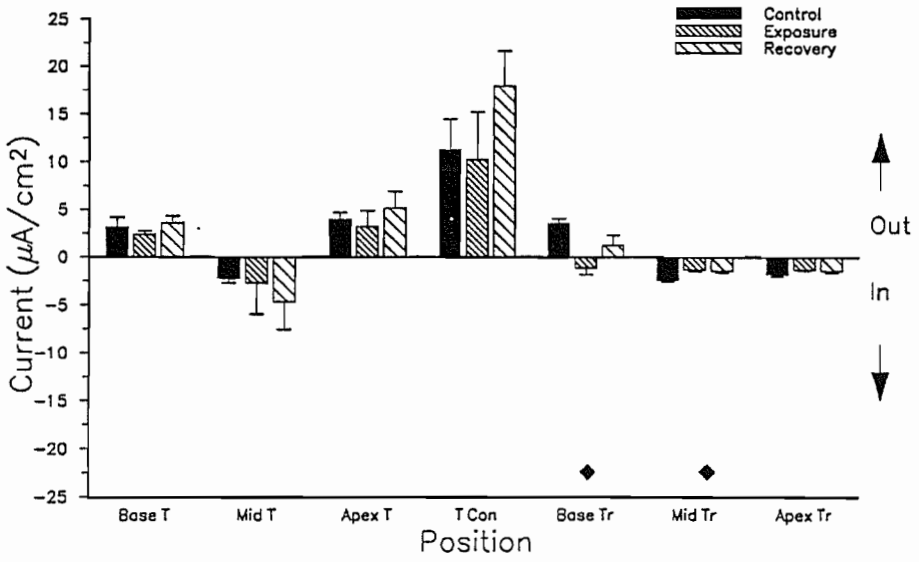
Diltiazem Exposure
Control
Exposure
Recovery
Current (μA/cm²)
25
20
15
10
5
0
−5
−10
−15
−20
−25
Out
In
Base T
Mid T
Apex T
T Con
Base Tr
Mid Tr
Apex Tr
Position

A.

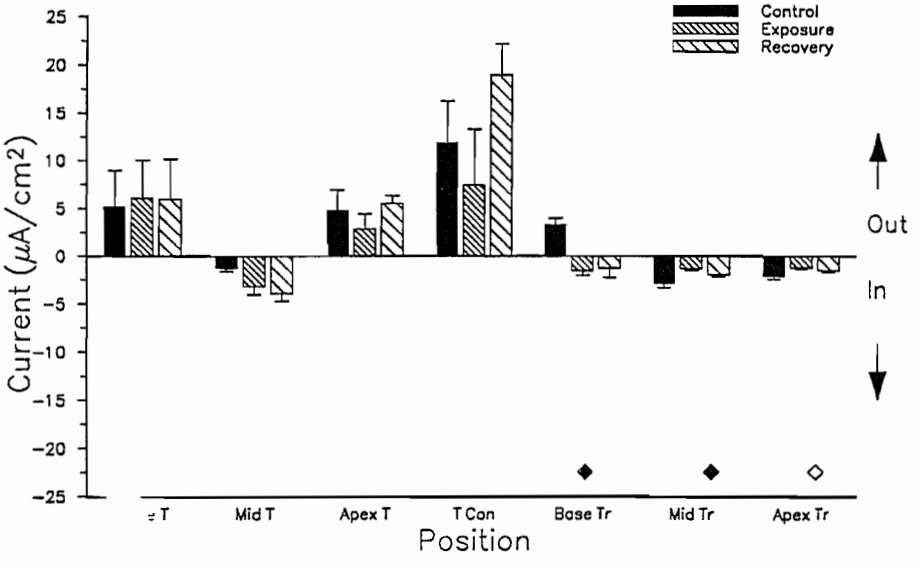
Verapamil Exposure
Control
Exposure
Recovery
Current (μA/cm²)
25
20
15
10
5
0
−5
−10
−15
−20
−25
Out
In
Mid T
Apex T
T Con
Base Tr
Mid Tr
Apex Tr
Position

Figure 11

Mean extracellular current densities around ovarioles in Ringers with TMB8. ◊ = marginally significant difference (0.10>P>0.05). *a)* Combined data (aggregate), including ovarioles with putative inward Ca^{+2} current at Apex T. Differences are not significant. N=7. *b)* Ovarioles with putative inward Ca^{+2} currents only. Differences are not significant. N=4. *c)* Ovarioles with current efflux at Apex T. There are increases in current density at all positions except Apex T; these are marginally significant at positions over the tropharium. N=3.

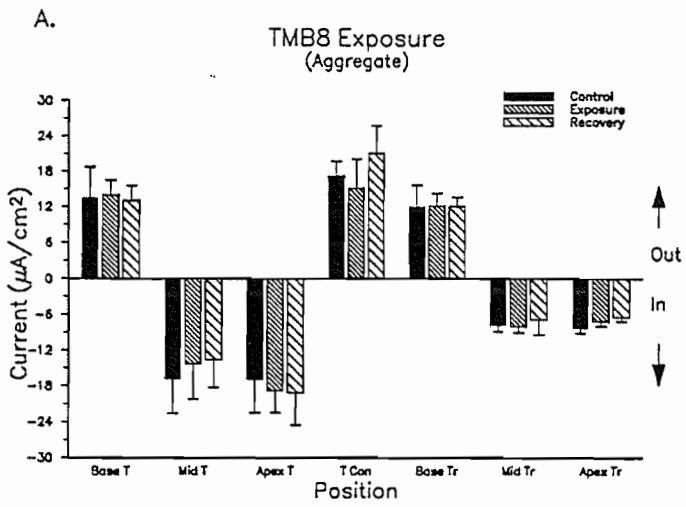
A.
TMB8 Exposure
(Aggregate)
Control
Exposure
Recovery
Current (μA/cm²)
30
24
18
12
6
0
−6
−12
−18
−24
−30
Out
In
Base T
Mid T
Apex T
T Con
Base Tr
Mid Tr
Apex Tr
Position

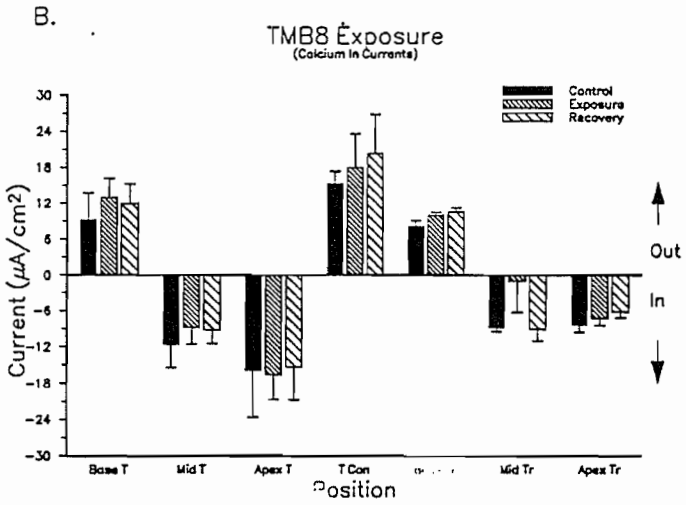
B.
TMB8 Exposure
(Calcium In Currents)
Control
Exposure
Recovery
Current (μA/cm²)
30
24
18
12
6
0
−6
−12
−18
−24
−30
Out
In
Base T
Mid T
Apex T
T Con
Mid Tr
Apex Tr
Position

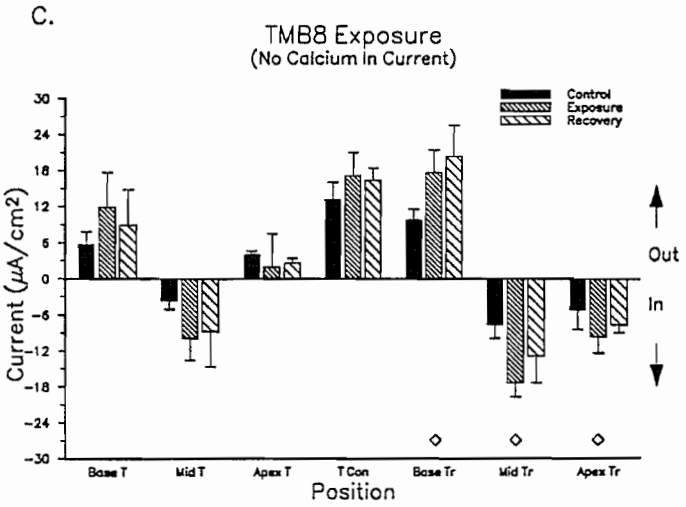
C.
TMB8 Exposure
(No Calcium In Current)
Control
Exposure
Recovery
Current (μA/cm²)
30
24
18
12
6
0
−6
−12
−18
−24
−30
Out
In
Base T
Mid T
Apex T
T Con
Base Tr
Mid Tr
Apex Tr
Position

Figure 12

Mean extracellular current densities around ovarioles in Ringers with Cl^- channel blockers. ♦ = significant difference ($P<0.05$). *a)* 9-anthracene carboxylic acid exposure. There is a significant decrease in current influx at Mid T, and noticeable but not significant decreases in current efflux at Base T and Apex T. N=7. *b)* DIDS exposure. There are no significant differences. N=4.

A.

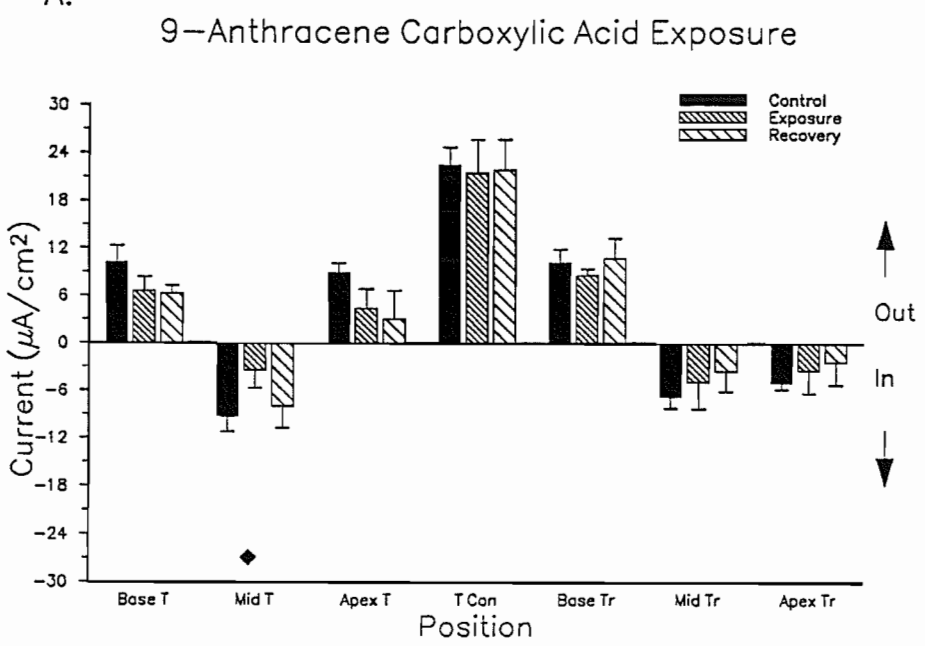
9—Anthracene Carboxylic Acid Exposure
Control
Exposure
Recovery
Current (μA/cm²)
30
24
18
12
6
0
−6
−12
−18
−24
−30
Out
In
Base T
Mid T
Apex T
T Con
Base Tr
Mid Tr
Apex Tr
Position

B.

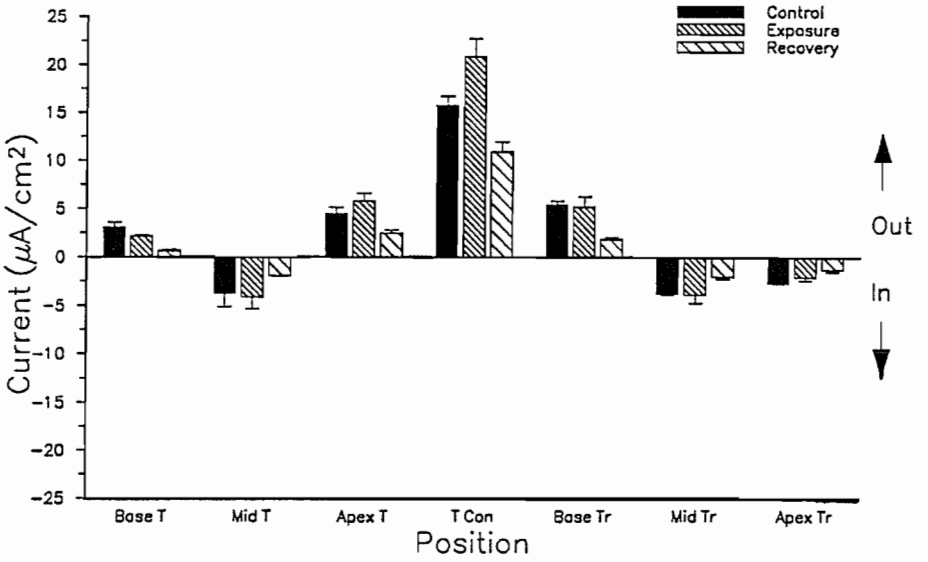
DIDS Exposure
Control
Exposure
Recovery
Current (μA/cm²)
25
20
15
10
5
0
−5
−10
−15
−20
−25
Out
In
Base T
Mid T
Apex T
T Con
Base Tr
Mid Tr
Apex Tr
Position

Figure 13

Mean extracellular current densities around ovarioles in Ringers with Na^+ transport blockers. ♦ = significant difference ($P<0.05$); ◊ = marginally significant difference ($0.10>P>0.05$). *a)* Ethacrynic acid exposure. Change in current influx at Mid Tr is obvious though not statistically significant. N=6. *b)* Ouabain exposure (after brief trypsinization). N=5.

A.

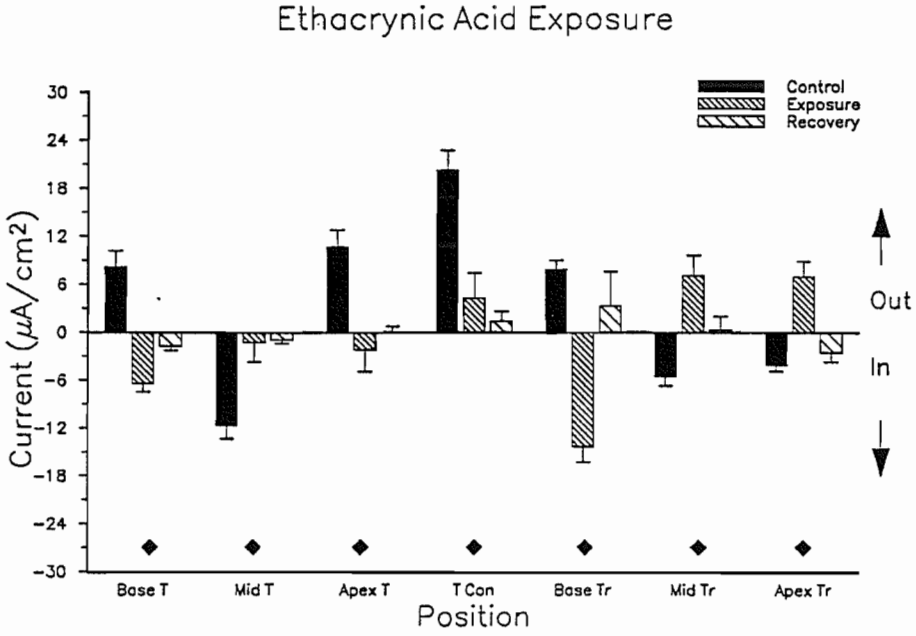
Ethacrynic Acid Exposure
Control
Exposure
Recovery
Current (μA/cm²)
30
24
18
12
6
0
-6
-12
-18
-24
-30
Out
In
Base T
Mid T
Apex T
T Con
Base Tr
Mid Tr
Apex Tr
Position

B.

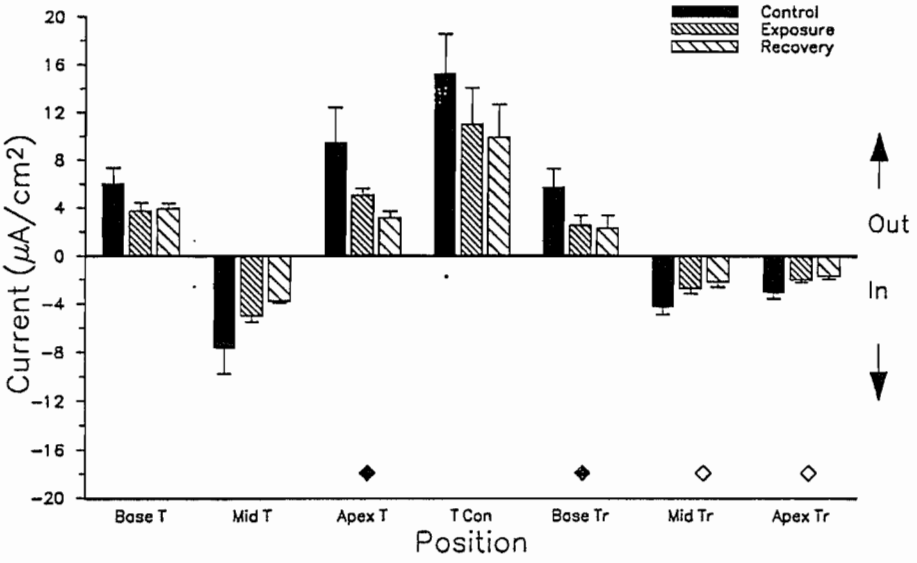
Ouabain Exposure
Control
Exposure
Recovery
Current (μA/cm²)
20
16
12
8
4
0
-4
-8
-12
-16
-20
Out
In
Base T
Mid T
Apex T
T Con
Base Tr
Mid Tr
Apex Tr
Position

Figure 14

Mean extracellular current densities around ovarioles in Ringers with sodium orthovanadate. ♦ = significant difference ($P<0.05$); ◊ = marginally significant difference ($0.10>P>0.05$). *a)* Combined data (aggregate). There are obvious changes in current direction or magnitude at all locations; these are significant only at Apex T, T Con, and Base Tr. There is a significant increase in current efflux at T Con. N=8. *b)* Group 1. Ovarioles in this group do not show significant differences in current flux over the tropharium. N=6. *c)* Group 2. Significant reversal in current direction occur over the tropharium; other differences are obvious but not significant due to low sample size. N=2.

A.

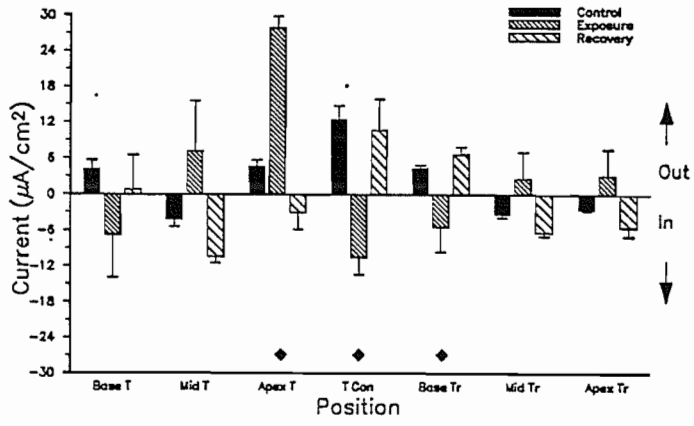
Sodium Orthovanadate Exposure
(Aggregate)
Control
Exposure
Recovery
Current (μA/cm²)
Out
In
Base T
Mid T
Apex T
T Con
Base Tr
Mid Tr
Apex Tr
Position

B.

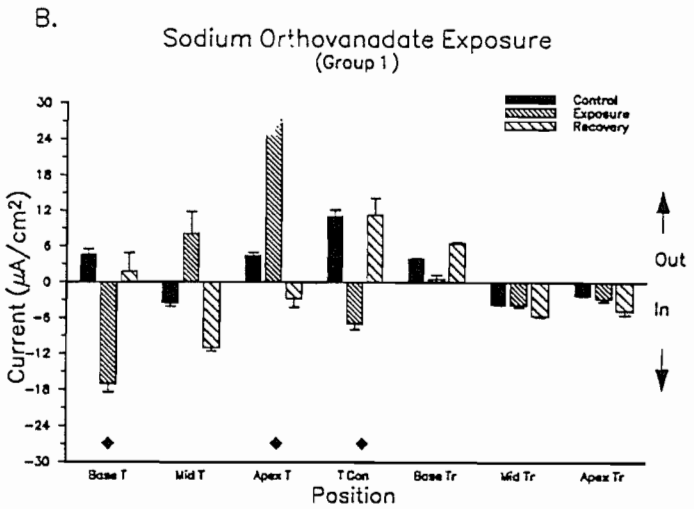
Sodium Orthovanadate Exposure
(Group 1)
Control
Exposure
Recovery
Current (μA/cm²)
Out
In
Base T
Mid T
Apex T
T Con
Base Tr
Mid Tr
Apex Tr
Position

C.

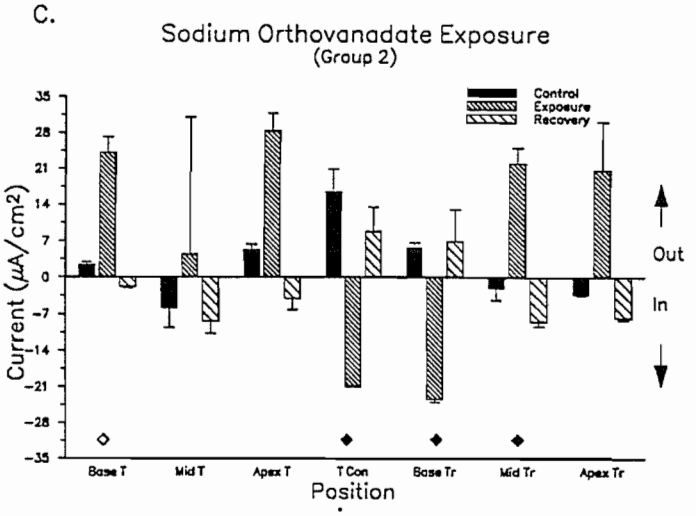
Sodium Orthovanadate Exposure
(Group 2)
Control
Exposure
Recovery
Current (μA/cm²)
Out
In
Base T
Mid T
Apex T
T Con
Base Tr
Mid Tr
Apex Tr
Position

Figure 15

Micropipette application of inhibitors. Currents were measured before inhibitor application with a micropipette. *a)* Pharmacological agents were administered in 30 sec pulses, and *b)* the currents measured within 15 sec post-application. MP = micropipette; VP = vibrating probe. Mag. = 130X.

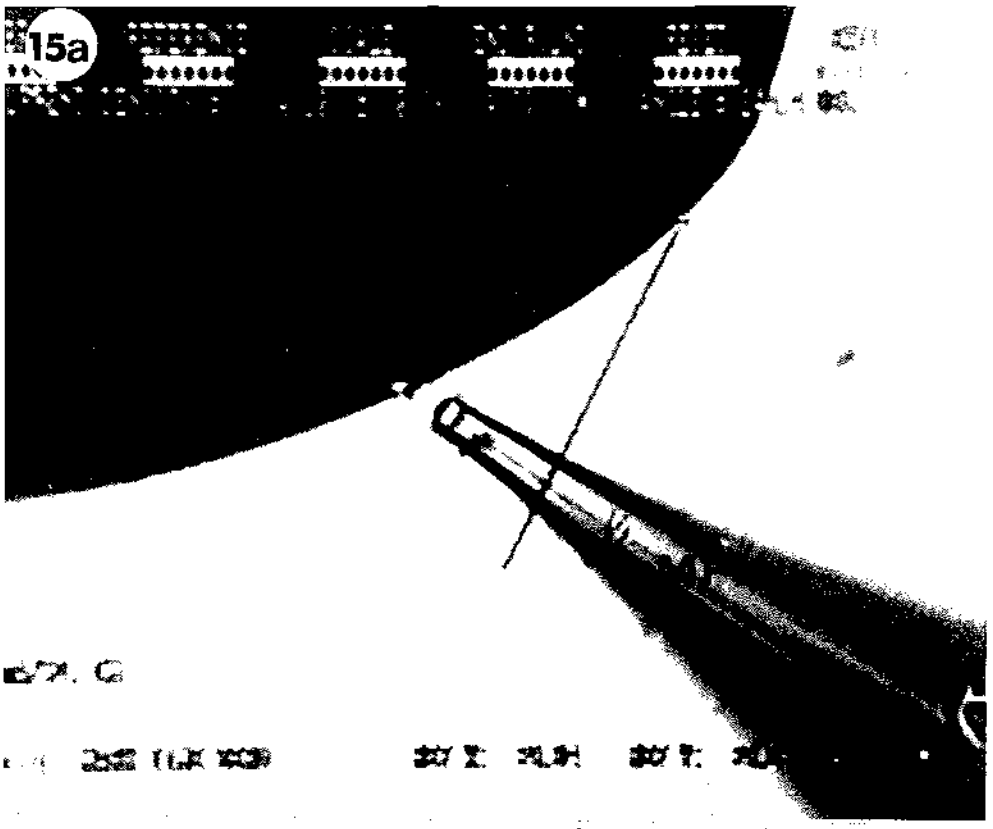
15a

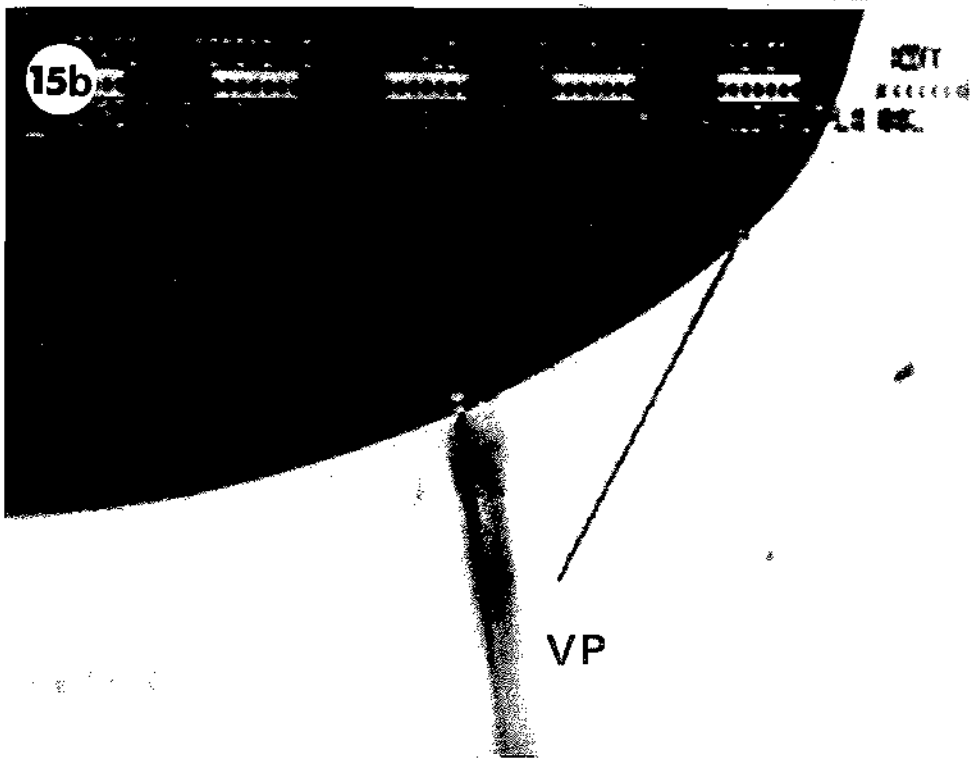
15b
VP

Figure 16

Results of micropipette inhibitor applications. Solid bars are controls, empty bars show currents after inhibitor experiments. Bars directed toward the ovariole represent current influx, bars directed outward represent current efflux. Sample sizes are given on the axes.

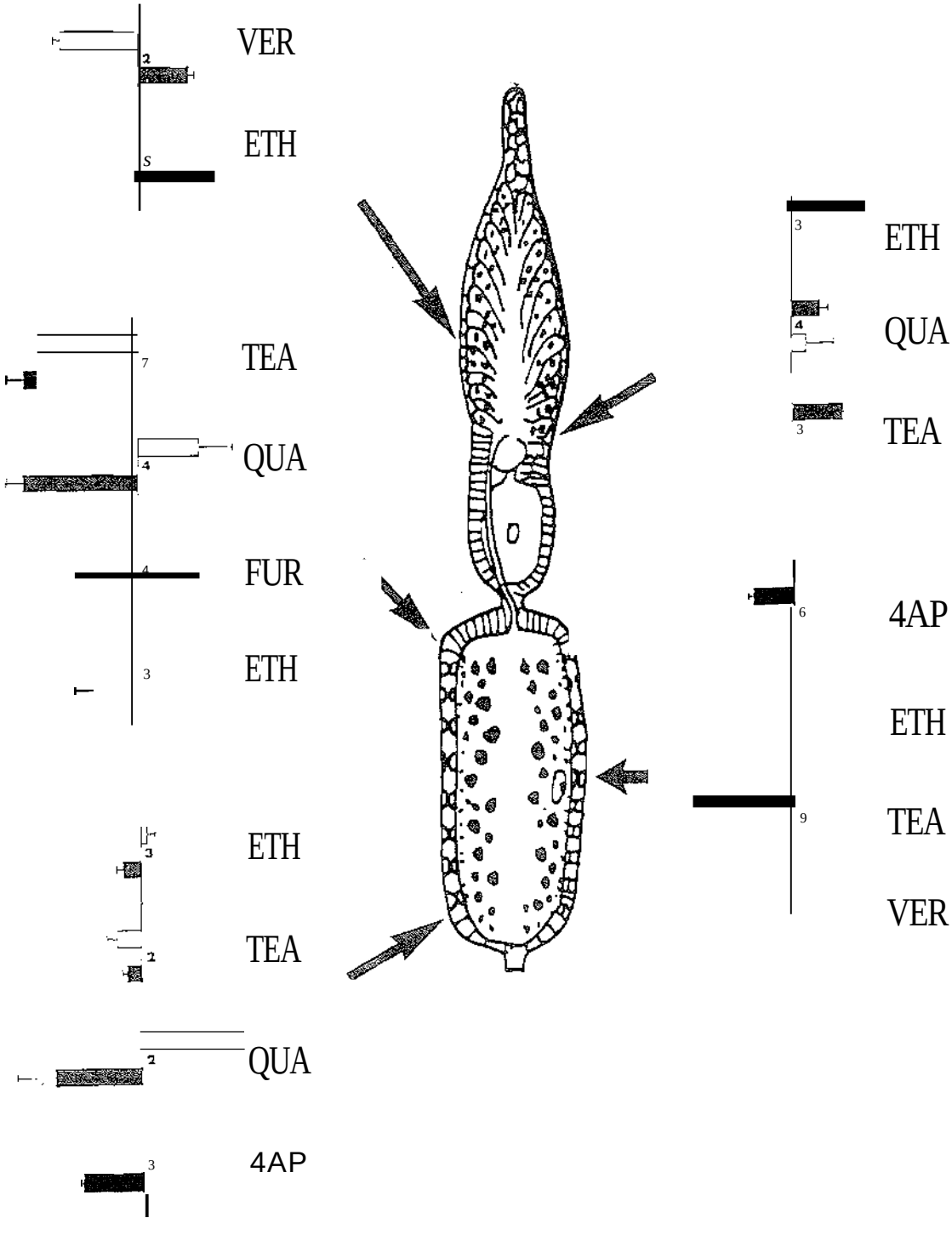
VER
ETH
TEA
QUA
FUR
ETH
ETH
TEA
QUA
4AP
ETH
QUA
TEA
4AP
ETH
TEA
VER

Figure 17

Effects of channel blockers and ion substitutions on inward currents over the apex of the T follicle. *a)* Summary of effects of verapamil, TEA, Ca^{+2}-free Ringers on current influx. High potassium induces current influx. Video still images illustrate the effect of Ca^{+2} free Ringers on the current *b)* before exposure and *c)* after exposure. Arrow highlights the location of the current. Mag. = 120X.

17a

Inward Apex T Currents

Effects of Channel Blockers and Ion Substitutions

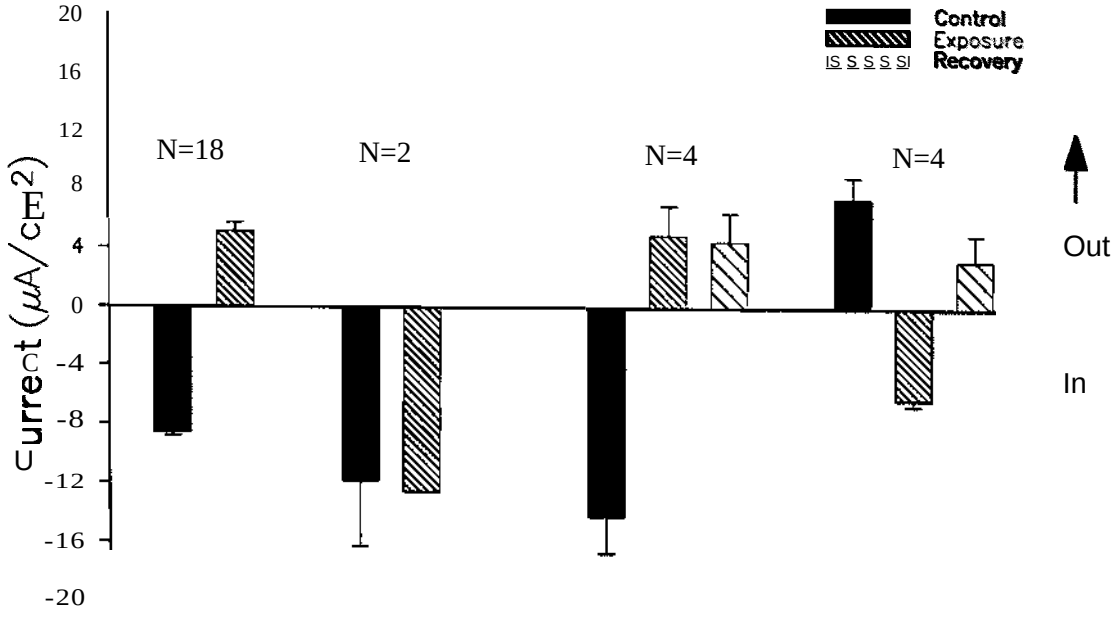

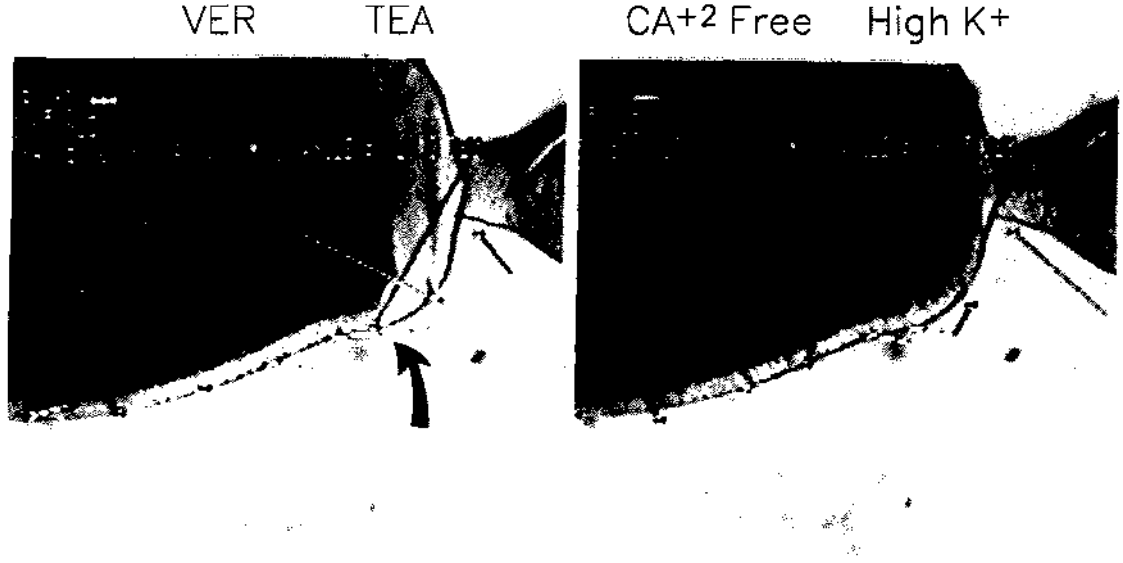

17b

Figure 18

Video still images illustrating the effects of Ca^{+2} channel blockers, Ba^{+2}, and high K^{+} on currents over the tropharium. In this specific example, Ba^{+2} was used to perturb currents. *a)* Before exposure to Ba^{+2}; and *b)* 2 min after exposure to Ba^{+2}. Mag. = 200X.

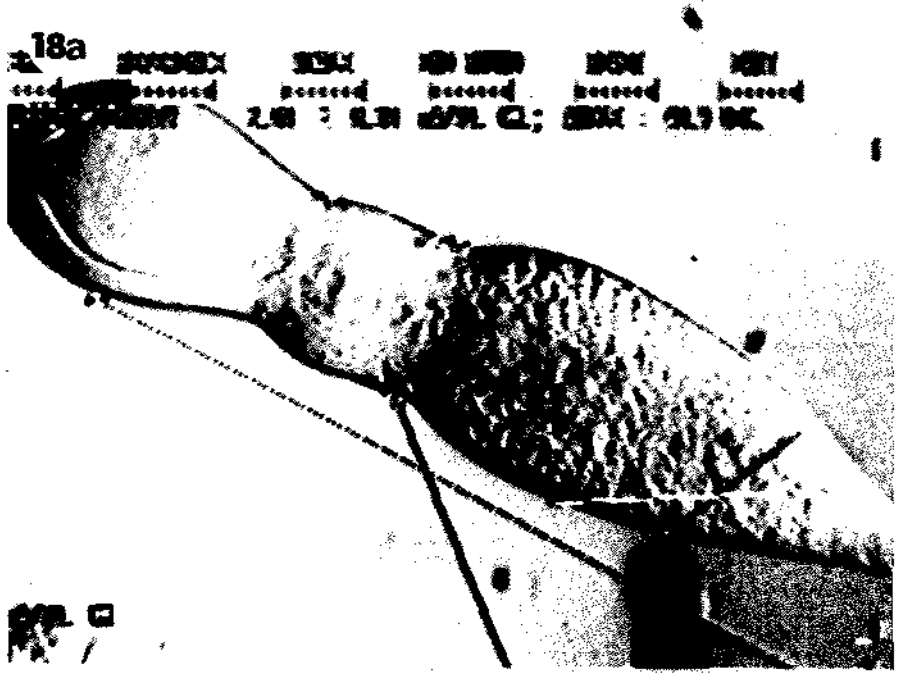

18a

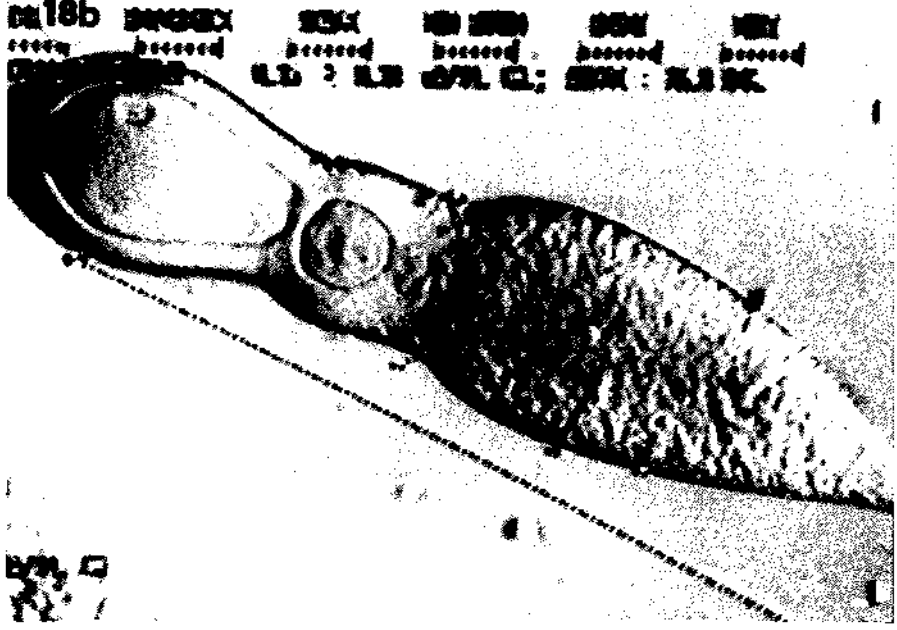

18b

Figure **19**

Schematic representation of *a)* "trans-tropharium" current, depicting the effects of *b)* Mn^{+2} and *c)* Ba^{+2}. C = cytoplasmic side; E = extracellular side; X^- and X^+ represent unidentified anion or cation conductances, respectively. Dashed line and arrows represent direction of current flow. See text for details.

A

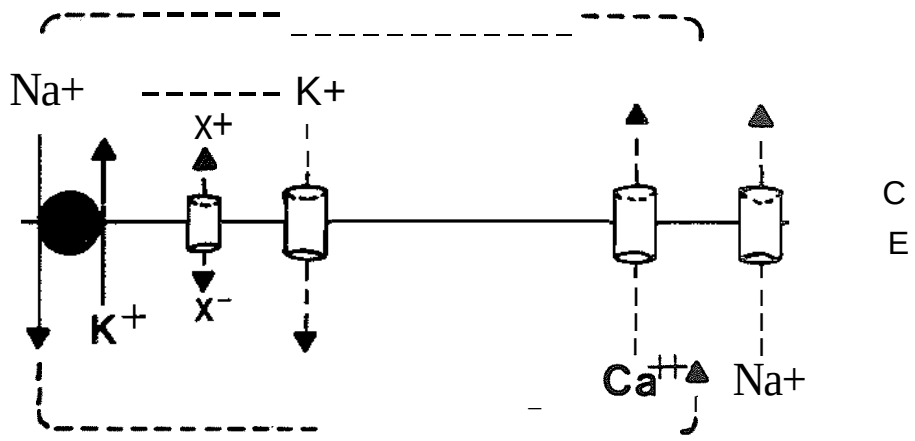

B

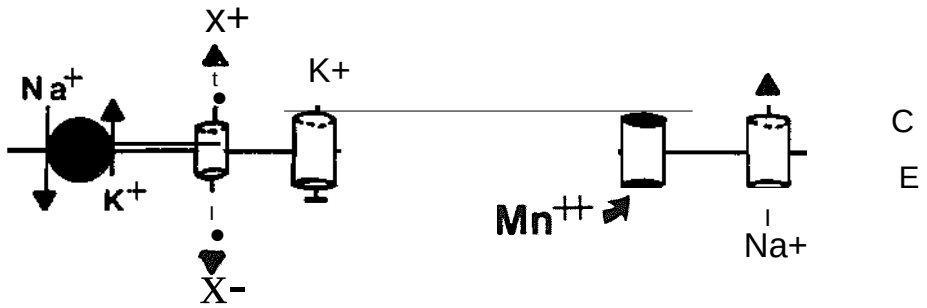

C

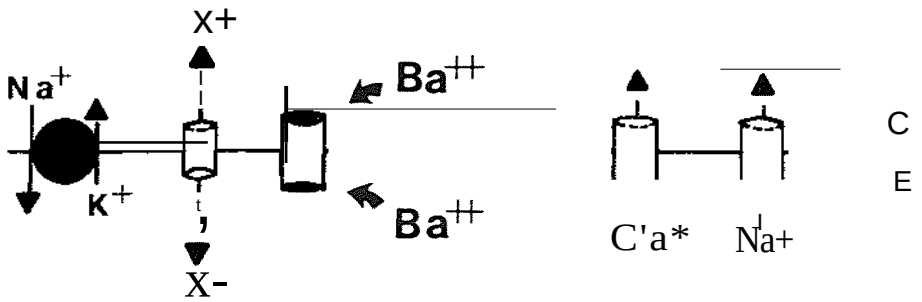

Figure 20

Overview of the ionic basis of extracellular currents around Rhodnius ovarioles. A vitellogenic terminal follicle is depicted at the bottom of the idealized ovariole; the T follicle and penultimate oocytes are shown connected to the tropharium via trophic cords. Dashed lines and arrows represent direction of current flow. Putative electrogenic Na" pumps at the base and apex of the T follicle and the base of the tropharium could be either Na+/K+ ATPases and/or Na+ ATPases. The Ca^{+2} channel depicted at the apex of the T follicle corresponds with the site of transient inward Ca^{+2} currents. Note that the relative contributions of follicle cells and germ cells are not explicitly represented.

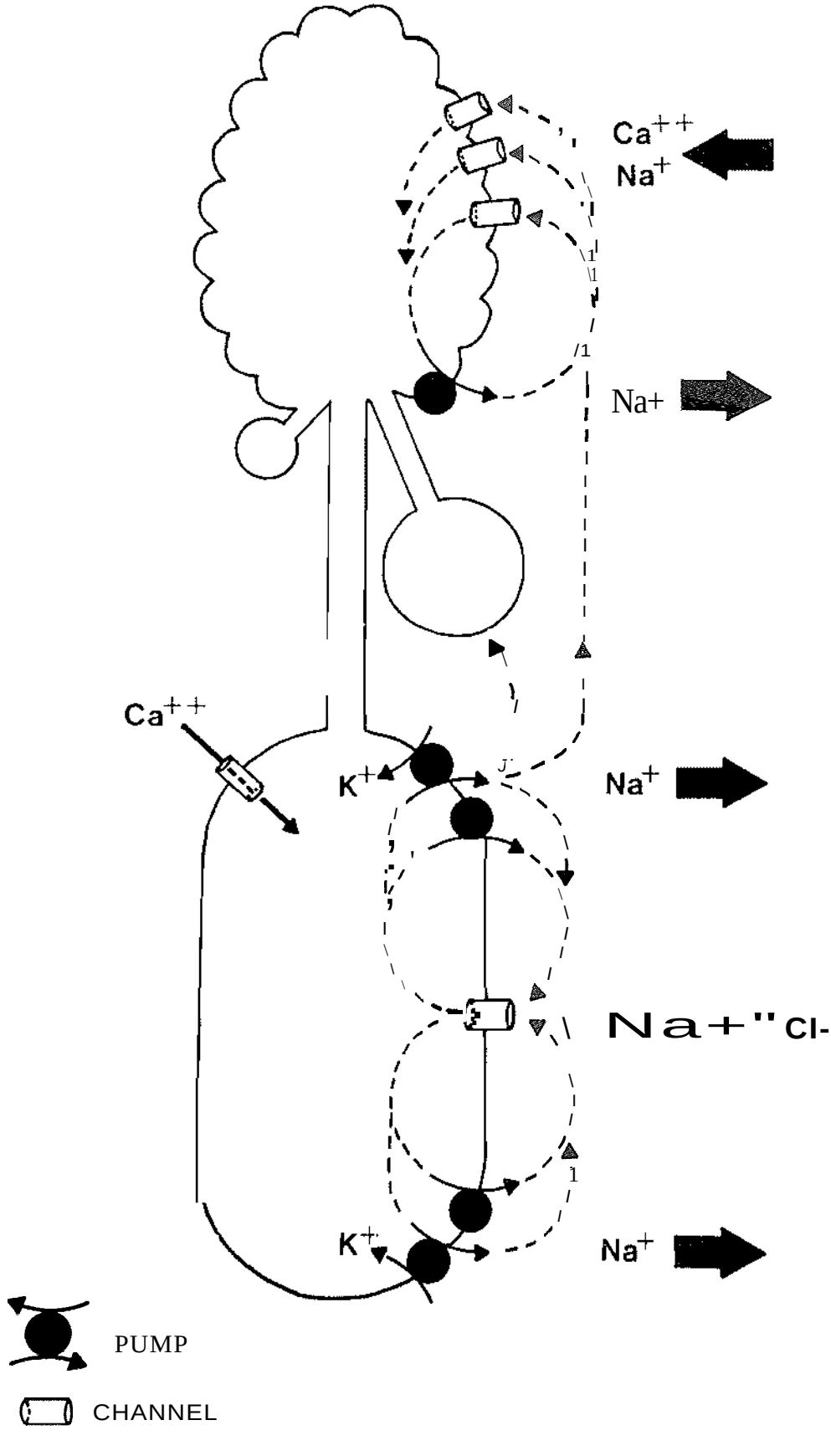
Ca++
Na+
Na+
Ca++
K+
Na+
Na+ Cl-
K+
Na+
PUMP
CHANNEL

CHAPTER III

EFFECTS OF ION SUBSTITUTIONS AND ION INHIBITORS ON FLUID-PHASE. ENDOCYTOSIS IN *Rhodnius prolixus* OVARIOLES

INTRODUCTION

The electrical properties of egg cell membranes have been investigated in almost every major animal phylum (Hagiwara and Jaffe, 1979). In several instances, electrical phenomena are directly associated with physiological responses. For example, the electrical fast block to polyspermy (Jaffe, 1976), Ca^{+2}-induced activation waves (Kline and Nucdtelli, 1985), and transmembrane proton fluxes (Shen and Steinhardt, 1978; Begg and Rebhun, 1979), are all electrical events at the cell membrane which have distinct effects on the oocyte.

Steady-state, transmembrane ionic currents are an almost ubiquitous property of developmental systems (Jaffe, 1981; Nucdtelli, 1990), yet there are few examples where these have been correlated with specific cellular responses. Roles attributed to extracellular ionic currents include pattern formation (Jaffe and Woodruff, 1979), control of gene expression (DeLoof, 1983), intracellular

electrophoretic transport (Telfer et al., 1981b) and vitellogenin uptake (Kindle et al., 1990).

Background work on Rhodnius prolixus ovarioles has delineated both the changing pattern of extracellular ionic currents (Sigurdson, 1984; Huebner and Sigurdson, 1986) and its ionic basis (Diehl-lones and Huebner, 1989a; this thesis). These currents are due at least in part to the germ cell membranes (Chapter 1). A current loop over the terminal follicle is carried by active Na" efflux from the base and apex, and is completed by passive Na" influx and chloride efflux over the middle of the follicle (Chapter 2). One possible function of active Na" transport in Rhodnius ovarioles includes modulation of follicle cell volume (Abu-Hakima and Davey, 1977), which is important in allowing access of yolk precursors to the oocyte cell membrane (Huebner and Davey, 1973; Huebner and Injeyan, 1980; Telfer et al., 1982; Oliviera et al., 1986).

One of the principal activities of the developing insect oocyte is endocytotic uptake of hemolymph proteins, including vitellogenin (Telfer, 1960; Stay, 1965; Hagedorn and Kunkel, 1979; Kunkel and Nordin, 1985). A tremendous amount of metabolic and biosynthetic activity is dedicated to this task: Telfer et al. (1982) calculate that Hyalophora oocytes generate approximately 300 times their initial surface membrane area. There is evidence that Ca^{+2} in particular has a key function in both binding and endocytotic uptake of vitellogenin in Nauphoeta cinerea follicles (Konig et al., 1988; Kindle et al., 1990). This finding correlates with the presence of voltage-dependent Ca^{+2} channels (see Kindle et al., 1990).

Aside from the transient inward Ca^{+2} currents during mid- to late vitellogenesis (Chapter 2) and Ca^{+2} action potentials (O'Donnell, 1985), inward Ca^{+2} flux is not a major component of the extracellular current pattern around Rhodnius ovarioles. However, other ions, most notably Na", are involved in regulating pinocytosis (Allison and Davies, 1974; Helenius et al., 1983). With the aid of a low-light video camera and computer image processing, I demonstrate pinocytotic uptake of the fluorescent marker Lucifer Yellow carbohydrazide (CH) by Rhodnius oocytes. I also report on the effects of ion substitutions and inhibitors on pinocytotic uptake in mid-vitellogenic ovarioles.

MATERIALS AND METHODS

Tissue

Rhodnius prolixus were reared and ovarioles dissected as previously described (Chapter 1). Ovarioles from 5 different size classes (2, 4, 6, 8, and 9) were used, and these corresponded to various stages of development, from very early vitellogenesis to late vitellogenesis/chorion formation (see Chapter 1 for a full description). Vitellogenic ovarioles (size class 4) were used to assay the effects of various experimental media.

Incubation Procedures

Ovarioles were incubated in 0.5 ml Microwell plates for 15 min, 60 min, or 180 min in 1 mg/ml Lucifer Yellow carbohydrazide in Rhodnius Ringers, then thoroughly washed in regular Rhodnius Ringers for either 15 min, 60 min, or 180 min. The Lucifer Yellow was a generous gift from Dr. W. Stewart (National Institute of Health, Bethesda, MD). To determine the effects of ion substitutions on Lucifer Yellow uptake, class 4 ovarioles were washed for 10 min in either Na", K^+, Ca^{+2}/Mg^{+2} or Cl-free Ringers (Media I, 2, 3, and 6, Chapter 2) or in K'-rlch Ringers (100 Mm by equi-molar substitution with Na'). Ovarioles were then incubated in the same respective medium with 1 mg/ml Lucifer Yellow for 15 min, then washed for 15 min. Ovarioles were exposed in the same manner to Ringers containing either 0.5 mM ouabain, 1 mM ethacrynic acid, 100 µM anthracene-9-carboxylic acid (9AC), or 100 mM tetraethylammonium chloride (TEA), and subsequently washed. Ovarioles were prepared for microscopy by mounting them on glass slides under coverslips supported by strips of Whatman No.1 filter paper.

Microscopy

Ovarioles were observed on a Zeiss Photo II epifluorescence microscope with a 75 W Xenon bulb and appropriate barrier and excitation filters for Lucifer Yellow fluorescence. A 25X neofluar objective lens (N.A.=0.6) and a 1.25X optivar were in the optical path, and a Dage MTI series 66 SIT (silicon-intensified target)

camera on manual gain of contrast was used to acquire fluorescence images. Live SIT images were frame averaged 256 times and background-subtracted on the Image-1 image processing system (Universal Imaging Co., Medea, PA). The system consisted of Image-1 software and hardware installed in a Compaq Deskpro 386S computer and a Sony Trinitron high resolution colour monitor (model no. PVM1342Q). Unenhanced, frame-averaged, and background-subtracted images were stored either on floppy disc or on a 40 MB magnetic tape drive (Irwin Magnetics Inc., model no. 140). Hard copies of video images were produced on a Polaroid video freeze frame (model no. FFVR-2) using TMax 100 professional 35 mm film and were printed on Ilford Multigrade III RC Rapid paper.

The Image-1 object measurement mode was used to provide a quantitative measure of pinocytotic uptake. Briefly, ovarioles incubated in Lucifer Yellow for 15 min were mounted in saline and fluorescence images were acquired in the uppermost discernible focal plane of the oocyte cortex. Digital video image threshold was manually adjusted until images were binarized into background video grey levels and those representing vesicles containing Lucifer Yellow. Briefly, this involved converting pixels within one gray value range into "object of interest" (in this case, Lucifer Yellow-loaded endosomes), or white, and the remaining pixels into "background", or black. By convention, the video threshold was adjusted until the smallest discernable vesicles were still visually distinguishable. One hundred such vesicles were selected at random from class

2 ovarioles, and the calculated mean surface area was used to discriminate or filter pinocytotic vesicles into small and large size categories. Numbers of small and large vesicles were counted within a standard surface area over ovarioles pulsed for 15 min in Lucifer Yellow, then chased for 15 min with normal Ringers. A one-way analysis of variance was used to determine if the differences between number of small and large vesicles in each size group were significant, and to determine significance between control and experimental treatments (Kleinbaum et al., 1988).

RESULTS

General Observations

Initial experiments in which ovarioles were incubated (or pulsed) for 30 min in Lucifer Yellow and washed (or chased) for an additional 30 min revealed a narrow band of fluorescence localized in the cortex of the terminal oocyte (Fig. 1). After a 180 min pulse followed by a 60 min chase, vesicles of various sizes were clearly visible at higher magnification, and a region approximately 20 urn wide delineated the extent of inward movement post incubation (Fig. 2). Fewer large pinocytotic vesicles were evident in the ooplasm under the apical follicle cells.

Early vitellogenic (class 2) ovarioles enabled better visualization of the relative rate of internalization of vesicles. Optical sections in the middle of the T follicle revealed >5 pm diameter vesicles 5-10 μm from the oolemma by 30 min post-incubation (Fig. 3a,b). By 60 min post-incubation, larger vesicles (approximately 15 urn in diameter) were observed approximately 30-35 urn from the oolemma (Fig. 4a,b).

T follicles in class 4 ovarioles were large enough to yield a reasonably flat optical field near the cortex, yet were thin enough to enable visualization of smaller endosomes. After a 15 min pulse and a 60 min chase, a variety of sizes of vesicles were visible in the cortex (Fig. 5a,b). After a 15 min pulse and a 180 min chase, there were clearly fewer small pinocytotic vesicles in the cortex (Fig. 6a,b). Since class 4 ovarioles had the best optical properties, this size class was chosen for analysis of the effects of ion substitutions and inhibitors.

Size Class Differences

Representative enhanced video images of pinocytotic vesicles in size class 2-9 ovarioles are presented in Fig. 7a-e. Fig. 8a,b illustrates the result of performing a digital threshold on a region of interest and filtering large from small pinosomes. One obvious difference between size classes is a marked decrease in Lucifer Yellow uptake in class 9 ovarioles. Other differences were not immediately apparent; however, a plot of the average number of large and small pinosomes in each size class revealed a marked trend (Fig. 9). There was no

significant difference between numbers of large and small pinosomes in early vitellogenic ovarioles, but in classes 4, 6, and 8 there were significantly fewer smaller pinosomes than large pinosomes (P<O.OOl, P=O.OOl, and P=O.014, respectively). By size class 9, there were approximately the same number of small vesicles as large vesicles.

Effects of Inhibitors and Ion Substitutions

Ethacrynic acid and Nat-free media induced the most dramatic differences (Figs. 10a,b and Lla-c, respectively). Large (up to 35 urn diameter) vesicles were induced after a 15 min chase, and few vesicles were under 5 urn in diameter. Nat-free Ringers also induced the formation of large vesicles, but there were relatively more smaller and intermediate-sized vesicles.

Figure 12 summarizes the effects of ion inhibitors and substitutions on the mean number of large and small pinocytotic vesicles. There were no significant differences between control and experimental groups in K'-free, high K^+, or Ca^{+2}-free Ringers. However, the number of large vesicles in Nat-free Ringers was significantly lower than in the control (P<O.OOl). There were also fewer small vesicles, although this was not significantly different. In the Cl-free Ringers, there were significantly more small vesicles than in the control (P=O.003). As well, there were significantly more small vesicles (P=O.046) and marginally fewer large vesicles (P=O.0971) in ovarioles treated with 9AC than in controls. Ethacrynic acid exposure resulted in fewer small and large vesicles than in the

controls (P=0.003 and P<0.001, respectively). Ouabain exposure did not result in any significant differences. TEA exposure resulted in significantly fewer large vesicles (P=0.037).

DISCUSSION

Low-light video and digital-image enhancement have enabled the visualization of a dynamic cellular process within Rhodnius oocytes. These observations compare with the ultrastructural studies by Huebner (1982) who described coated vesicles in Rhodnius oocytes. While in the present work fine ultrastructural details could not be discerned, two novel observations on fluid phase endocytosis were made. First, internalization of endocytotic vesicles proceeds at a remarkably uniform rate around the periphery of oocytes. This is shown by the uniform distance of Lucifer Yellow-loaded vesicles from oocyte periphery after 30 and 60 min post-incubation. Second, there is a significant decrease in the number of small pinocytotic vesicles after early vitellogenesis. This implies that either the primary pinosomes are larger or that they fuse more rapidly with other endocytotic vesicles. The latter is a more plausible explanation, and this could facilitate faster recycling of clathrin and membrane constituents which are not incorporated into yolk spheres (Telfer et al., 1981a).

Technical limitations prevent differentiation between the relative sizes of larger vesicles; neither can anything be concluded about the total amount of Lucifer Yellow uptake. Although such parameters can be quantified with computer image analysis (Benveniste et al., 1989), there are several limitations which complicate these' measurements. 'For example, overlapping fluorescent vesicles and background autofluorescence can interfere with the fluorescence signal of interest. Additionally, it is difficult to assess when an object is precisely in the focal plane, and this can dramatically influence area and intensity measurements (Maxfield and Dunn, 1990). Measurement of light intensity at precise intervals through the focal plane and subsequent integration of these values can be used to normalize digitized grey values (Benveniste et al., 1989), but this was not technically possibly in our setup. For these reasons, the analysis in the present study is restricted to measurement of the relative numbers of large and small pinosomes which could be measured with reasonable accuracy. Since I have shown the feasibility of optically examining pinocytotic vesicles in living Rhodnius oocytes, refinements of my technique will likely enable the measurement of other parameters of endosomal uptake. For example, it should be possible to use probes such as BCECF or fluorescein to measure pinosome pH in various parts of the endocytotic pathway (Paradiso et al., 1987; Yamashiro and Maxfield, 1987; Maxfield, 1989).

The effects of Cl-free media and Cl- channel blockers support the finding that Cl' efflux carries a portion of the inward current over the T follicle.

However, the mechanism by which this occurs is unclear. Chloride ions may influence Na" activity, although the fact that high K+ Ringers -- which depolarizes Rhodnius oocytes (O'Donnell, 1986) -- has no obvious effect on pinocytosis makes this unlikely. By extension, the fact that neither low K+ nor high K+ Ringers produced a visible effect on pinocytosis strongly suggests that the effect of TEA is pharmacologicallyrather than physiologically relevant.

The effects of Na" and ethacrynic acid on pinosome fusion strongly suggest a link between the extracellular current pattern and pinocytosis. These effects are not due to membrane depolarization, since high K+ Ringers did not induce a noticeable difference in pinosome fusion, although changes in membrane resistance have been correlated with pinocytosis (Allison and Freeman, 1967). Other ions and inhibitors had no obvious effects on pinocytosis, which would suggest that Na" influx is the major modifying influence.

There is ample precedence for the involvement of Na" currents in pinocytosis. As stated by Klopocka and Grebecka (1985): "The influx of Na" to the cell seems to control several steps of pinocytosis.... Therefore, the agents affecting Na" movements should be expected to influence pinocytosis." According to Allen et al. (1974), anionic sites on the surface of Amoeba selectively bind cations such as Na". Intracellular Na" is in turn able to release Ca^{+2} from intracellular stores, which triggers microfilament contraction (Taylor, 1977) and subsequent pinosorne formation (Stockem et al., 1983). It is evident that perturbation of Na" flux across the cell membrane could perturb Na" homeostasis

and have profound effects on pinocytosis. These findings do not, however, provide an obvious answer as to how a perturbation of Na^+ flux can induce the formation of large endocytotic vesicles.

One possible link between Na^+ flux and endosome fusion is intracellular pH. In particular, it is well established that pH regulates a variety of endosomal functions, from receptor-ligand dissociation and recycling to endosomal fusion rates (Tycko et al., 1983; Mellman et al., 1986; Yamashiro and Maxfield, 1988). Large endocytotic vesicles have been shown invariably to have a lower pH than small vesicles, and this acidification is largely due to membrane-bound proton ATPases (Al-Awqati, 1986). Aside from differences in the number of endosomal ATPases or the direct regulation of their activity, it has long been suggested that cation/proton exchangers may be involved in regulating endosomal pH (Mellman et al., 1986).

One possible candidate for regulating pH is the electrically-silent Na^+/H^+ antiport. This exchanger appears to exist in almost all animal cells, where it has been implicated in the regulation of cytoplasmic pH and Na^+ concentration (see Grinstein and Rothstein, 1986). The Na^+/H^+ antiport is activated by a variety of stimuli, including osmotic shock and hormones, and is not affected by changes in membrane potential (Grinstein and Rothstein, 1986). I hypothesize that inhibitions of active Na^+ transport and Na^+-free media both decrease intracellular Na^+ concentrations, the former by reducing the inward driving force on Na^+, the latter by restricting Na^+ entry over the middle of the T oocyte. Putative Na^+/H^+

antiports from the oolemma would probably be incorporated into endosomes such that Na" influx and H+ efflux are favoured. If cytoplasmic Na" is decreased, proton efflux would diminish, and the contents of endosomes would be further acidified via the inward-directed proton ATPase. This in turn could promote vesicle fusion and the formation of larger endosomes.

A major supposition in this model is that Na"/H+ antiporters exist in these endosomes. If this is not the case, other perhaps less direct mechanisms may be responsible for the formation of larger endosomes. Clearly, the connection between inhibition of Na" transport and vesicle fusion has yet to be defined. The significance of the present findings is that inhibition of specific transmembrane ion fluxes have been linked with a visible perturbation of a major physiological activity - that of fluid-phase endocytosis. Obviously, no assumptions can be made from this work as. to the relevance .of Na" transport to receptor-mediated endocytosis of vitellogenins. Other researchers have demonstrated influences of extracellular Ca^{+2} (Konig et al., 1988; Kindle et al., 1990) and pH (DiMario and Mahowald, 1986) on vitellogenin uptake, and this certainly should be investigated in Rhodnius. However, ion fluxes which modulate underlying processes of pinocytosis can reasonably be expected to impact on receptor-mediated endocytosis.

Figure 1

Low light, computer-enhanced fluorescence image showing the T follicle after a 30 min pulse in Lucifer Yellow, followed by a 15 min chase. Note that a diffuse band of fluorescence localizes in the cortex of the oocyte. The double arrow indicates the extent of follicle cells along the lateral aspect of the follicle. TO = terminal oocyte; TC = entry point of the trophic cord to the T oocyte; AFC = apical follicle cells. Mag. = 110X.

Figure 2

Enhanced fluorescence image of T follicle after a 180 min pulse, followed by a 60 min chase. The double arrows indicate the extent of vesicle internalization. FC = outer boundary of follicle cells. Mag. = 260X.

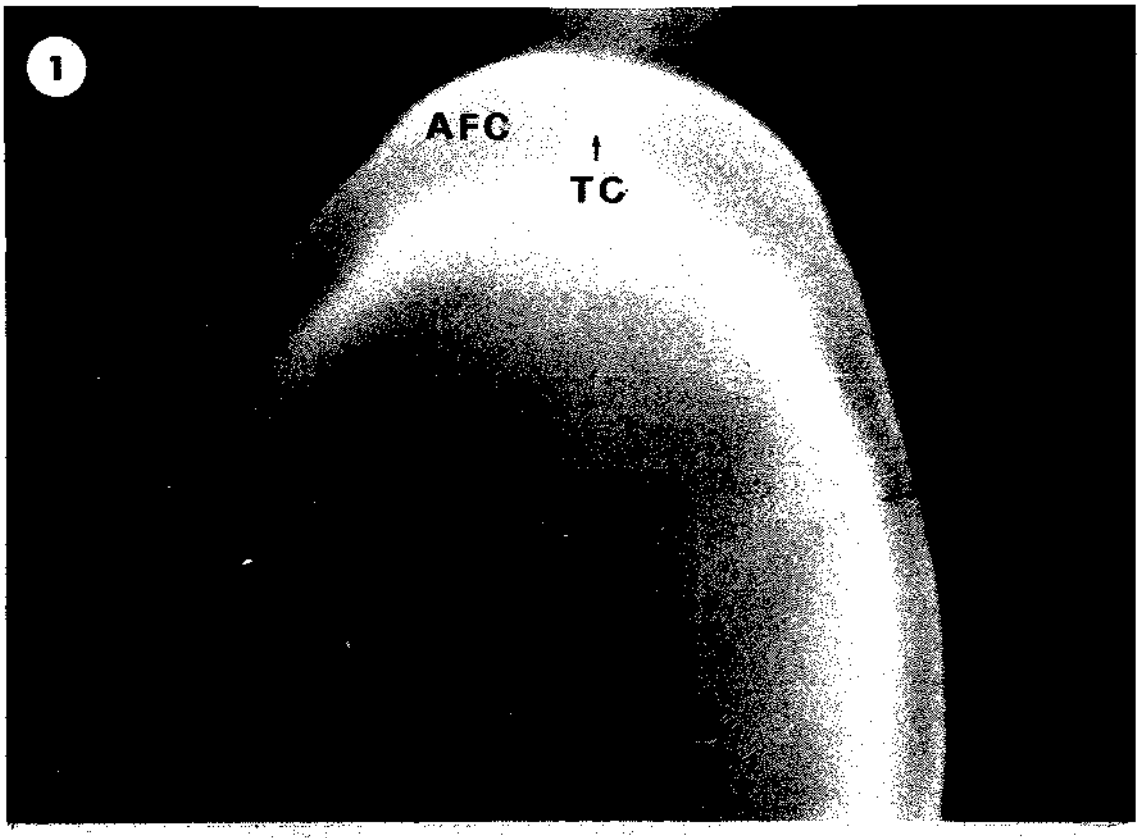
1
AFC
TC

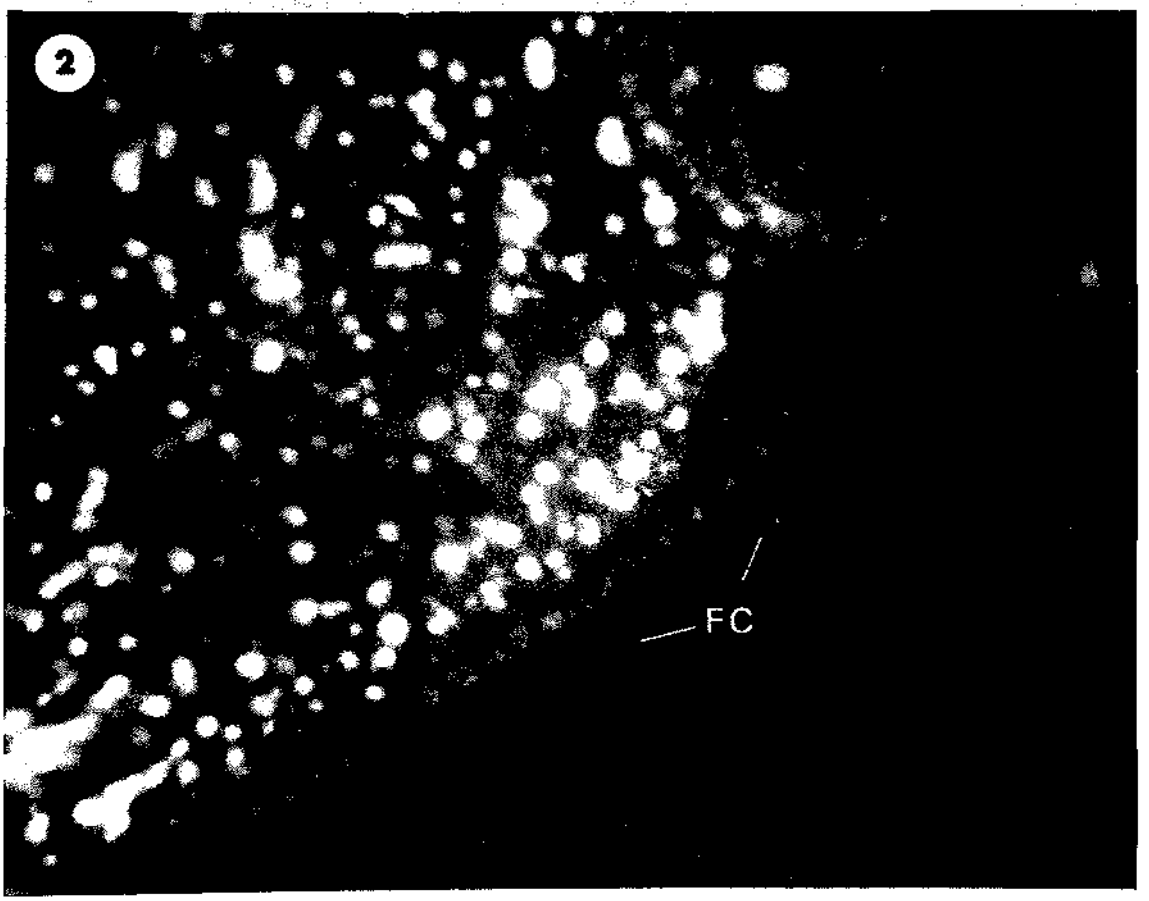
2
FC

Figure 3

a) Enhanced fluorescence image of a class 2 T follicle after a 15 min pulse, 30 min chase. The focal plane is in the middle of the follicle. Clusters of small endosomes are visible at the periphery of the oocyte. *b)* Three-dimensional line intensity profile of *a)* shows the relative size of vesicles. In this and subsequent line intensity profiles, pixel brightness has been mapped as a third graphical dimension to yield a three dimensional plot of intensity distribution. Mag. = 425X.

Figure 4

a) Enhanced fluorescence image of a class 2 T follicle after a 15 min pulse, 60 min chase. *b)* Three-dimensional line intensity profile of *a)* shows the increase in fluorescence intensity concomitant with the increased size of vesicles. Mag. = 425X.

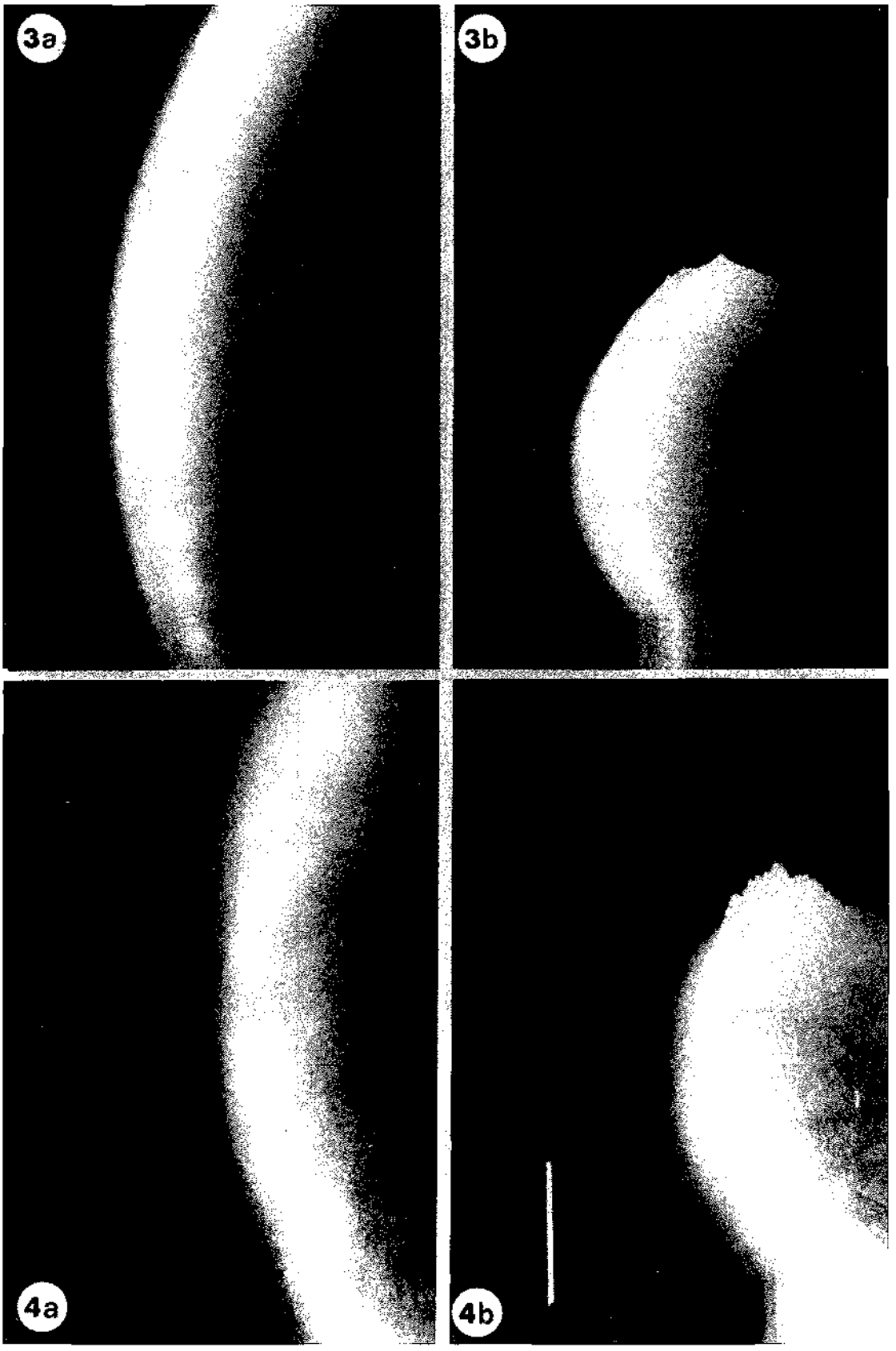
3a
3b
4a
4b

Figure 5

a) Enhanced fluorescence image of a class 4 T oocyte, immediately below the follicle cells. This oocyte received a 15 min pulse, followed by a 60 min chase. *b)* Three-dimensional line intensity profile of *a)* shows the relative intensities of pinocytotic vesicles. Mag. = 425X.

Figure 6

a) Enhanced fluorescence image of a class 4 T oocyte after a 15 min pulse, 180 min chase. *b)* Three-dimensional line intensity profile of *a)* dramatically emphasizes the extent of pinosome fusion. Mag. = 425X.

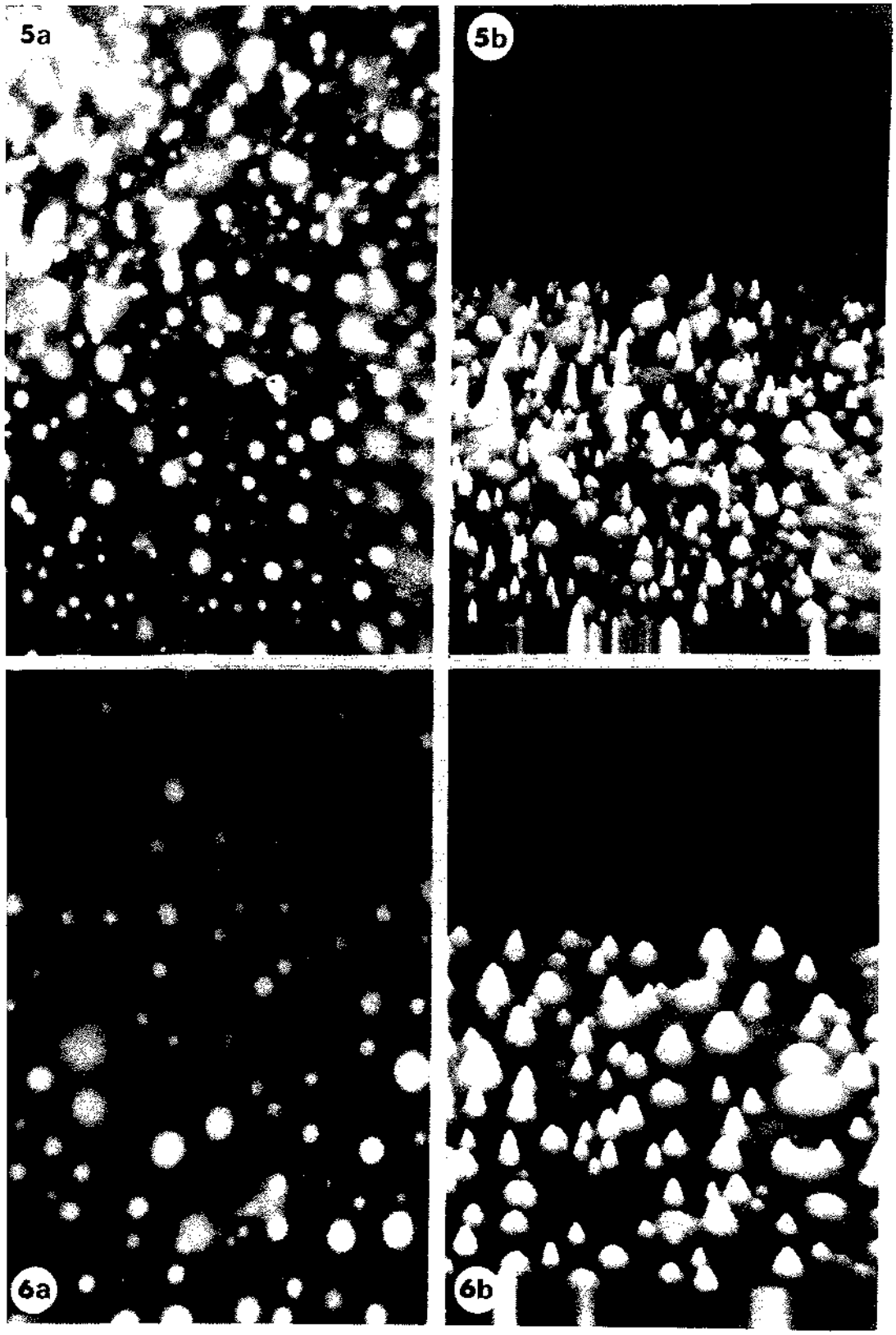
5a
5b
6a
6b

Figure 7a-e

Representative video images of class 2 (a), 4 (b), 6 (c), 8 (d), and 9 (e) ovarioles after a 15 min pulse, 15 min chase. Mag. = 425X.

Figure 8

Enhanced fluorescence image *a)* before and *b)* after digital thresholding. The basis for digital threshold formation is described in the text. The white square in Fig. 8b represents the standard area for object counting. Endosomes have been filtered into small «2 urn) and large (>2 urn). Mag.= 425X.

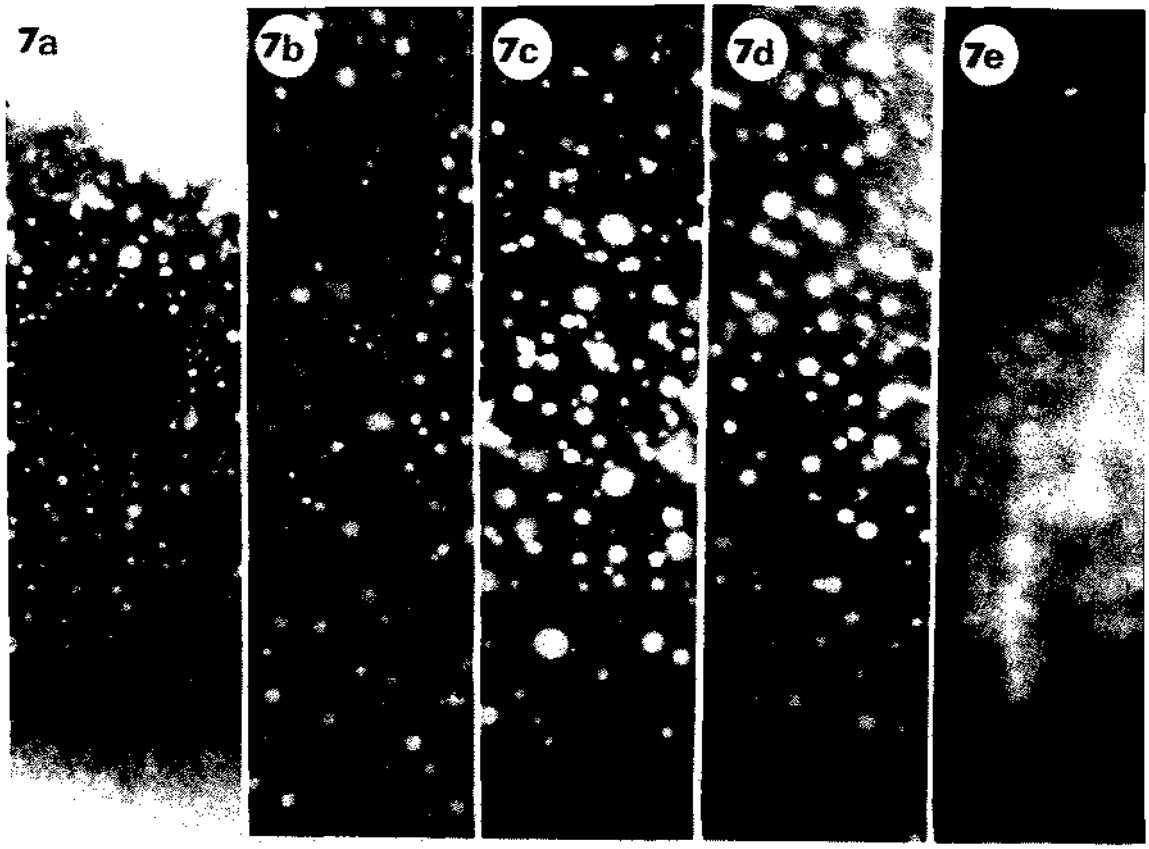
7a
7b
7c
7d
7e

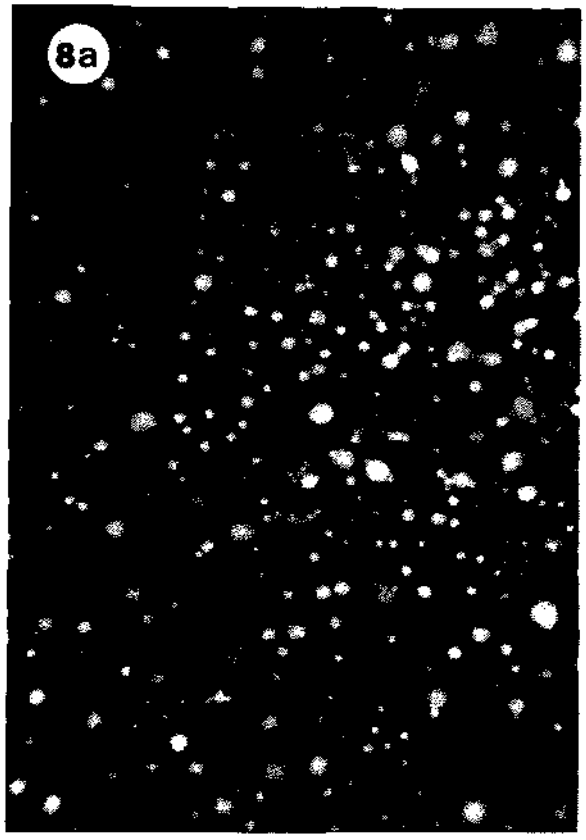
8a

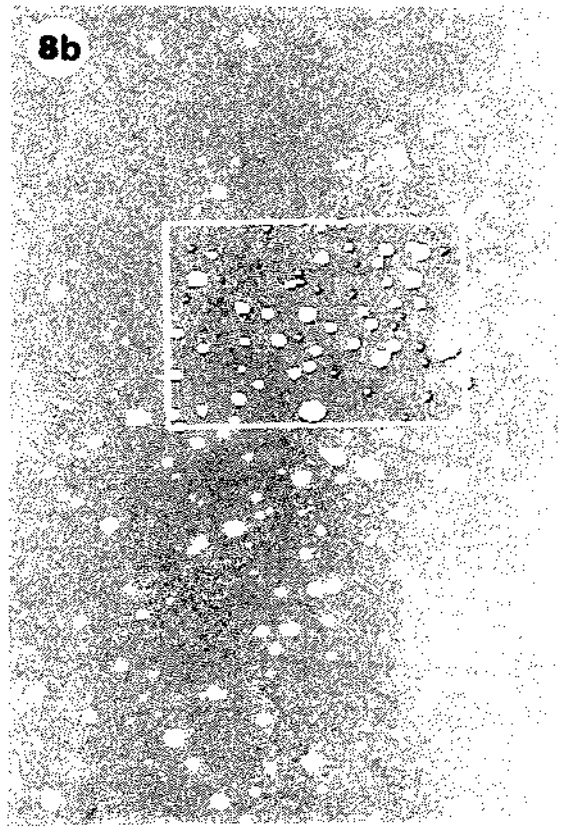
8b

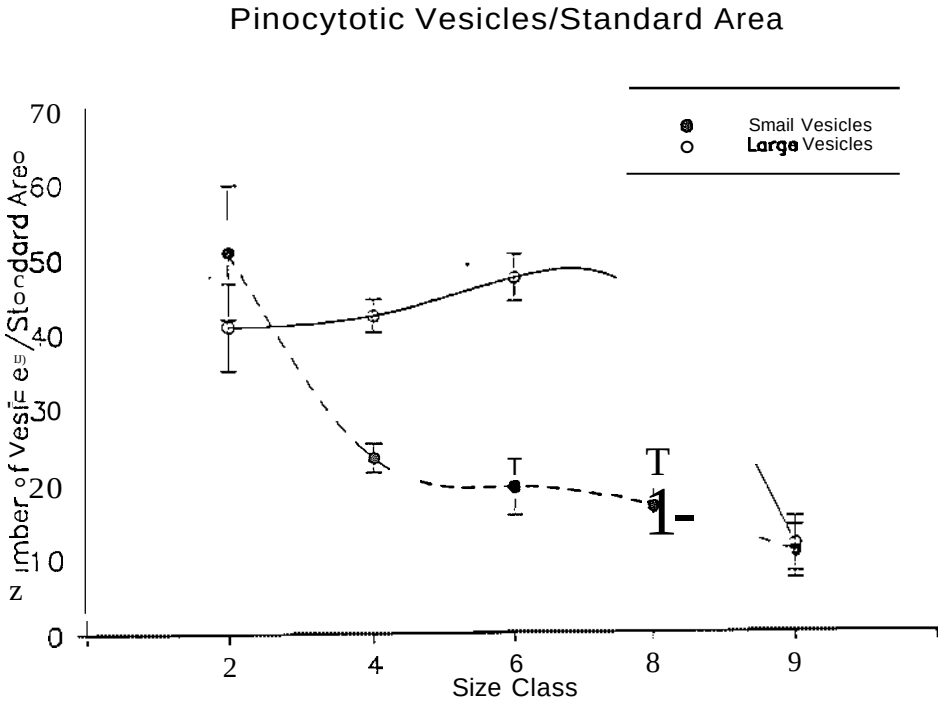

Figure 9

Lowess plot of the mean number of large and small vesicles/standard area (±SEM) in ovariole size classes 2, 4, 6, 8, and 9. Numbers of small and large pinosomes were counted as illustrated in Fig. 8. There are significantly fewer small pinosomes in size classes 4, 6, and 8 (P<O.05). N=5.

Figure 10

Effect of ethacrynic acid on pinocytosis. The treated ovarioles had markedly larger vesicles (up to 35 μm in diameter). Mag. = 425X.

Figure 11

Effect of Na+-free Ringers on pinocytosis. a) enhanced fluorescence image of control follicle. b) In 6 out of 7, large (up to 20 μm) vesicles were evident. c) Normal-sized vesicles were observed in 4 out of 7 follicles. Mag. = 425X.

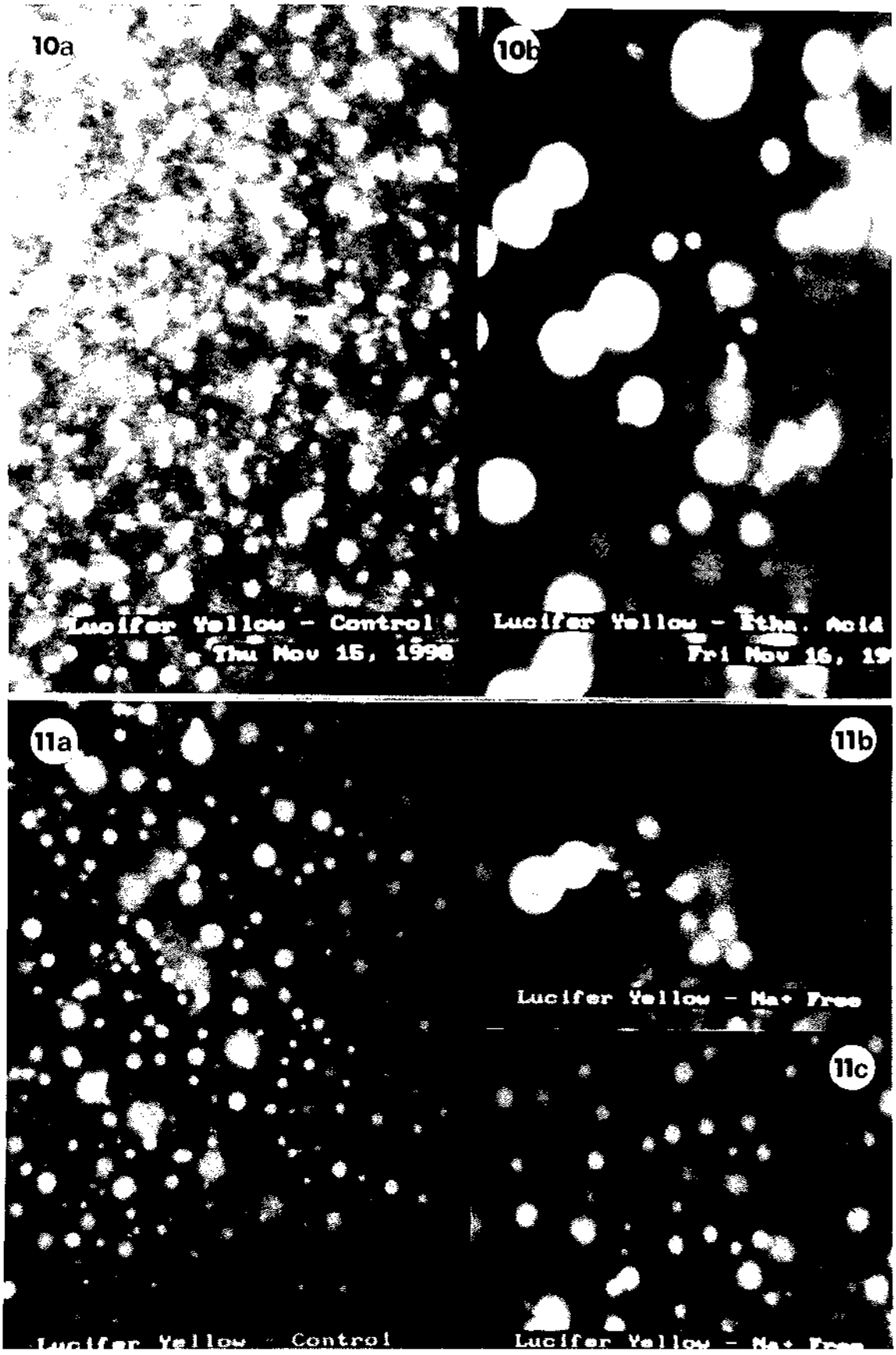
10a
Lucifer Yellow - Control
Thu Nov 15, 1990
10b
Lucifer Yellow - Etha. Acid
Fri Nov 16, 19
11a
Lucifer Yellow - Control
11b
Lucifer Yellow - Na+ Free
11c
Lucifer Yellow - Na+ Free

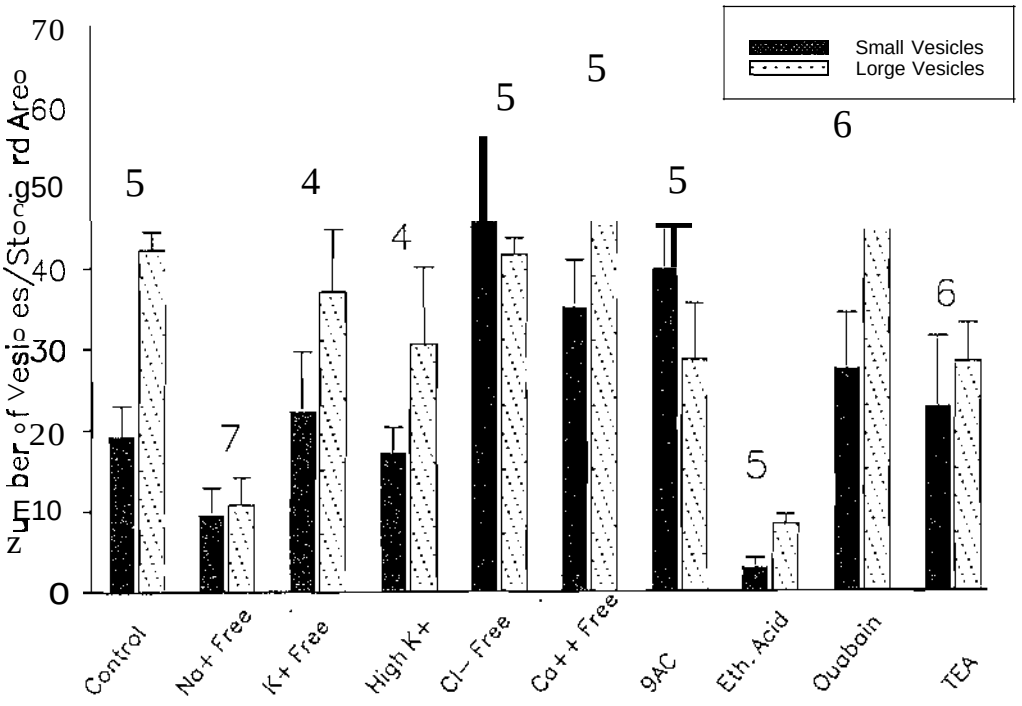

Figure 12

Effects of ion inhibitors, and substitutions on mean number of pinocytotic vesicles/standard area (±SEM). See text for details. Eth Acid = ethacrynic **acid. The number of replicates per treatment are indicated above each bar.**

CHAPTER IV

INTRAOVARIOLE BEAD TRANSPORT IN *Rhodnius prolixus*

INTRODUCTION

Speculation and research on the mechanisms underlying nurse-cell oocyte transport has continued for nearly twenty years (Bier, 1963; Woodruff and Telfer, 1980; Bohrmann, 1991). It is thought that intracellular voltage gradients effect electrophoretic transport of charged proteins in the polytrophic ovarioles of Hyalophora (Woodruff and Telfer, 1980; Telfer et al., 1981b) and in Drosophila (Woodruff et al., 1988; Woodruff, 1989; for dissenting opinions, see Bohrmann and Gutzeit, 1987, and Bohrmann, 1991). Electrically polarized transport between the trophic core and the nurse cell lobes occurs in the telotrophic ovarioles of Rhodnius (Telfer et al., 1981b), the milkweed bug Oncopeltus fasciatus (Woodruff and Anderson, 1984), and the cotton bug, Dysdercus intermedius (Munz and Dittmann, 1987).

A major difference between telotrophic and polytrophic ovarioles is the length of the trophic connection with developing oocytes. Woodruff and

Anderson (1984) point out that, in mid-vitellogenic telotrophic ovarioles, a nurse cell-oocyte electropotential difference of 150 mV is necessary to produce a voltage gradient of 1 V/em. It is therefore not surprising that electrically-polarized transport between the T follicle and tropharium has not been observed in the telotrophic ovarioles studied thus far. Another structural difference between polytrophic and telotrophic ovarioles is the high density of microtubules in the trophic core and cords of the latter (Hyams and Stebbings, 1977, 1979a,b,c; Huebner,1984a). The presence of abundant microtubules strongly implicates a microtubule-based transport system (Stebbings, 1981; Gutzeit, 1986). Dittmann et al. (1987) indicate that micro-injected mitochondria move along the trophic cords of Dysdercus at rates approximating fast and slow axonal transport, and suggest that both electrophoretic and microtubule-based transport systems are operative (Munz and Dittmann, 1987). To develop an assay for intraovariole transport, I utilized microinjection of charged fluorescent latex beads into Rhodnius ovarioles.

MATERIALS AND **METHODS**

FITC-conjugated 0.1- and 0.9 urn carboxylated latex microspheres (Polysciences) were washed, centrifuged, and resuspended 3 times in a microinjection buffer at pH 6.8 to remove unbound dye (Zavortink et al., 1983).

For both pressure and iontophoretic rnicroinjection, Pyrex glass tubes (inner diameter=0.6 mm; outer diameter=0.8 mm) were pulled on a vertical pipette puller (David Kropf Instruments, Tujunga, CA). Two technical problems arose during these microinjections. First, the size of the beads necessitated a relatively large tip diameter to avoid clogging. Secondly, the basal lamina around Rhodnius ovarioles presents an especially tough barrier to electrode penetration.

To enable oocyte penetration with relatively large micropipette tips, a bevelling method after Lederer et al. (1979) was adopted. Briefly, electrode tips were immersed in a thick slurry of 3 M KCI and 0.05 µm aluminium silica particles. The slurry was rotated past electrodes at approximately 20 rpm, and a wick electrode in the overlying KCI supernatant allowed monitoring of the electrode resistance. Final electrode resistance after 30 min was usually of the order of 2 megohm.

To insure microinjections were not simply "pressuring" beads away from the injection site, both pressure and iontophoretic injections were done. A 2 ml Gilmont micrometer syringe (Great Neck, NY) was used to inject approximately 500 pl volumes into ovarioles. Iontophoretic injections were made with 100 Hz, 150 nAmp command pulses through a WPI iontophoresis unit (Model No. S-7061A). Beads were injected into the trophic core at the base of the tropharium. To visualize single beads or groups of beads in situ, the epifluorescence, low light video, and computer enhancement system described in Chapter 3 was used, and ovarioles were each observed once between 10 min and 48 hrs post-injection.

RESULTS

The results of microinjections are summarized in Fig. 1. Of 60 ovarioles successfully injected (no gross degeneration at the time of observation), 32 ovarioles (22 pressure-injected, 10 iontophoretically-injected) exhibited some degree of intracellular movement. Single beads and clumps of beads were found at the top of the trophic cords (Fig. Ib), at the cortex of the T-l oocyte (Fig. Ic), and in the trophic cord and cortex of the T oocyte (Fig. 1d, inset.) In two instances, 0.1 urn beads were successfully microinjected into the T-l oocyte; in neither case was movement of the beads towards the tropharium observed (Fig. Ie).

DISCUSSION

These preliminary results indicate that negatively-charged latex spheres are transported unidirectionally from the tropharium to the subterminal and terminal oocytes. While this certainly does not definitively prove either electrophoretic- or microtubule-based transport, the movement of beads into but not out of subterminal oocytes is consistent with the electrophoretic theory of transport. Current influx is observed in the subterminal oocytes of ovarioles at this stage

(Chapter 1), which indicates the entry of positive charge; electromotive forces would therefore favour movement of beads from the tropharium into subterminal oocytes. On the other hand, the very weak voltage gradient along the trophic cord to the T oocyte suggests that other transport processes are involved in the movement of latex beads to the T oocyte.

The counter-experiment wherein positively-charged (possibly amide-linked) beads are injected into various parts of the ovariole is required. However, the present experiment shows the feasibility of using latex beads to study transport processes in Rhodnius ovarioles. Furthermore, latex beads can be covalently labelled with a variety of protein and carbohydrate moieties, and this could enable more precise dissection of the mechanisms underlying cytoplasmic transport.

Figure 1

FITC-conjugated carboxylated latex beads were microinjected into tropharia. Movement of beads to various positions (trophic cords, oocytes) is indicated in the line drawing. The insets in the micrographs are three-dimensional line intensity profiles which clearly delineate the beads from background autofluorescence. *a)* 0.1 urn beads in middle of the trophic core, 10 min post-injection. *b)* 0.1 urn beads at top of trophic cords and in subterminaloocytes. c) 0.9 urn bead near rear cortex of T-l oocyte. *d) 0.1* urn bead near cortex of T oocyte, 16 hours post-injection. Beads were found in the T oocyte of only 2 ovarioles out of 32 injected. Circular inset shows 0.1 urn bead in trophic cord. *e)* Controls (0.1 pm beads injected into T-1 oocytes) did not show reverse transport.

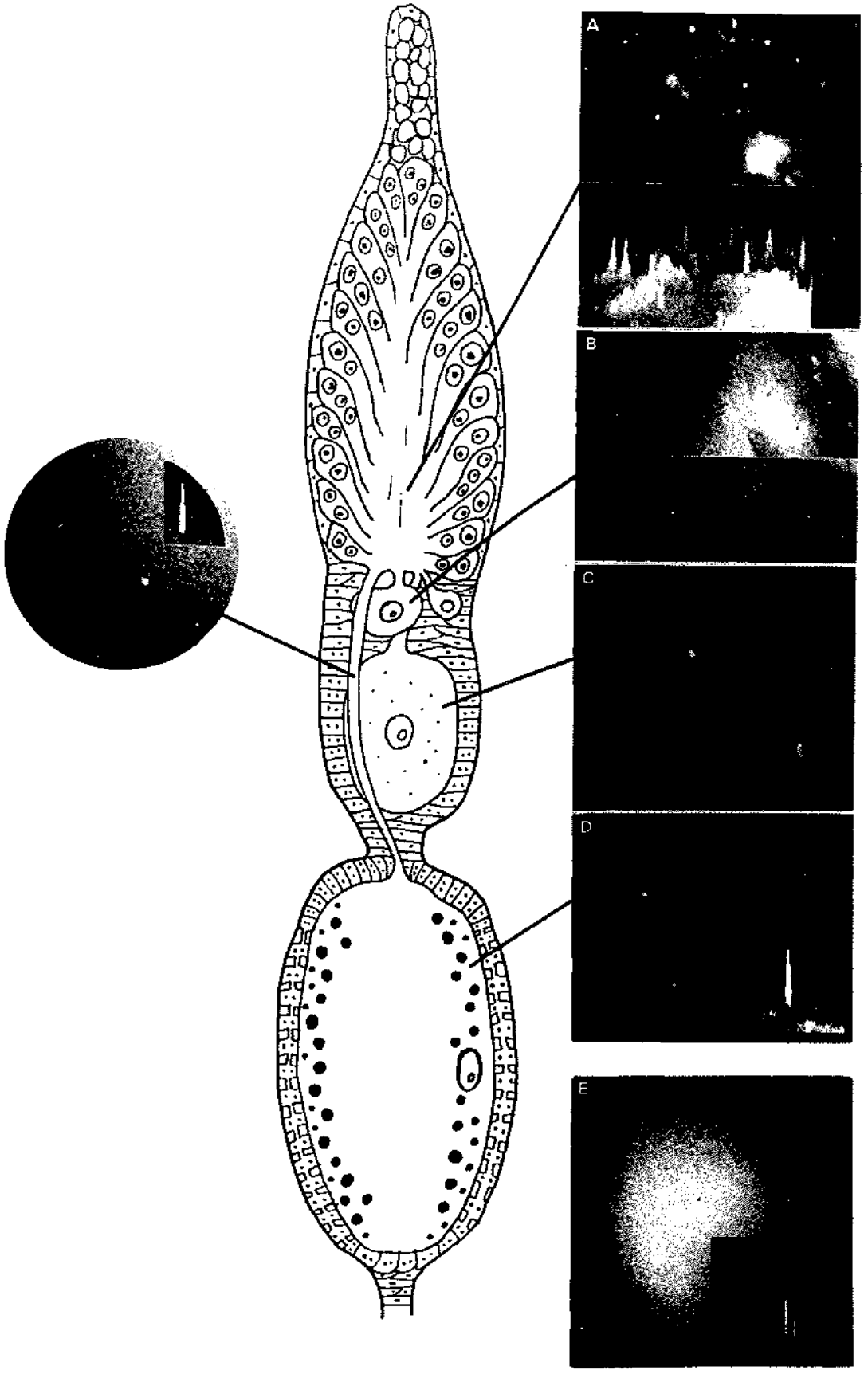
A
B
C
D
E

SUMMARY

This study presents several new findings. Radial asymmetries in the three-dimensional current pattern around Rhodnius prolixus ovarioles are now apparent, especially over the T follicle. It is not yet possible to say if these asymmetries are correlated with developmental axes, but future research aimed at uncovering whether or not mRNA or maternal gene products are localized in the oocyte may help to resolve this. Data from denuded ovarioles indicate that transcellular currents are at least in part generated by germ cells, and this opens the possibility that transcellular currents are involved in localization/delocalization of ooplasmic determinants (see Larabell and Capco, 1988).

The follicular epithelium in Rhodnius likely contributes to the pattern of extracellular currents, since currents around denuded germ cells are usually weaker. Additionally, currents over the base of the tropharium are masked or modulated by follicle cells. Clearly, the role of the follicular epithelium, both in current generation and in ovarian regulation, must be further explored, especially in light of recent findings by Woodruff and Telfer (1990) with respect to follicle cell-oocyte coupling and physiological activation in Hyalophora. Gap junctions also exist between germ cells and follicle cells of Rhodnius ovarioles (Huebner,

1981b; Telfer et al., 1982), and it is possible that the follicular epithelium in the telotrophic ovariole is important in the overall ion conductance pathways and in oocyte activation. The present study clearly shows dynamic changes in current direction over denuded subterminal oocytes which may play a key role - in conjunction with follicle cell-oocyte interactions -- in oocyte regulation and growth.

Active Na" efflux around Rhodnius ovarioles is in agreement with putative Na"/K+ ATPase activity in follicle cells (Ilenchuk and Davey, 1982) and with the results of studies with intracellular electrodes (O'Donnell, 1985, 1986). Perhaps the most noteworthy findings are that transient inward Ca^{+2} currents appear over the T follicle, and that Ca^{+2} is one of the ions involved in current influx over the tropharium. Given the prime role of Ca^{+2} as a second messenger and regulator of cellular function, these currents could have far-reaching effects on oocyte physiology. Future experiments could use Ca'<chelating buffers, pharmacological agents such as Diltiazem, and ionophores to perturb Ca^{+2} homeostasis. However, before this system can be fully exploited, a longer-term culture medium should be devised to assess the "effects of these treatments on in vitro development.

The "trans-tropharium" current correlates with the observations of Telfer et al. (1981b) on the electrophoretic movement of dye in the tropharium. The migration of basic dye to nurse cell lobes in the basal half of the tropharium would occur if positive charge leaves (or negative charge enters) this region of the tropharium. In addition, Mn^{+2}, high K^{+}, and Ba^{+2} substitution media, since they

uncouple the trans-tropharium current, provide useful experimental tools for examining the relationship between transcellular currents and electrophoretic transport. With this in mind, I am planning microinjection experiments with FLY and McFLY, as well as with charged latex beads.

The two main ions carrying current influx over the T follicle also affected pinocytosis, which forms a definite, though not definitive, link between spatially segregated ion currents and a dynamic cellular process. To clarify the function of these ions in regulating pinocytosis, substitution experiments coupled with measurements of endosomal pH and ooplasmic Ca^{+2} are presently being planned. In conclusion, a clearer picture of the role of bioelectric currents in oogenesis is emerging, although many critical elements remain to be explored.

LITERATURE CITED

Abu-Hakima, R, and Davey, KG. 1977. The action of juvenile hormone on the follicle cells of Rhodnius prolixus: the importance of volume changes. J. Exp. BioI. 69: 33-44.

Abu-Hakima, R, and Davey, K.G. 1979. A possible relationship between ouabain-sensitive, Na"/K'-dependent ATPase and the effect of juvenile hormone on the follicle cells of Rhodnius prolixus. Insect. Biochem. 9: 195-198.

Aickin, C.C., and Thomas, RC. 1977. An investigation of the ionic mechanisms of intracellular pH regulation in mouse soleus muscle fibres. J. PhysioI. 273: 295-316.

Al-Awquati, Q. 1986. Proton-translocating ATPases. Ann. Rev. Cell BioI. 2: 179-199.

Alberts, B., Bray, D., Lewis, J., Raff, M., Roberts, K., and Watson, J.D. 1990. Molecular Biology of the Cell. 2nd ed. Garland Publishing, New York.

Allen, H.J., Ault, G., Winzler, RJ., and Danielli, J.P. 1974. Chemical characterization of the isolated cell surface of Amoeba. J. Cell BioI. 60: 26-38.

Allison, A.C., and Davies, P. 1974. Mechanisms of endocytosis and exocytosis. Symp. Soc. Exp. BioI. 28: 419-446.

Allison, A.C., and Freeman, A.R 1967. Substructural changes correlated with electrical resistance and pinocytosis. Science 155: 582-585.

Almers, W., and Stirling, C. 1984. Distribution of transport proteins over animal cell membranes. J. Membr. Biol. 77: 169-186.

Anstee, J.H., and Bowler, K. 1979. Ouabain-sensitivity of insect epithelial tissues. Compo Biochem. Physiol. 62(A): 763-769.

Barker, A.T., Jaffe, L.F., and Vanable [r., J.W. 1982. The glabrous epidermis of cavies contains a powerful battery. Am. J. PhysioI. 242: R358-R366.

Bean, B.P. 1985. Two kinds of calcium channels in canine atrial cells. Differences in kinetics, selectivity, and parmacology. J. Gen. Physiol. 86: 1-30.

Begg, D.A., and Rebhun, 1.1. 1979. pH regulates the polymerization of actin in the sea urchin egg cortex. J. Cell BioI. 83: 241-248.

Benveniste, M., Schlessinger, J., and Kam, Z. 1989. Characterization of internalization and endosome formation of epidermal growth factor in transfected NIH-3T3 cells by computerized image-intensified three-dimensional fluorescence microscopy. J. Cell BioI. 109: 2105-2115.

Berridge, M.J., Lindley, B.D., and Prince, W.T. 1976. Studies on the mechanism of fluid secretion by isolated salivary glands of Calliphora. J. Exp. BioI. 64: 311-322.

Bier, K 1963. Synthese, interzellulare transport, und Abbau von Ribonukleinsaure im ovar der stubenfliege Musca domestica. J. Cell BioI. 16: 436-440.

Bjorkman, T. 1989. The use of bioelectric currents to study gravity perception in roots. BioI. Bull. 176(S): 49-55.

Bluh, 0., and Scott, B.1.H. 1950. Vibrating probe electrometer for the measurement of bioelectric potentials. Rev. Sci. Inst. 21: 867-868.

Bohrmann, J. 1991. In vitro culture of Drosophila ovarian follicles: the influence of different media on development, RNA synthesis, protein synthesis and potassium uptake. Roux's Arch Dev. Biol. 199: 315-326.

Bohrmann, J., Dorn, A., Sander, K, and Gutzeit, H. 1986a. The extracellular current pattern and its variability in vitellogenic Drosophila follicles. J. Cell Sci. 81: 189-206.

Bohrmann, J., Huebner, E., Sander, K, Gutzeit, H. 1986b. Intracellular electrical potential measurements in Drosophila follicles. J. Cell Sci. 81: 207-221.

Bohrmann, J., and Gutzeit, H. 1987. Evidence against electrophoresis as the principal mode of protein transport in vitellogenic ovarian follicles of Drosophila. Development 101: 279-288.

Bond, G.H., and Hudgins, P.M. 1980. Inhibition of red cell Ca^{+2} ATPase by vanadate. Biochim. Biophys. Acta 600: 781-790.

Borgens, RB., Vanable, J.W., [r, and Jaffe, L.F. 1979. Bioelectricity and regeneration. Bioscience 29: 468-494.

Bowdan, E., and Kunkel, J.G.· 1990. Patterns of ionic currents around the developing oocyte of the German cockroach, Blatella germanica. Dev. Biol. 137: 266-275.

Brandt, P.W., and Freeman, A.R 1967. Plasma membrane: structural changes correlated with electrical resistance and pinocytosis. Science 155: 582-585.

Brawley, S.H., and Robinson, KR 1985. Cytochalasin treatment disrupts the endogenous currents associated with cell polarization in fucoid zygotes: studies of the role of F-actin in embryogenesis. J. Cell Biol. 100: 1173-1184.

Browder, L.W., Erickson, CA., and Jeffrey, W.R 1991. Developmental Biology. Third Edition. Saunders College Publishing, Toronto.

Brown, KT., and Flaming, D.G. 1986. Advanced Micropipette Techniques for Cell Physiology. John Wiley & Sons, Chichester.

Brownlee, C 1989. Visualizing cytoplasmic calcium in polarizing zygotes and growing rhizoidsof Fucus serratus'. Biol, Bull. 176(S): 14-17.

Brownlee, C, and Wood, J.W. 1986. A gradient of cytoplasmic free calcium in growing rhizoid cells of Fucus serratus. Nature 320: 624-626.

Buning, J. 1978. Development of telotrophic-meroistic ovarioles of polyphage beetles with special reference to the formation of nutritive cords. J. Morph. 156: 237-256.

Buning, J. 1979. The telotrophic-meroistic ovary of megaloptera. 1. The ontogenic development. J. Morph. 162: 37-66.

Busa, W.B. 1982. Cellular dormancy and the scope of pl-I, mediated metabolic regulation. In Intracellular pH: Its Measurement, Regulation, and Utilization in Cellular Functions. R Nuccitelli and D.W. Deamer (eds.). Allan R Liss, New York. pp. 417-426.

Busa, W.B. 1986. Mechanisms and consequence of pH-mediated cell regulation. Ann. Rev. Physiol. 48: 389-402.

Busa, B.W., and Nuccitelli, R 1984. Metabolic regulation via intracellular pH. Am. J. Physiol. 246: R409-R438.

Capco, D., and Jeffrey, W. 1979. Origin and spatial distribution of messenger RNA during oogenesis of an insect, Oncopeltus fasciatus. J. Cell Sci. 39: 63-76.

Charnock, J.s., Potter, H.A., and McKee, D. 1970. Ethacrynic acid inhibition of (Na" + K+)-activated adenosine triphosphatase. Biochem. Pharm. 19: 1637-1641.

Chiou, c.Y., and Malagodi, M.J. 1975. Studies on the mechanism of the action of a new Ca^{2+} antagonist, 8-(N-N-diethylamine)-octyl-3,4,5,-trimethoxybenzoate hydrachloride in smooth and skeletal muscles. Brit. J. Pharmacol. 53: 279-288.

Chiu, S.Y., and Ritchie, J.M. 1980. Potassium channels in nodal and internodal axonal membrane of mammalian myelinated fibres. Nature 284: 170-171.

Cooper, M.S., and Schliwa, M. 1986. Transmembrane Ca^{+2} fluxes in the froward and reversed galvanotaxis of fish epidermal cells. In Ionic Currents in Development. Alan RUss, New York. pp.311-318.

Davenport, R 1974. Synthesis and intercellular transport of ribosomal RNA in the ovary of the milkweed bug, Oncopeltus fasciatus. J. Insect Physiol. 20: 1949-1956.

Davis, P.W. 1970. Inhibition of Renal Na'.K'vactivated adenosine triphosphatase activity by ethacrynic acid. Biochem. Pharm. 19: 1983-1989.

Del Castillo, J.R, and Robinson, J.W.L. 1985. Nat-stimulated ATPase activities in basolateral plasma membranes from guinea-pig small intestinal epithelial cells. Biochim. Biophys. Acta 812: 413-422.

Demarest, J.R, Scheffey, C., and Machen, T.E. 1986. Segregation of gastric sodium and chloride transport: a vibrating probe and microelectrode study. Am. J. Physiol. 251: C643-C648.

Diehl-lones, W., and Huebner, E. 1989a. Pattern and composition of ionic currents around ovarioles of the Hemipteran, Rhodnius prolixus (Stahl). BioI. Bull. 176(S): 86-90.

Diehl-lones, W., and Huebner, E. 1989b. Bead transport and ionic currents in an ovary. J. Cell BioI. 109(4-2): 32a, abs no. 157.

DiMario, P.J., and Mahowald, A.P. 1986. The effects of pH and weak bases on the in vitro endocytosis of vitellogenin by oocytes of Drosophila melanogaster. Cell and Tiss. Res. 246: 103-108.

Dinsmore, J.H., and Sloboda, RD. 1988. Calcium and calmodulin-dependent phosphorylation of a 62kd protein induces microtubule depolymerization in sea urchin mitotic aparatusses. Cell 53: 769-780.

Dittmann, F., Ehni, R, and Engels, W. 1981. Bioelectric aspects of the hemipteran telotrophic ovariole (Dysdercus intermedius). Roux's Arch. Dev. BioI. 190: 221-225.

Dittmann, F., Weiss, D.G., and Miinz, A. 1987. Movement of mitochondria in the ovarian trophic cord of Dysdercus intermedius (Heteroptera) resembles nerve axonal transport. Roux's Arch. Dev. Biol. 196: 407-413.

Dorn, A., and Weisinseel, M.H. 1982. Advances in vibrating probe techniques. Protoplasma 113: 89-96.

Duggon, D.E., and Noll, RM. 1965. Effects of ethacrynic acid and cardiac glycosides upon a membrane adenosine-triphosphatase of renal cortex. Arch Biochem. Biophys. 109: 388-396.

Dux, 1., and Martonosi, A. 1983. The regulation of ATPase-ATPase interactions in sarcoplasmic reticulum membrane. J. Biol. Chern. 258: 11896-11902.

Eckert, R, and Naitoh, Y. 1972. Bioelectric control of locomotion in the ciliates. J. Protozool. 19(2): 237-243.

Emanuelson, H., and Arlock, P. 1985. Intercellular voltage gradient between oocyte and nurse cells in a polychaete. Exp. Cell Res. 161: 558-561.

Ephrussi, B., and Beadle, G.W. 1936. A technique of transplantation for Drosophila. Amer. Naturalist 70: 218-225.

Erickson, C.A., and Nuccitelli, R 1984. Embryonic fibroblast motility and orientation can be influenced by physiological electric fields. J. Cell Biol. 98: 296-307.

Fathpour, H., Anstee, J.H., and Hyde, D. 1983. Effect of Na", *K+,* ouabain, amiloride and ethacrynic acid on the transepithelial potential across malpighian tubules of Locusta. J. Insect Physiol 29(10): 773-778.

Fawcett, D.W., Ito, S., and Slautterback, D. 1959. The occurrence of intercellular bridges in groups of cells exhibiting synchronous differentiation. J. Biophys. and Biochern. CytoI. 5: 453-460.

Forscher, P. 1989. Calcium and phosphoinositide control of cytoskeletal dynamics. TINS 12: 468-474.

Franchi, 1.1., and Mandl, A.M. 1962. The ultrastructure of oogonia and oocytes in the foetal and neonatal rat. Proc. Roy. Soc. B. 157: 99-114.

Freeman, J.A., Manis, P.B., Snipes, G.J., Mayes, B.N., Samson, P.c., Wikswo Jr., J.P., Freeman, D.B. 1985. Steady growth cone currents revealed by a novel circularly vibrating probe: a possible mechanism underlying neurite growth. J. Neurosci. Res. 13: 257-283.

Gee, J.D. 1976. Fluid secretion by the Malpighian tubules of the Tsetse fly Glossinia moritans: the effects of ouabain, ethacrynic acid and amiloride. J. Exp. BioI. 65: 323-332.

Geysen, [ohan. 1988. The morphology and molecular cytology of the egg follicles of the adult blowfly, Sarcophaga bullata. Ph.D. Thesis. Katholieke Universiteit Leuven, Belgium.

Gilbert, S.P. 1988. Developmental Biology. 2nd ed. Sinaver Assoc., Sunderland, Mass.

Grinstein, S., and Rothstein, A. 1986. Mechanisms of regulation of the Na+/H+ exchanger. J. Membr. BioI. 90: 1-12.

Gutzeit, H.O. 1986. Transport of molecules and organelles in meroistic ovarioles of insects. Differentiation 31: 155-165.

Hagedorn, H.H., and Kunkel, J.G. 1979. Vitellogenin and bitellin in insects. A. Rev. Ent. 24: 475-505.

Hagins, W.A., Penn, R.D., and Yoshikami, S. 1970. Dark current and photocurrent in retinal rods. Biophys. J. 10: 380-412.

Hagiwara, S., and Byerly, 1. 1983. The calcium channel. Trends Neurosci. 6: 189-193.

Hagiwara, S., and Jaffe, l.A. 1979. Electrical properties of egg cell membranes. Ann. Rev. Biophys. Bioeng. 8: 385-416.

Hajjar, J.-J., Zakko, S., and Tomicic, T.K. 1986. Effects of vanadate on water and electrolyte transport in rat jejunum. Biochim. Biophys. Acta 863: 325-328.

Hamill, a.p., Marty, A., Neher, E., Sakmann, B., and Sigworth, P.J. 1981. Improved patch-clamp techniques for high resolution current recording from cells and cell-free membrane patches. Pfliigers Arch. 391: 85-100.

Harold, F.M. 1986. Transcellular ion currents in tip growing organisms: where are they taking us? In Ionic Currents in Development. R Nuccitelli (ed.). Prog. Clin. Biol, Res., Vol 2, 210. Alan R. Liss, Inc., New York. pp. 359-366.

Harvey, B.J., Thomas, S.R., and Ehrenfeld, J. 1988. Intracellular pH controls cell membrane Na" and K+ conductances and transport in frog skin epithelium. J. Gen. Physiol, 92: 767-791.

Hay, B., Ackerman, L., Barbel, L., Jan, L.Y., and Jan, Y. N. 1988. Identification of a component of Drosophila polar granules. Development 103: 625-640.

Heiple, J.M., and Taylor, D.L. 1982. pH changes in pinosomes and phagosomes in the Ameba, Chaos carolinensis. J. Cell Biol. 94: 143-149.

Helenius, A., Mellman, L, Wall, D., and Hubbard, A. 1983. Endosomes. Trends Biochem. Sci. 8: 245-250.

Hermann, A., and Gorman, A.L.F. 1981. Effects of tetraethylammonium on potassium currents in a molluscan neuron. J. Gen Physiol, 78: 87-110.

Hermsmeyer, K., and Sperelakis, N. 1970. Decrease in K+ conductance and depolarization of frog cardiac muscle produced by Ba'". Am. J. Physiol. 219: 1108-1114.

Highsmith, S., Barker, D., and Scales, D.J. 1985. High-affinity and low-affinity vanadate binding to sarcoplasmic reticulum $Ca^{+2\text{-ATPase}}$ labeled with fluorescein isothiocyanate. Biochim. Biophys. Acta 817: 123-133.

Hille, B. 1984. Ionic Channels of Excitable Membranes. Sinauer Associates Inc., Sunderland, USA.

Hinkle, L., McCaig, CD., and Robinson, K.R. 1981. The direction of growth differentiating neurons and myoblasts from frog embryos in an applied electrical field. J. Physiol. (London) 314: 121-135.

Huebner, E. 1981a. Nurse cell-oocyte interactions in the telotrophic ovarioles of an insect, Rhodnius prolixus. Tissue Cell 13: 105-125.

Huebner, E. 1981b. Oocyte-follicle cell interaction during normal oogenesis and atresia in an insect, Rhodnius prolixus. J. Ultrastruct. Res. 74: 95-103.

Huebner, E. 1982. Ultrastructure and development of the telotrophic ovary. In The Ultrastructure and Functioning of Insect Cells. H. Akai, RC. King, and S. Morohoshi (eds.). Soc. for Insect Cells, Japan. pp.9-12.

Huebner, E. 1983. Oostatic hormone-antigonadotropin and reproduction. In Endocrinology of-Insects. RG.H. Downer and H. Laufer (eds.). Alan R Liss, New York. pp.319-329.

Huebner, E. 1984a. Developmental cell interactions in female reproductive organs. In Advances in Invertebrate Reproduction, Vol 3. W. Engels (ed.). Elsevier North Holland and Biomedical Publishers, Amsterdam. pp.97-105.

Huebner, E. 1984b. The ultrastructure and development of the telotrophic ovary. In Insect Ultrastructure, Vol 2. RC. King and H. Akai (eds.). Plenum Press, New York. pp. 3-48.

Huebner, E., and Anderson, E. 1970. The effects of vinblasting sulfate on the microtubular organization of the ovary of Rhodnius prolixus. J. Cell Biol. 46: 191-198.

Huebner, E., and Anderson, E. 1972a. A cytological study of the ovary of Rhodnius prolixus. I. The ontogeny of the follicular epithelium. J. Morph. 136: 459-494.

Huebner, E., and Anderson, E. 1972b. A cytological study of the ovary of Rhodnius prolixus. II. Oocyte differentiation. J. Morph. 137: 385-416.

Huebner, E., and Anderson, E. 1972c. A cytological study of the ovary of Rhodnius prolixus. III. Cytoarchitecture and development of the trophic chamber. J. Morph. 138: 1-40.

Huebner, E., and Davey, K.G. 1973. An antigonadotropin from the ovaries of the insect Rhodnius prolixus Stal. Can. J. Zoo1. 51: 113-120.

Huebner, E., and Injeyan, H. 1980. Patency of the follicular epithelium in Rhodnius prolixus: a reexamination of the hormone response and technique refinement. Can. J. Zoo1. 58: 1617-1625.

Huebner, E., and Injeyan, H. 1981. Follicular modulation during oocyte development in an insect: formation and modification of septate and gap junctions. Dev. BioI. 83: 101-113.

Huebner, E., and Sigurdson, W.J. 1986. Extracellular currents during insect oogenesis: special emphasis on telotrophic ovarioles. In Ionic Currents in Development. R Nuccitelli (ed.). Prog. Clin. BioI. Res., Vol 2, 210. Alan R Liss Inc., New York. pp. 155-164.

Hush, J.M., and Overall, RL. 1989. Steady ionic currents around pea (Pisum sativum L.) root tips: the effects of tissue wounding. BioI. Bull. 176(5): 56-65.

Hyams, J.S., and Stebbings, H. 1977. The distribution and function of microtubules in nutritive tubes. Tissue Cell 9: 537-545.

Hyams, J.S., and Stebbings, H. 1979a. The formation and breakdown of nutritive tubes: massive microtubular organelles associated with cytoplasmic transport. J. Ultrastruct. Res. 68: 46-57.

Hyams, J.S., and Stebbings, H. 1979b. The mechanism of microtubule associated cytoplasmic transport. Cell Tissue Res. 196: 103-116.

Hyams, J.S., and Stebbings, H. *1979c.* The mechanism of microtubule-based cytoplasmic transport. J. Ultrastruct. Res. 68: 46-57.

Ilenchuck, T.T., and Davey, KG. 1982. Some properties of Na+-K+ ATPase in the follicle cells of Rhodnius prolixus. Insect Biochem. 12: 675-679.

Ilenchuck, T.T., and Davey, KG. 1983. Juvenile hormone increases ouabain-binding capacity of microsomal preparations from vitellogenic follicle cells. Can. J. Biochem. Cell BioI. 61: 826-831.

Inoue, S. 1986. Video Microscopy. Plenum Press, New York.

Jaffe, L.p. 1966. Electrical currents through the developing Fucus egg. Proc. Nat!. Acad. Sci. USA. 56: 1102-1109.

Jaffe, L.A. 1976. Fast block to polyspermy in sea urchin eggs is electrically mediated. Nature 261: 68-71.

Jaffe, L.F. 1977. Electrophoresis along cell membranes. Nature 265: 600-602.

Jaffe, L.F. 1979. Control of development by ionic currents. In Membrane Transduction Mechanisms. RA. Cone and J.E. Dowling (eds.), Soc. Gen. Physiol. Symp. 33. Raven Press, New York. pp. 100-231.

Jaffe, L.F. 1981. The role of ionic current in establishing developmental pattern. Phil. Trans. R Soc. Lond. B. 295: 553-566.

Jaffe, L.F. 1986. Ion currents in development: an overview. Prog. Clin. Biol. Res. 210: 351-358.

Jaffe, L.F., and Nuccitelli, R 1974. An ultrasensitive vibrating probe for measuring steady extracellular currents. J. Cell BioI. 63: 614-628.

Jaffe, L.F., and Poo, M.-M. 1979. Neurites grow faster toward the cathode than the anode in a steady field. J. Exp. Zool. 209: 115-128.

Jaffe, L.F., Robinson, K.R, and Nuccitelli, R 1974. Local cation entry and self-electrophoresis as an intracellular localization mechanism. Ann. N.Y. Acad. Sci. 238: 372-389.

Jaffe, L.F., and Stern, C.D. 1979. Strong electrical currents leave the primitive streak of chick embryos. Science 206: 569-571.

Jaffe, L.F., and Woodruff, RI. 1979. Large electrical currents traverse developing cecropia follicles. Proc. Natl. Acad. Sci. USA 76: 1328-1332.

[amrich, M., et al. 1984. Histone RNA in amphibian oocytes visualized by in situ hybridization to methacrylate-embedded tissue sections. EMBO J. 3: 1939-1943.

Kakiuchi, S., and Sobue, K. 1983. Control of the cytoskeleton by calmodulin and calmodulin-binding proteins. Trends Biochem. Sci. 8: 59-62.

Kastern, W.H., Watson, CA., and Berry, S.J. 1990. Maternal messenger RNA distribution in silkmoth eggs I. Clone Ec4B is associated with the cortical cytoskeleton. Development 108: 497-505.

Kindle, H., Konig, R, and Lanzrein, B. 1988. In vitro uptake of vitellogenin by follicles of the cockroach Nauphoeta cinerea: comparison of artificial media with haemolymph media and role of vitellogenin concentration and of juvenile hormone. J. Insect Physiol. 34: 541-548.

Kindle, H., Lanzrein, B., and Kunkel, J.G. 1990. The effect of ions, ion channel blockers, and ionophores on uptake of vitellogenin into cockroach follicles. Dev. BioI. 142: 386-391.

Kindle, J.G., and Nordin, J.H. 1985. Yolk proteins. In Comprehensive Insect Physiology, Biochemistry, and Pharmacology, vol 1. 1.1. Gilbert, G.A. Kerkut (eds.), Pergamon Press, New York. pp.83-111.

King, RC., and Akai, H. 1971. Spermatogenesis in Bombyx mori. 1. The canal system joining sister spermatocytes. J. Morph. 134: 47-55.

King, RC., and Barklis, W. 1985. Regional distribution of maternal messenger RNA in the amphibian oocyte. Dev. BioI. 112: 203-212.

King, RC., and Burring, J. 1985. The origin and functioning of insect oocytes and nurse cells. In Comprehensive Insect Physiology, Biochemistry, and Pharmacology, Vol 1, Embryogenesis and Repreduction. G.A. Kerkut, 1.1. Gilbert (eds.). Pergamon Press, Oxford, New York. pp. 37-82.

Kleinbaum, D.G., Kupper, 1.1., and Muller, K.E. 1988. Applied Regression Analysis and Other Multivariable Methods. 2nd ed. PWS-Kent Publishing, Boston.

Kline, D. 1986. A direct comparison of the extracellular currents observed in the activating frog egg with the vibrating probes and the patch clamp techniques. In Ionic Currents in Development. R Nuccitelli (ed.). Prog. Clin. BioI. Res., Vol 2, 210. Alan R Liss, Inc., New York. pp. 97-104.

Kline, D., and Nuccitelli, R 1985. The wave of activation currents in the Xenopus egg. Dev. BioI. 111: 471-487.

Kline, D., Robinson, K.R, and Nuccitelli, R 1983. Ion currents and membrane domains in the cleaving Xenopus egg. J. Cell BioI. 97: 1753-1761.

Klopocka, W., and Grebecka, 1. 1985. Effects of bivalent cations on the initiation of Na-induced pinocytosis. Protoplasma 126: 207-214.

Komukai, M., Fujiwara, A., Fujino, Y., and Yasumasu, 1. 1985. The effects of several ion channel blockers and calmodulin antagonists on fertilization-induced acid release and $^{45}Ca^{+2}$ uptake in sea urchin eggs. Exp. Cell Res. 159:463-472.

Konig, R, Kindle, H., Kunkel, J.G., and Lanzren, B. 1988. Vitellogenesis in the cockroach Nauphoeta cinerea: separation of two classes of binding sites and calcium effects on binding and uptake. Arch. Insect Biochem. Physiol. 9: 323-337.

Kropf, D.L. 1986. Intracellular potential recording as a means to investigate the tranhyphal current in Achlya. In Ionic Currents in Development. Alan R Liss, New York. pp.97-104.

Kropf, D.L. 1989. Calcium and early development in fucoid algae. Biol. Bull. 176(S): 5-8.

Kropf, D.L., Caldwell, J.H., Gow, N.A.R, and Harold, F.M. 1984. Transcellular ion currents in the water mold Achyla. Amino acid proton symport as a mechanism of current entry. J. Cell Biol. 99: 486-496.

Kropf, D.L., and Quatrano, RS. 1987. Localization of membrane-associated calcium during development of fucoid algae using chlorotetracycline. Planta 171: 158-170.

Kuffler, S.W., Nichols, J.G., and Martin, A.R. 1984. From Neuron To Brain. 2nd ed. Sinauer Associates Inc., Sunderland, USA.

Kuhtreiber, W.M., and Jaffe, L.F. 1990. Detection of extracellular calcium gradients with a calcium-specific vibrating electrode. J. Cell Biol.

Kunkel, J.G. 1986. Dorsoventral currents are associated with vitellogenesis in cockroach ovarioles. In Ionic Currents in Development. R Nuccitelli (ed.). Prog. Clin. BioI. Res., Vol 2, 210. Alan R Liss, Inc., New York. pp. 165-172.

Kunkel, J.G., and Nordin, J.H. 1985. Yolk proteins. In Comprehensive Insect Physiology, Biochemistry, and Pharmacology, vol 1. Ll. Gilbert, G.A. Kerkut (eds.). Pergamon Press, New York. pp.83-111.

Larabell, CA., and Capco, D.G. 1988. Role of calcium in the localization of maternal poly *(A)*+ RNA and tubulin mRNA in Xenopus oocytes. Roux's Arch. Dev. BioI. 197: 175-183.

Lederer, W.J., Spindler,' A.J., and Eisner; D.A. 1979. Thick slurry bevelling. Pflug. Arch. 381: 287-288.

Lee, KS., and Tsien, R.W. 1983. Mechanism of calcium channel blockade by verapamil, D600, diltiazem and nitrendipine in single dialysed heart cells. Nature 302: 790-794.

Luther, P.W., Peng, H.B., and Lin, J.J.-C 1983. Changes in cell shape and actin distribution induced by constant electric fields. Nature (London): 303: 61-64.

MacKnight, A.D.C, and Leaf, A. 1977. Regulation of cellular volume. Phys. Reviews 57(3): 510-573.

Maddrell, S.H.P. 1969. Secretion by the malphigian tubules of Rhodnius. The movement of ions and water. J. Exp, Biol. 57:71-98.

Mahowald, A.P. 1971. Polar granules of Drosophila. III. The continuity of the life cycle of Drosophila. J. Exp. Zoo1. 176: 329-343.

Maxfield, F.R. 1989. Measurement of vacuolar pH and cytoplasmic calcium in living cells using fluorescence microscopy. Meth. in Enzymology 173: 765-771.

Maxfield, P.R., and Dunn, K 1990. Studies of endocytosis using image intensification fluorescence microscopy and digital image analysis. In Optical Microscopy for Biology. B. Herman, K Jacobson (eds.), Wiley-Liss Inc., New York. pp. 357-371.

McCaig, CD. 1989. On the mechanism of nerve galvanotropism. Biol. Bull. 176(S): 136-139.

McCloskey, M.A., Liu, Z.-Y., and Poo, M.-M. 1984. Lateral electromigration and diffusion of Fce receptors on rat basophilic leukemia cells: effects of IgE binding. J. Cell BioI. 99: 778-787.

Mellman, I., Fuchs, R., and Helenius, A. 1986. Acidification of the endocytic and exocytic pathways. Ann. Rev. Biochem. 55: 663-700.

Melton, A.A. 1987. Translocation of a localized maternal mRNA to the vegetal pole of Xenopus oocytes. Nature (Lond.) 328: 80-82.

Miller, A.L., Raven, J.A., Sprent, J.L, and Weisenseel, M.H. 1986. Endogenous ion currents traverse growing roots and root hairs of Trifolium repens. Plant. Cell Envir. 9: 79-83.

Miller [r., F. 1977. College Physics. 4th ed. Harcourt, Brace, Jovanovich, New York.

Miyazaki, S.-I., and Hagiwara, S. 1976. Electrical properties of the Drosophila egg membrane. Dev. BioI. 53: 91-100.

Miinz, A., and Dittmann, F. 1987. Voltage gradients and microtubules both involved in intercellular protein and mitochondria transport in the telotrophic ovariole of Dysdercus intermedius. Roux's Arch. Dev. Biol. 196: 391-396.

Nielsen, R 1979. A 3 to 2 coupling of the Na-K pump responsible for the transepithelial Na transport in frog skin disclosed by the effect of Ba. Acta. PhysioI. Scand. 1979: 189-191.

Nuccitelli, R 1983. Transcellular ion currents: signals and effectors of cell polarity. In Modern Cell Biology, Vol 2. Alan R Liss, New York. pp.451-481.

Nuccitelli, R 1984. The involvement of transcellular ion currents and electric fields in pattern formation. In Pattern Formation. G.M. Malasinski, S.V. Bryant (eds.), MacMillan Publishing, New York. pp.23-46.

Nuccitelli, R 1986. A two-dimensional vibrating probe with a computerized graphics display. In Ionic Currents in Development. Alan R Liss, New York. pp. 13-20.

Nuccitelli, R 1988. Physiological electrical fields can influence cell motility, growth and polarity. Adv. Cell Biol. 2: 213-233.

Nuccitelli, R 1990. Vibrating probe technique for studies of ion transport. Noninvasive Techniques in Cell Biology. Wiley-Liss, New York. pp.273-310.

Nuccitelli, R, and Jaffe, L.F. 1974. Spontaneous current pulses through developing Fucus eggs. Proc. Natl. Sci. USA 71: 4855-4859.

Nuccitelli, R, and Jaffe, L.F. 1976. The ionic components of the current pulses generated by developing fucoid eggs. Dev. Biol. 49: 518-531.

Nuccitelli, R, and Smart, T. 1989. Extracellular calcium levels strongly influence neural crest cell galvanotaxis. Biol. Bull. 176(S): 130-135.

Nuccitelli, R, and Wiley, L.M. 1985. Polarity of isolated blastomeres from mouse morulae: detection of transcellular ion currents. Dev. BioI. 109: 452-463.

O'Donnell, M.J. 1985. Calcium action potentials in the developing oocytes of an insect, Rhodnius prolixus. J. Exp. BioI. 119: 287-300.

O'Donnell, M.J. 1986. Action potentials in Rhodnius oocytes: repolarization is sensitive to potassium channel blockers. J. Exp. Biol. 126: 119-132.

O'Donnell, M.J., and Singh, B. 1988. Cyclic amp modulates electrical excitability of insect oocytes (Rhodnius prolixus). J. Insect PhysioI. 34(6): 499-506.

Oiki, 5., Ohno-Shosaku, T., and Okada, Y. 1989. Electric currents associated with directed migration of fibroblasts. Biol. Bull. 176(5): 123-125.

Olivieri, P.L., Gondim, *K.C.,* Guedes, D.M., and Masudo, H. 1986. Uptake of yolk proteins in Rhodnius prolixus. J. Insect Physiol. 32: 859-866.

Orida, N. and Poo, M.-M. 1978. Electrophoretic movement and localization of acetylcholine receptors in the embryonic muscle cell membrane. Nature (London) 275: 31-35.

Overall, R, and Jaffe, L.P. 1985. Patterns of ionic current through Drosophila follicles and eggs. Dev. BioI. 108: 102-119.

Owen, M.E., and Villereal, M.L. 1982. Effect of the intracellular Ca^{2+} antagonist TMB-8 on serum-simulated Na" influx in human fibroblasts. Biochem. Biophys. Res. Comm. 109: 762-768.

Paradiso, A.M., Tsien, RY., and Machen, T.E. 1987. Digital image processing of intracellular pH in gastric oxyntic and chief cells. Nature (London) 325: 447-450.

Perez-Gonzalez de la Manna, M., Proverbio, F., and Whittembury, G. 1980. In Current Topics in Membranes and Transport, Vol 13. F. Bronner, A. Kleinzeller (eds.). Academic Press. pp. 315-335.

Phillips, D.M. 1970. Insect sperm: their structure and morphogenesis. J. Cell BioI. 44: 243-277.

Poenie, M., Alderton, J., Steinhardt, R, and Tsien, R 1986. Calcium rises abruptly and briefly throughout the cell at the onset of anaphase. Science 233: 886-889.

Poo, M.-M. 1981. In situ electrophoresis of membrane components. Ann. Rev. Biophys. Bioeng. 10: 245-276.

Poo, M.-M., and Robinson, KR 1977. Electrophoresis of concanavalin A receptors along embryonic muscle cell membrane. Nature (London) 265: 602-605.

Pratt, G.E., and Davey, KG. 1972a. The corpus allatum and oogenesis in Rhodnius prolixus (Stal). I. The effects of allatectomy. J. Exp. BioI. 56: 210-214.

Pratt, G.E., and Davey, K.G. 1972b. The corpus allatum and oogenesis in Rhodnius prolixus (Stal). II. The effects of starvation. J. Exp. Biol, 56: 215-221.

Pratt, G.E., and Davey, KG. 1972c. The corpus allatum and oogenesis in Rhodnius prolixus (Stal). III. The effect of mating. J. Exp. BioI. 56: 223-237.

Purves, RD. 1981. Microelectrode Methods for Intracellular Recording and Ionophoresis. Academic Press, London.

Robb, J.A. 1969. Maintenance of imaginal wing discs of Drosophila melanogaster in chemically defined media. J. Cell Biol, 41: 876-885.

Robinson, KR 1979. Electrical currents through full-grown and maturing Xenopus oocytes. Proc. Natl. Acad. Sci. USA 76: 837-841.

Robinson, KR 1985. The responses of cells to electrical fields: a review. J. Cell BioI. 101: 2023-2027.

Robinson, KR, and Cone, R 1980. Polarizing of fucoid eggs by a calcium ionophore gradient. Science 207: 77-78.

Robinson, KR, and Jaffe, L.P. 1975. Polarizing fucoid eggs drive a calcium current through themselves. Science 187: 70-72.

Rodeau, J.C., and Vilain, J.P. 1987. Changes in membrane potential, membrane resistance, and intracellular H^+, K^+, Na^+, and Cl^- activities during the progesterone-induced maturation of urodele amphibian oocytes. Dev. Biol. 120: 481-493.

Roos, A., and Boron, W.F. 1981. Intracellular pH. Physiol, Rev. 61: 297-421.

Scheffey, e. 1986. Electric fields and the vibrating probe, for the uninitiated. In Ionic Currents in Development. R Nuccitelli (ed.), Prog. Clin. Biol, Res., Vol 2, 210. Alan R. Liss, New York. pp. xxv-xxxvii.

Scheffey, e. 1988. Two approaches to construction of vibrating probes for electrical current measurement in solution. Rev. Sci. Instr. 59: 787-792.

Schwartz, A., Lindenmayer, G.E., and Allen, J.e. The sodium-potassium adenosine triphosphatase: pharmacological, physiological and biochemical aspects. Pharmacol. Rev. 27(1): 3-117.

Shen, S.S., and Steinhardt, RA. 1978. Direct measurement of intracellular pH during metabolic derepression of the sea urchin egg. Nature (London) 272: 253-254.

Shen, S.S., and Steinhardt, RA. 1979. Intracellular pH and the sodium requirement at fertilization. Nature 282: 87-89.

Sigurdson, W.J. 1984. Bioelectric aspects of the Rhodnius prolixus ovariole: extracellular current mapping during oogenesis. Ph.D. Thesis. University of Manitoba, Winnipeg.

Sigurdson, W.J., and Huebner, E. 1984. Extracellular currents during oogenesis in an insect. J. Cell Biol. 99(4): 55a, abst 206.

Simoncini, L., Block, M.L., and Moody, W.J. 1988. Lineage-specific development of calcium currents during embryogenesis. Science 242: 1572-1575.

Skou, J.e. 1969. The role of membrane ATPase in the active transport of ions. In Molecular Basis of Membrane Function. D.e. Tostesin (ed.), Prentice-Hall, Englewood Cliffs, N.J. pp. 455-482.

Sonnenblick, B.P. 1950.· The early embryology of Drosophila melanogaster. In Biology of Drosophila. M. Demenec (ed.), John Wiley & Sons, New York. pp.62-167.

Speksnijder, J.E., Miller, A.L., Weisenseel, M.H., Chen, T.-H., and Jaffe, L.F. 1989. Calcium buffer injections block fucoid egg development by facilitating calcium diffusion. Proc. Natl. Acad. Sci. USA 86: 6607-6611.

Standen, N.B., and Stanfield, P.R. 1978. A potential- and time-dependent blockade of inward rectification in frog skeletal muscle fibres by barium and strontium ions. J. Physiol. 280: 169-191.

Stay, B. 1965. Protein uptake in the oocytes of the Cecropia moth. J. Cell BioI. 26: 49-62.

Stebbings, H. 1981. Observations on cytoplasmic transport along ovarian nutritive tubes of polyphagous coleopterans. Cell Tissue Res. 220: 153-161.

Stirling, C.E., and Lee, A. 1980. [3H] ouabain autoradiography of frog retina. J. Cell Biol. 85: 313-324.

Stockem, W., Naib-Majani, W., Wohlfarth-Botterman, KE., Osbor, M., and Weber, K. 1983. Pinocytosis and locomotion in amoebae. XIX. Immunocyto-chemical demonstration of actin and myosin in Amoeba proteus. Eur. J. Cell BioI. 29: 171-178.

Stollberg, J., and Fraser, S.E. 1989. Electric field-induced redistribution of ACh receptors on cultured muscle cells: electromigratin, diffusion, and aggregation. BioI. Bull. 176(S): 157-163.

Strange, K, and Phillips, J.W. 1985. Cellular mechanism of HC03- and CI-transport in insect salt gland. J. Membrane Biol, 83: 25-37.

Stump, RF., and Robinson, KR 1986. Ionic current in Xenopus embryos during neurulation and wound healing. In Ionic Currents in Development. R. Nuccitelli (ed.). Alan R Liss, New York. pp. 223-230.

Sun, Y.A., and Wyman, RJ. 1987. Lack of an oocyte to nurse cell voltage difference in Drosophila. Neuroscience 13: 1139.

Sun, Y.-A., Wyman RJ. 1989. The Drosophila egg chamber: external ionic currents and the hypothesis of electrophoretic transport. Biol. Bull. 176: 79-85.

Taylor, D.L. 1977. The contractile basis of amoeboid movement. IV. The visco-elasticity and contractility of amoeba cytoplasm in vivo. Exp. Cell Res. 105: 413-426.

Telfer, W.H. 1960. The selective accumulation of blood proteins by the saturnid moths. BioI. Bull. 118: 338-351.

Telfer, W.H. 1975. Development and physiology of the oocyte-nurse cell syncytiun. In Advances in Insect Physiology, Vol, 11. J.E. Treherne, M.J. Berridge and V.B. Wigglesworth (eds.). Academic Press, New York. pp. 223-319.

Telfer, W.H., Huebner, E., and Smith, D.S. 1982. The cell biology of vitellogenic follicles in Hyalophora and Rhodnius. In Insect Ultrastructure, Vol I. R'C. King, H. Akai (eds.). Plenum Press, New York. pp. 118-149.

Telfer, W.H., Rubinstein, E.e., and Pan, M.e. 1981a. How the ovary makes yolk in Hyalophora. In Regulation of Insect Development and Behaviour. F. Sehnal, A. Zabza, J.J. Menn, and B. Cymborowski (eds.). Wroclaw Technical University, Wroclaw. pp. 637-654.

Telfer, W.H., Woodruff, RI., and Huebner, E. 1981b. Electrical polarity and cellular differentiation in meroistic ovaries. Am. Zool. 21: 675-686.

Tilney, L.G., Kiehart, D.P., Sardet, e., and Tilney, M. 1978. Role of Ca^{+2} and H+ on the assembly of actin and in membrane fusion in the acrosomal reaction of echinoderm sperm. J. Cell BioI. 77: 536-550.

Tombes, RM., and Borisy, *G.G.* 1989. Intracellular free calcium and mitosis in mammalian cells: anaphase onset is calcium modulated, but is not triggered by a brief transient. J. Cell BioI. 109: 627-636.

Towle, D.W. 1984. Membrane-bound ATPases in athropod ion-transporting tissues. Amer. Zool. 24:177-185.

Tycko, *B.,* Keith, e.H., and F.R Maxfield. 1983. Rapid acidification of endocytic vesicles containing asialoglyco-protein in cells of a human hepatoma line. J. Cell BioI. 97: 1762-1776.

Vanderburg, J.P. 1963. Synthesis and transfer of DNA, RNA and proteins during vitellogenesis in Rhodnius prolixus (Hemiptera). Biol. Bull. 125: 556-575.

Van Der Meer, J.M., and Jaffe, L.F. 1983. Elemental composition of the perivitelline fluid in early Drosophila embryos. Dev. BioI. 95: 249-252.

Verachtert, B. 1988. Electrical polarity in the ovarian follicles of Sarcophaga bullata, Drosophila melanogaster and Locusta migratoria. Ph.D. Thesis. Katholieke Universiteit Leuven, Belgium.

Verachtert, B., and DeLoof, A. 1986. Electric currents around the polytrophic ovarian follicles of Sarcophaga bullata and the panoistic follicles of Locusta migratoria. In Ionic Currents in Development. R Nuccitelli (ed.). Prog. Clin. BioI. Res., Vol 2, 210. Alan R Liss, New York. pp. 173-180.

Verachtert, B., and DeLoof, A. 1989. Intra- and extracellular electrical fields of vitellogenic polytrophic insect follicles. Biol. Bull. 176(S): 91-95.

Vilain, J.P., Moumene, M., and Moreau, M. 1989. Chloride current modulation during meiosis in Xenopus oocytes. J. Exp. Zool. 250: 100-108.

Weeks, D.C., and Melton, D.A. 1987. A maternal mRNA localized to the animal pole of Xenopus eggs encodes a subunit of mitochondrial ATPase. Proc. Natl. Acad. Sci. USA 84: 2798-2802.

Weisinseel, M.H., Dorn, A., and Jaffe, L.P. 1979. Natural H+ currents traverse growing roots and root hairs of barley (Hordeum vulgare). Plant Physiol. 64: 512-518.

Weisinseel, M.H., Nuccitelli, R., and Jaffe, L.F. 1975. Large electrical currents traverse growing pollen tubes. J. Cell Biol. 66: 556-567.

Winkel, G.R., and Nuccitelli, R. 1989. Large ionic currents leave the primitive streak of the 7.5-day mouse embryo. Biol. Bull. 176(5): 110-117.

Wollberg, A., Cohen, E., and Kalina, M. 1975. Electrical properties of developing oocytes of the migratory locust, Locusta migratoria. J. Cell Physiol. 88: 145-158.

Woodruff, R.I. 1979. Electrotonic junctions in Cecropia moth ovaries. Dev. Biol. 69: 281-295.

Woodruff, R.I. 1989. Charge-dependent molecular movement through intercellular bridges in Drosophila follicles. Bio. Bull. 176(5): 71-78.

Woodruff, R.I., and Anderson, K.L. 1984. Nutritive cord connection and dye coupling of the follicular epithelium to the growing oocytes in the telotrophic ovarioles on Oncopeltus fasciutus, the milkweed bug. Roux's Arch. Dev. Biol. 193: 158-163.

Woodruff, R.I., Huebner, E., and Telfer, W.H. 1986. Ion currents in Hyalophora ovaries: the role of the epithelium and the intercellular spaces of the trophic cap. Dev. BioI. 117: 405-416.

Woodruff, R.I., Kulp, J.H., and LaGaccia, *B.D.* 1988. Electrically mediated protein movement in Drosophila follicles. Roux's Arch. Dev. Biol. 197: 231-238.

Woodruff, R.I., and Telfer, W.H. 1973. Polarized intercellular bridges in ovarian follicles of the cecropia moth. J. Cell Biol. 58: 172-188.

Woodruff, R.I., and Telfer, W.H. 1974. Electrical properties of ovarian cells linked by intercellular bridges. Ann. N.Y. Acad. Sci. 238: 408-419.

Woodruff, R.I., and Telfer, W.H. 1980. Electrophoresis of proteins in intercellular bridges. Nature (London) 286: 84-86.

Woodruff, R.I., and Telfer, W.H. 1990. Activation of a new physiological state at the onset of vitellogenesis in Hyalophora follicles. Dev. BioI. 138: 410-420.

Yamashiro, D.J., and Maxfield, F.R. 1987. Acidification of morphologically distinct endosomes in mutant and wild type Chinese hamster cells. J. Cell BioI. 105: 2723-2733.

Yamoshiro, D.J., and Maxfield, F.R. 1988. Regulation of endocytic processes by pH. Trends in Pharm. Sci. 9: 190-193.

Yisraeli, J.K., and Melton, D.A. 1988. The maternal mRNA Vgl is correctly localized following injections into Xenopus oocytes. Nature (London) 336: 592-595.

Yisraeli, J.K., Sokol, S., and Melton, D.A. 1990. A two-step model for the localization of maternal mRNA in Xenopus oocytes: involvement of microtubules and microfilaments in the translocation and anchoring of Vgl mRNA. Development 108: 289-298.

Zamboni, L., and Gondos, B. 1967. Intercellular bridges and synchronization of germ cell differentiation during oogenesis in the rabbit. J. Cell Biol. 36: 276-282.

Zavortink, M., Welsh, M.J., and McIntosh, J.R. 1983. The distribution of calmodulin in living mitotic cells. Exp. Cell Res. 149: 375-385.

Zivkovic, D. 1990. Steady transcellular ionic currents during early molluscan development. Ph.D. Thesis. Rikjsuniversiteit te Utrecht, Holland.

APPENDIX

TWO-DIMENSIONAL VIBRATING PROBE

Equipment Layout

The general layout of the vibrating probe is depicted in Fig. 1. A Zeiss AM35 inverted microscope, Narishige Micromanipulator, probe micromanipulator, preamplifier, and thermocouple sensor all rest on a vibration-free table (Micro-g) enclosed in a wire-mesh Faraday cage. The push-pull syringe system was mounted for easy access during experiments. Not shown in Fig. 1 is a vacuum line which connected to the outflow port on the specimen chamber. The preamplified signal output connected to the lock-in amplifier which in turn fed into an IBM PCXT computer. A microscope video image from a Panasonic CCD camera and computer graphics were superimposed on a Panasonic black-and-white video monitor via a PC-Microkey board (model 1300, Video Associates Labs, Austin, TX). Current vectors were displayed on the video monitor by touching the screen with a light pen (FTG Co., Onyx Systems, Wausau, WI), which also selected software menu options displayed on the video monitor. Other components of the system, including the parallelogram bender are described by Nuccitelli (1986).

Details of the recording chamber design are illustrated in Fig. 2a. Essentially, the entire chamber was constructed from two pieces of Plexiglass. The upper fluid reservoir was enclosed by a ring of Plexiglass glued with acrylic cement to the base of the chamber. Platinum-blacked reference and ground electrodes were permanently installed in the lower reference chamber. A 22 X 40 mm coverslip formed the bottom of the specimen chamber. Holes drilled into the base of the recording chamber enabled the introduction of a suction pipette which was used to hold ovarioles by the base of the pedicel (Fig. 2b).

Probe Construction

An improved wire probe design greatly facilitated probe fabrication and use. Either platinum-iridium or stainless steel, paraline-coated electrodes (Cat. no. SS300305A) were purchased from Micro Probe Inc. (Clarksburg, MD). These had an impedance of 6.7-7.3 megohms. Electrodes were trimmed to 1.6-1.8 ern in length and mounted in gold socket connectors with cold #-solder conductive adhesive (Acme Division Allied, New Haven, CT) and cured for 2 hrs at 60C. Unfinished probe tips were cleaned in chromosulfuric acid, rinsed in distilled water. A 30 μm gold and platinum tip was elecroplated on with a model AR-1 Probe Maker (Vibrating Probe Co., Davis, CA). The final 20% of the probe diameter was added via 0.5 sec, 2 p.Amp "shots." Capacitance was checked by passing a triangle-wave test pulse. Probes were frequently acid-cleaned and/or replated.

Probe Calibration

The most critical procedure before any experiment was to calibrate the probe properly. This was accomplished by passing a known current with a current-injecting electrode (described in General Materials and Methods). If one considers the electrical field around a point source of current to be symmetrical, then the current density at a given radius from the center will be equal to

$$\frac{I}{4\pi r^2}$$

(from Scheffey, 1986). By making I equal to the known current being passed, and r equal to the radius of the sphere (or distance from the electrode), it is possible to calculate the theoretical current density at the probe tip. Probes were calibrated at 5 equidistant locations from the microelectrode tip. Calibrations were accepted as valid when the measured current was within 80% of the known, and if angular derivatives were less than approximately 10 degrees (inset, Fig. 1).

In addition to calibration, probes were also checked for barrier artifact by placing the probe close (within approximately 50 urn) to the side of the recording chamber. If reference current values were different from those in the center of the recording chamber, probes were replated and recalibrated. If platinum loss from a probe was excessive, it was subjected to brief sonication (10 sec) in distilled water followed by an acid wash, and then replated.

Probe Noise

A recurrent problem with the vibrating probe technique was electrical noise. Common sources of noise include:

1) loss of capacitance, either by probe fouling or platinum loss;
2) air bubbles or platinum loss on the reference electrode;
3) interference from harmonics of the vibration frequency;
4) loss of ground;
5) AC line "spikes" in room power supply;
6) unshielded AC power sources too near to the probe;
7) breaks in the paraline coat.

With the aid of an oscilloscope and some practice, these problems can usually be quickly diagnosed and fixed. For another description of commonly encountered probe artifacts, see Scheffey (1986).

Figure 1

General layout of the two-dimensional vibrating probe. AD = analogue-to-digital converter; C = CCD camera; FC = Faraday cage; LA = lock-in amplifier; LP = light pen; P = pre-amplifier; S = push-pull syringe; T = thermocouple sensor.

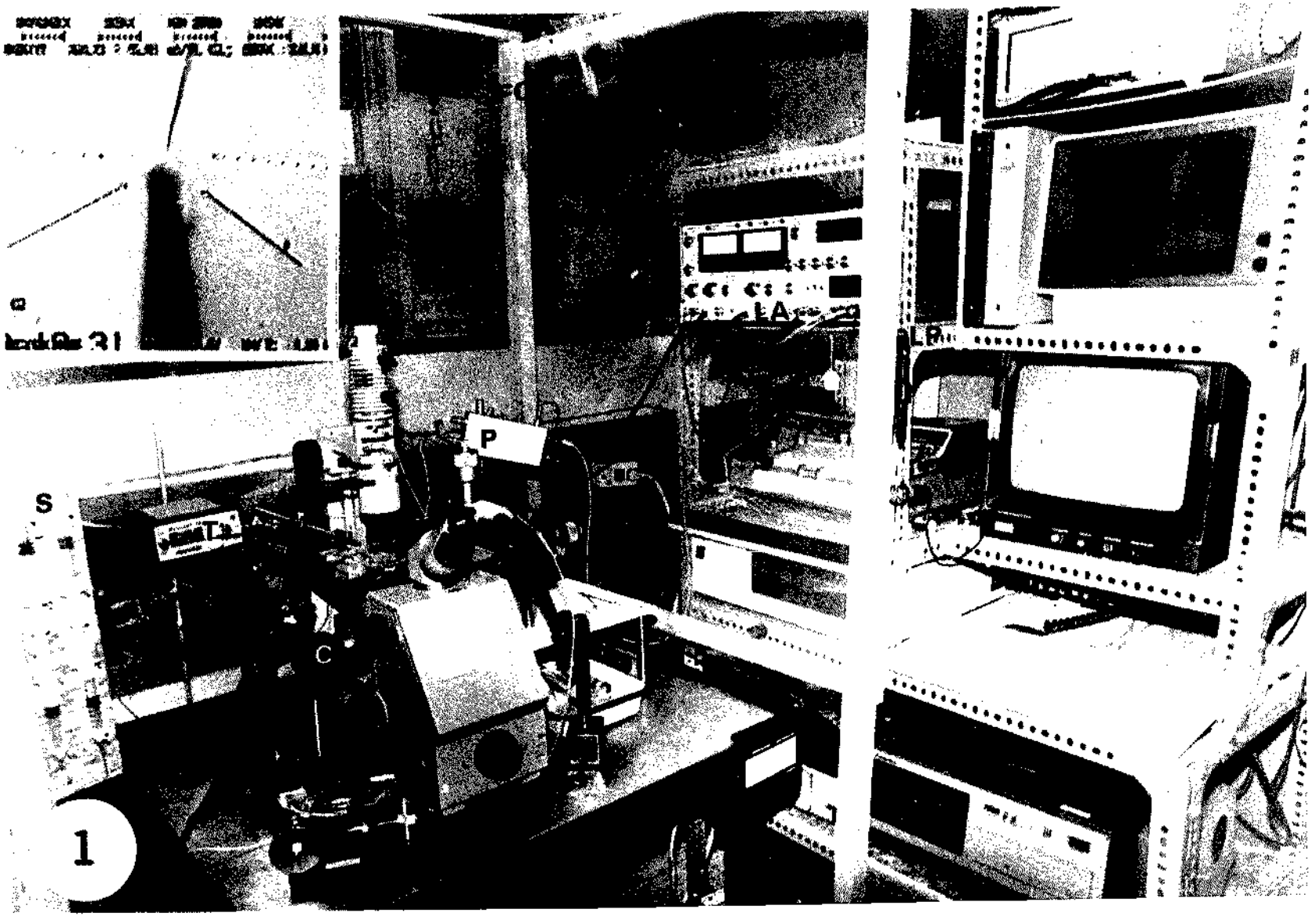
P
S
C
1

Figure 2

Details of *a)* recording chamber and *b)* suction pipette. GND = equal ground; IF = inflow; IP = iontophoresis pipette; OF = outflow; REF = reference; SP = suction pipette; VP = vibrating probe.

2a

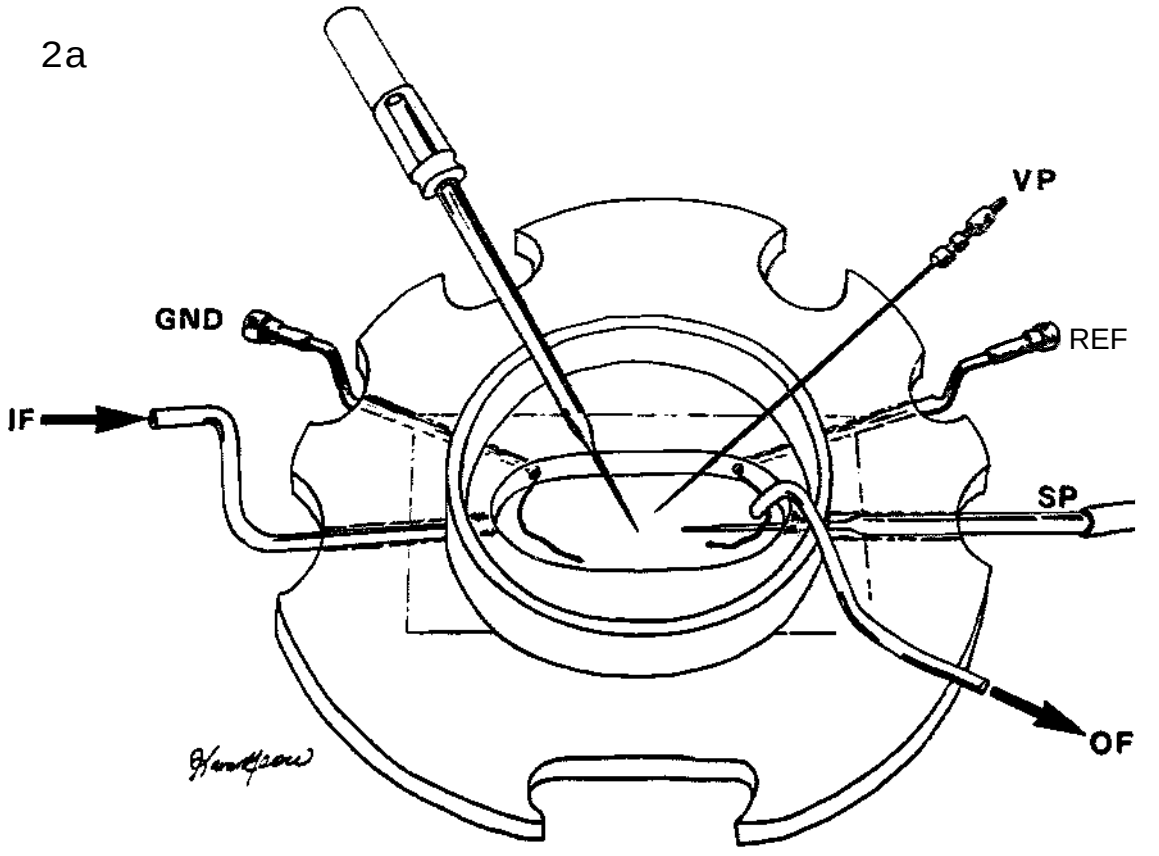

2b